THE FORMATION AND ORIGIN OF CARBONATE MINERALS IN THE DARLING AND YZERFONTEIN HYPERSALINE PANS, WESTERN CAPE, SOUTH AFRICA

Carla Mauger
B. Sc. (Hons) (Geology) (UCT)

Submitted in complete fulfillment of the requirements of the degree of
MASTER OF SCIENCE
in the
Department of Geological Sciences
Faculty of Science
University of Cape Town
February 2009

Preface

The work in this thesis was conducted in the Department of Geological Sciences at the University of Cape Town, under the supervision of Assoc. Prof. John Compton and Dr. Alakendra Roychoudhury.

This study represents original work of the author, and has not been submitted in any other form to another university. Where use was made of the work of other authors, it has been duly acknowledged in the text.

Signed: Signed by candidate Date: 15/02/2009

C.L. Mauger

Acknowledgements

The author would like to thank the following:

Assoc. Prof. John Compton for his invaluable supervision and guidance throughout the year;

Dr. Alakendra Roychoudhury for supervision and organization of the original project, and help with lab equipment;

NRF for funding;

Assoc. Prof. Chris Harris and Fayrooza Rawoot for assistance with stable isotope preparation and analysis;

Ian Newton for analyzing organic carbon samples on the mass spectrometer;

Dr. Petrus Le Roux and Shireen Govender for help with Sr isotope preparation and analysis;

Ronel August for assistance with the XRD;

Miranda Waldron, for SEM analysis;

Nicholas, Kirsten, Catherine, Anne, Anthony and Donovan for their hard work on sampling trips, and all my post grad classmates for their good company and critical discussion;

Marius from Yzerfontein gypsum mine and the owners of Rooipan and Zwartwater farm for access to their property.

Abstract

The Darling and Yzerfontein hypersaline pans are located on the western coastal plain of South Africa. The area has an arid, Mediterranean type climate. The carbonate minerals calcite and dolomite have precipitated in the pans through the evaporation and concentration of ions derived from weathering of bedrock, marine aerosols and coastal rainfall. Five pans were studied, the brine-type pans Rooipan South, Zwartwater North and Zwartwater South, the brackish saline pan Rooipan North, and the coastal Yzerfontein pan. Directly below the surficial halite crust of the three brine-type pans is a black organic-matter rich layer in which bacterial sulphate reduction is occurring (hydrogen-sulphide smell). All of the pans contain disseminated calcite, with only the Zwartwater North and Zwartwater South pans containing a mixture of dolomite and calcite. Yzerfontein and Zwartwater North pans contain small aragonitic gastropod shells (*Tomichia ventricosa)* which are no longer active in the pans due to the high present-day salinities of the pan waters. Low-magnesian calcite is likely the first evaporite mineral to precipitate in the pans because of its low solubility. The removal of Ca^{2+} leads to a higher Mg/Ca ion ratio of pan waters and results in the precipitation of high-magnesian calcite. As the Mg/Ca ion ratio of the pan sediment pore waters rises further, dolomite or a poorly ordered form of dolomite (protodolomite) forms, either through direct precipitation, or by dolomitization of calcite by Mg-rich evaporative brine water. The $\delta^{18}O_{PDB}$ of the carbonate minerals varies from -8.85 to -1.87‰ and indicates precipitation from warm, evaporative waters. The $\delta^{13}C$ values of the carbonate minerals varies from -5.56 to -2.41‰ and suggests that organic matter degradation is at least partly the source of carbonate ions. Carbonate ions are made available for precipitation of diagenetic carbonate minerals during organic matter degradation by sulphate-reducing bacteria. Reduction of sulphate may also enhance dolomite precipitation. The $^{87}Sr/^{86}Sr$ ratios of pan carbonate minerals range from 0.710797 to 0.71159. These somewhat higher than seawater (0.709) ratios indicate that the source of the calcium ions in the carbonate minerals is a mixture of seawater (seaspray and marine aerosol rainout) and chemical weathering of the Cape Granite and Malmesbury Group bedrock. The knobby texture of the carbonate minerals, with subspherical structures common in SEM images, suggests that the precipitation of the carbonate minerals, particularly dolomite, was intimately tied to bacteria and microbial processes.

TABLE OF CONTENTS

Abstract ..... *i*
Acknowledgements ..... *ii*
Table of Contents ..... *iii*
List of Figures ..... *vi*
List of Tables ..... *ix*

1 Introduction 1-1

1.1 Motivation for study **1-1**

1.2 Aims of the study **1-2**

1.3 Study area **1-3**
1.3.1 General Geology 1-3
1.3.2 Soils, flora and land use 1-5
1.3.3 Climate 1-6

1.4 Pans **1-7**
1.4.1 Pan development 1-8
1.4.2 Darling and Yzerfontein Pans 1-9
1.4.3 Brine Evolution and Evaporite minerals 1-11
1.4.4 Precipitation of Carbonate minerals 1-12

2 Methods **2-1**

2.1 Sample collection **2-1**

2.2 Sample Preservation and Preparation **2-1**

2.3 X-Ray Diffraction Analysis (XRD) **2-1**

2.4 Scanning Electron Microscope (SEM) **2-2**

2.5 Carbonate mineral and organic carbon content and organic carbon $\delta^{13}C$ 2-3

2.6 Carbon and oxygen isotope composition of the carbonate minerals 2-4

2.7 Sr Isotope Analysis 2-6

3 Results 3-1

3.1 Pan Stratigraphy 3-1
3.1.1 Sample nomenclature 3-1
3.1.2 Sampling Localities 3-1

3.2 Sediment Analysis 3-14
3.2.1 Grain size analysis 3-14
3.2.2 Mineralogy (XRD) 3-16
3.2.3 Sediment texture (SEM) 3-20
3.2.4 Organic Carbon and $\delta^{13}C$ 3-20
3.2.5 Stable and Radiogenic Isotopes 3-21

4 Discussion 4-1

4.1 Origin of carbonate minerals 4-1
4.1.1 Oxygen isotope evidence for the extent of evaporation during carbonate mineral precipitation 4-1
4.1.2 Source of carbonate ions 4-3
4.1.3 Source of Ca^{2+} and Mg^{2+} ions 4-16

4.2 Evolution of pans 4-19
4.2.1 Brine type pans 4-19
4.2.2 Brackish-saline Pan 4-24
4.2.3 Coastal Yzerfontein Pan 4-24

4.3 Factors enhancing carbonate mineral precipitation 4-26

4.4 Regional differences in pan carbonate minerals 4-27

4.5 Comparison to pans within southern Africa.....4-30
4.5.1 Present-day pan environments 4-30
4.5.2 Palaeo-lake and palaeo- playa environments..... 4-31

5 Summary and Conclusions.....5-1

6 References 6-1

Appendix: XRD Scans.....A-1

List of Figures

Figure 1.1. Location map of Darling and Yzerfontein pans (Based on 1:250 000 series, Geological map (3318 Cape Town), Geological Survey, 1990) 1-4

Figure 1.2. Google Earth image of the study area, showing pans in the study area 1-5

Figure 1.3. The distribution of pans in southern Africa (from Goudie and Wells, Fig. 2) 1-8

Figure 3.1. Orthophotograph of Rooipan South indicating sample pit (Trigonometric Survey). 3-2

Figure 3.2. Pan stratigraphy of Rooipan South Pan, indicating sample numbers 3-2

Figure 3.3. Orthophotograph of Zwartwater North Pan indicating sample pits. Note ploughed fields to west, east and south of pan 3-3

Figure 3.4. Pink halite crust, black sulphate reducing mud, and underlying green mud of Zwartwater North Pan, East sampling pit. 3-4

Figure 3.5. Pan stratigraphy of sample pits at Zwartwater North Pan, indicating sample numbers. 3-4

Figure 3.6. Orthophotograph of Zwartwater South Pan and Slangkop hill indicating sample pits at the pan, and sample locality of Slangkop Hill Gully 3-5

Figure 3.7. Pan stratigraphy of Zwartwater South Pan at different sample pits, showing sample numbers 3-6

Figure 3.8. Rooipan North Pan showing sample pits RNN and RNC (Google Earth image) 3-7

Figure 3.9. View towards southwest of Rooipan North. Note dry surface, the lack of halite crust, and the vegetated pan margin 3-8

Figure 3.10. Pan stratigraphy of Rooipan North with sample names 3-8

Figure. 3.11. View of Yzerfontein Pan looking north 3-9

Figure 3.12. Orthophotograph of Yzerfontein pan, showing sample pits, and area mined for gypsum 3-10

Figure 3.13. Pan stratigraphy of Yzerfontein Pan at sample sites, showing sample numbers.....3-10

Figure 3.14. Inner margin of Yzerfontein Pan, orange *Tomichia ventricosa* shells, deposited on the surface mud. 3-11
Figure 3.15. Sample YZ1A: burrowed calcitic grey mud at inner edge of Yzerfontein Pan. Sediment block ~20 cm wide 3-11

Figure 4.1. Plot of $\delta^{13}C$ versus $\delta^{18}O$ isotope values for the disseminated pan dolomite, calcite, calcite nodule, and biogenic carbonate. Dotted lines join calcite and dolomite from the same sample.. 4-3

Figure 4.2. Plot of $\delta^{13}C$ versus $\delta^{18}O$ values for carbonate minerals in the pans compared to carbonate minerals from other studies precipitated in sulphate reduction and methanogenesis zones, such as East Salina Caicos (Perkins et al., 1994), Monterey Formation (Burns and Baker, 1987) and Lagoa Vermelha (Vasconcelos and McKenzie, 1997) 4-6

Figure 4.3. Plot showing the distribution of $\delta^{13}C$ values of the bulk organic carbon in pan sediment samples. The pan sediment is interpreted to be a mixture of algal (-19 to -21‰) and woody C3 plants (-25 to -27‰). 4-8

Figure 4.4. The weight percent of organic carbon versus weight percent calcite+ dolomite of samples, mostly from black surface mud layers, shows a positive correlation ($R^2 = 0.71$). YZ2 sample is from the Yzerfontein coastal pan. 4-8

Figure 4.5. A) SEM images of fine silt fraction of sample ZNMA (from Zwartwater North) showing quartz grains and small laths of organic matter B) Fine silt fraction of sample ZNMB (Zwartwater North) showing carbonate mineral coating on organic matter C) Biogenic carbonate - aragonitic *T. ventricosa* shell fragment from coarse silt fraction of sample ZNMB (Zwartwater North) D) Organic matter (small irregular fragments) and carbonate mineral precipitate in fine silt fraction of sample ZNMB (from Zwartwater North).....4-14

Figure 4.6. SEM images from A)Yzerfontein pan (sample YZ1A) gypsum and calcite crystals (note smooth crystal faces of calcite and small platey gypsum crystals), B) Dolomite with possible interlocking dumbbell structure in silt fraction of sediment from Zwartwater North pan (sample ZNED), C) Knobby anhedral carbonate mineral possibly coating nanobacteria from Zwartwater North pan (sample ZNNC) D) knobby texture of carbonate minerals in fine silt fraction of sediment from Zwartwater South (sample ZSNC). XRD indicates that these are a mixture of calcite and dolomite. These are interpreted to be dolomite. 4-15

Figure 4.7. Diagram of precipitation of carbonate minerals during pan evolution. A) brackish-saline stage with active *T. ventricosa* ; B) saline pan with moderate salt and calcite precipitation during early stages of evaporation, and C) hypersaline

pan with well developed halite crust in summer Mg/Ca ratio rise and sulphate reduction leading to dolomite precipitation 4-20

Figure 4.8. XRD scan of sample ZNSB, showing mineralogy of 2-38 μm and 38-63 μm size fractions. Kao=kaolinite, Qtz=quartz, Cc=calcite, Mg-cc=magnesian calcite, Dol=dolomite, Hal=halite 4-22

Figure 4.9. XRD scan of sample ZSSA, showing mineralogy of 2-38 μm and 38-63 μm size fractions. Kao=kaolinite, Qtz=quartz, Cc=calcite, Mg-cc=magnesian calcite, Dol=dolomite, Hal=halite 4-22

Figure 4.10. Cropped XRD scans of sample A) ZNSB and B) ZSSA, showing main low magnesian calcite (cc), high magnesian calcite (Mg-cc) and dolomite (dol) peaks. Note the broad magnesian calcite peaks, indicating the range of magnesium content 4-23

Figure 4.11. Schematic diagram showing the sequential progradation of the Yzerfontein coastline, leading to the formation of Coastal Rooipan (not in the study) and Yzerfontein pans. A) Last interglacial highstand of the sea (Eemian), 120-130 ka, B) Progradation of beach and build up of dunes as sea level fell during the early stages of the last glaciation. C) Present-day abandoned lagoons transformed into salt pans. The lagoon would have been intermittently connected to the sea between stages A and B related to sea-level fluctuations and build up of beach and dune sand deposits. 4-25

List of Tables

Table 3.1 Pan names, abbreviations, pan type and location 3-1

Table 3.2 Sample descriptions 3-12

Table 3.3. Grain size distribution of sediment samples 3-14

Table 3.4. Mineralogy of pan sediments obtained by X-Ray Diffractometry (patterns presented in Appendix) ordered in relative decreasing abundance. Results shown for each separate size fractions: 38-63 μm coarse silt fraction, 2-38 μm fine silt fraction and <2 μm clay fraction. Qtz=quartz, K-fsp = K-feldspar, kao= kaolinite, cc = calcite, Mg-cc=magnesian calcite, dol=dolomite, ill=illite, hal=halite, gyps = gypsum, goe=goethite, smec=smectite, ?=unidentified peak 3-18

Table 3.5. Organic carbon (OC) content and carbon isotope composition of bulk pan sediment samples 3-20

Table 3.6. Carbon, oxygen and strontium isotope analyses of pan calcite and dolomite 3-21

Table 4.1 Major ion chemistry of pan water samples (concentrations in mmol/kg) from Smith, 2000, Table 4.2) and molar Mg/Ca ratio 4-10

Table 4.2 Regional groundwater borehole data from the DWAF geohydrological database (concentrations in mmol/kg) (from Smith, 2000, Table 4.8.) and molar Mg/Ca ratio 4-18

1 Introduction

1.1 Motivation for study

Carbonate sediments are produced through either chemical or biochemical precipitation of carbonate minerals from supersaturated waters. The most common carbonate minerals in modern sediments are aragonite, calcite and dolomite. Carbonate rocks compose roughly a quarter of the sedimentary rock record (Ronov, 1983) and are of economic importance as they can often be found in conjunction with petroleum and metallic elements (Boggs, 2001). Dolomite is especially of interest because of the "Dolomite Problem", which refers to the poor understanding surrounding the process of dolomitization and dolomite precipitation (Purser et al., 1994). The first part of the dolomite problem is that while dolomite rock can be found in abundance in the sedimentary record, as vast marine platforms for example, there are few modern (i.e. Holocene) analogues for the precipitation of dolomite on a similar large scale as observed in the rock record. This is despite dolomite's thermodynamic stability and the fact that surface seawater is currently supersaturated with respect to dolomite. Holocene dolomite is only found in relatively small amounts in varying environments, including deep sea environments, marine shelf environments, and sabkha lake/ hypersaline pan evaporative environments (Baker and Kastner, 1981; Morrow, 1982; Purser et al., 1994). The second part of the dolomite problem is the inability to synthesize dolomite in the laboratory under conditions found in Earth surface environments (i.e. temperatures below 80° C, and pressures below 20 atm) (Purser et al., 1994).

Sediments from the Quaternary Darling and Yzerfontein Pans have been identified as containing carbonate minerals (Smith, 2000; Smith and Compton, 2004), specifically calcite, dolomite and biogenic aragonite. These pans provide an opportunity to study an environment presently precipitating these carbonate minerals. The pan sediments have also been identified as environments in which bacterial sulphate reduction is occurring (Porter, 2007). Bacterial sulphate reduction is a possible influencing factor in the precipitation of carbonate minerals and specifically dolomite at low (i.e. Earth's surface) temperatures (Vasconcelos and McKenzie, 1997). Methanogenesis may also be an important process enhancing dolomite precipitation in anoxic, organic rich sediments (Mazzulo, 2000).

1.2 Aims of the study

The first aim of this study is to determine the mineralogy and texture of pan sediments with a particular focus on the carbonate minerals. The second aim of this study is to determine the oxygen, carbon and strontium isotope composition of the carbonate minerals in order to understand better the origin of the carbonate minerals. The source of the carbonate ions in the carbonate minerals, whether from degradation of organic matter, or from the chemical weathering of bedrock, may be determined by carbon isotopes of the carbonate minerals. Oxygen isotopes can be used to determine the extent of evaporation of the brine during the period of carbonate mineral precipitation. The source of the calcium and magnesium ions in the carbonate minerals can be identified from the strontium isotope composition of the carbonate mineral. Sr isotope ratios ($^{87}Sr/^{86}Sr$) can be used as a proxy for the origin of calcium ions, especially to differentiate between marine and bedrock sources (Compton et al., 2001). The source of the calcium ions in the

carbonate minerals of the pans could be weathering of the Cape Granite or Malmesbury Group bedrock, or the calcium could be of marine origin.

1.3 Study area

The study area is located between the towns of Yzerfontein and Darling, on the West Coast of the Western Cape, South Africa (Figure 1.1). Five hypersaline pans are the focus of this study: The first is the coastal Yzerfontein Pan, outside the town of Yzerfontein. Zwartwater North Pan and Zwartwater South Pans are located on the Zwartwater farm, about 10 kilometers west of the town of Darling. Rooipan North and Rooipan South are located on Rooipan farm and lie about 3 km northeast of the Zwartwater pans.

1.3.1 Gene ral Geology

The bedrock in the study area consists the Tygerberg terrane of the Late Precambrian Malmesbury Group (1200-510 Ma), as well as the Cape Granite Suite of the Darling Batholith. The Malmesbury Group here consists of metamorphosed mudstone, schist and quartzite. The Cape Granite is of NeoProtozoic to Cambrian age (547± 6 Ma), intruded into the Malmesbury Group during the Saldahnian orogeny (Da Silva et al., 2000) (Figure 1.1). The Darling pluton/batholith consist of an S-type (sedimentary type), which is composed of alkali feldspar, plagioclase, quartz, biotite and cordierite, and a relatively small amount of Aa-type granite. At the coast near Yzerfontein lies the Yzerfontein pluton, which consists of younger, approximately 519±7 Ma, calc-alkaline, intermediate and mafic intrusions, also of the Cape Granite Suite. These are predominantly gabbros, monzogabbros and monzosyenites (Da Silva et al., 2000). The area surrounding the batholith is covered by loamy, gravelly clay, and light grey sandy Quaternary sediments.

Pleistocene marine calcrete and limestone of the Langebaan Formation, and the aeolian white calcareous dune sands of the Holocene Witzand Formation underlie the town of Yzerfontein and the surrounding coastal areas (Compton and Franceschini, 2005). The Colenso Fault cuts NW/SE through the study area. The Colenso Fault originated during the Saldahnian orogeny and separates the Swartland and Tygerberg terranes (Schoch, 1976).

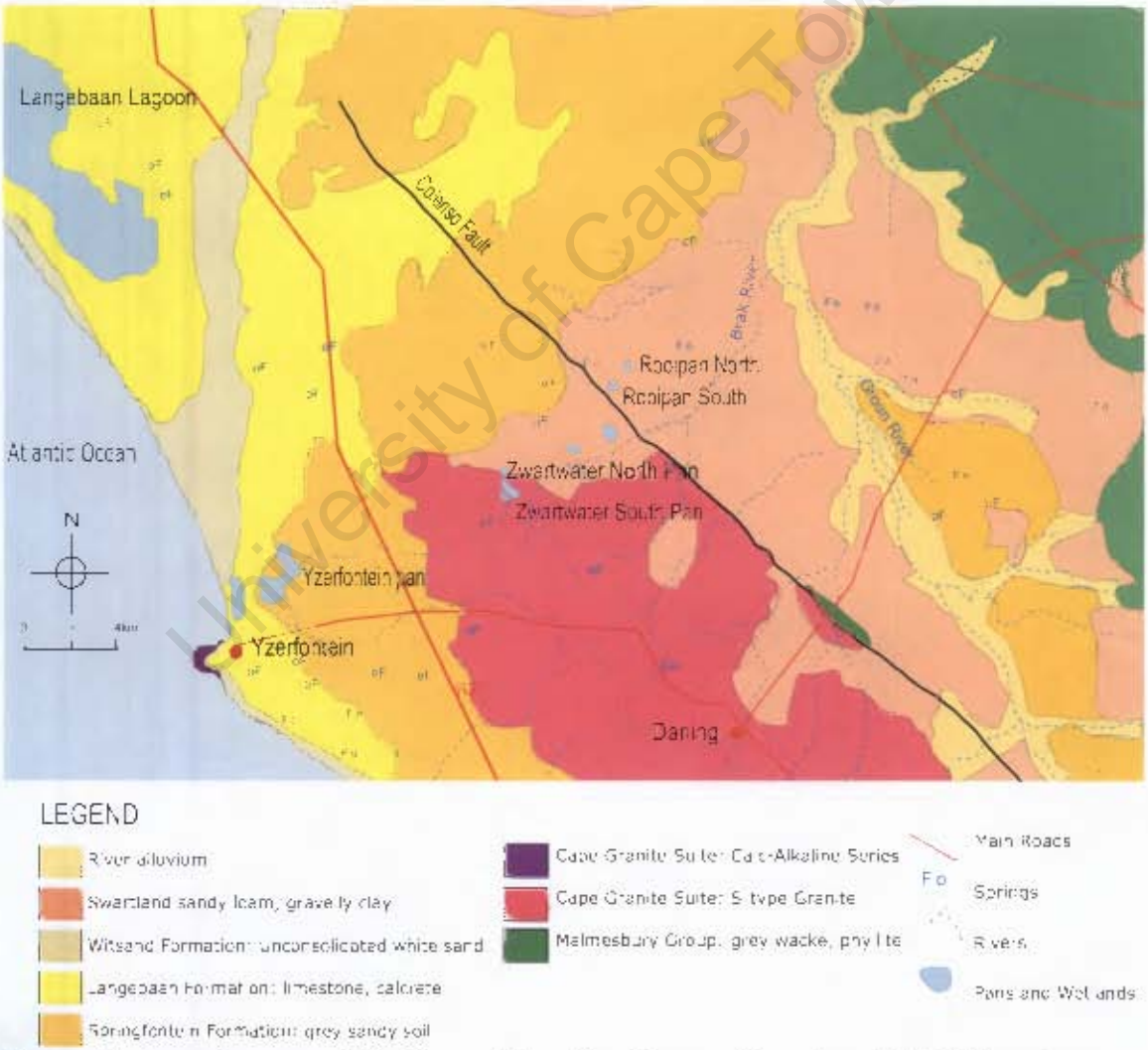

Figure 1.1. Location map of Darling and Yzerfontein pans (Based on 1:250 000 series, Geological map (3318 Cape Town), Geological Survey, 1990)

Figure 1.2. Google Earth image of the study area, showing pans in the study area.

1.3.2 Soils, flora and land use

The coastal soils are calcareous and sandy, derived from the Langebaan and Witzand formations. Low lying, shrub-type coastal *strandveld* vegetation dominates in these low nutrient soils. Soils on the Cape Granite hill slopes consist of granitic, thin porous silty sand. The soils of the valley bottoms consist of grey, brown quartzitic sand. Further inland are sandy horizons over clayey loam derived from the Malmesbury Group, soils tending towards aquifer formation, as the clay acts as an aquitard (Lambrechts, 1981).

Renosterveld vegetation, characterized by dark bushes and C3 grasses, thrives in these clay rich soils inland.

The land has been cultivated to a large extent and the Darling Pans (excluding Yzerfontein Pan) are surrounded by agricultural land. Dairy cattle, sheep, ostrich and wheat are all farmed in the area. Yzerfontein pan is mined for gypsum at present, and in the past was mined for salt. Since the high salt concentrations of the pans and their immediate surrounds are not conducive to agriculture, the pans are fenced off from the cultivated land, and are surrounded by both indigenous fynbos vegetation and alien vegetation, such as the Australian gum, *Acacia cyclops.* The pan's outer margins are either unvegetated or vegetated by halophilic plants.

1.3.3 Clim ate

The Darling Pans are located in the Western Cape which has a Mediterranean-type climate. It experiences hot, dry summers and cool, wet winters with the highest average rainfall occurring in July. Winter temperatures range from 5°C to 19°C on average, while summer temperatures average from 12°C to 28°C and precipitation is between 250-300 mm per annum (South African Weather Service). The pans occur within the catchment of the Berg River.

Two main factors influence the climate of the Darling West Coast area. The first is the cool descending air of the Hadley Cell. The Hadley Cells are belts of low pressure in the subtropical regions, around 15-45 degrees North and South of the equator. These low pressure cells are associated with arid desert regions. The second factor is the cold

Benguela Current. Upwelling cools the air, decreasing its ability to carry moisture, lowering humidity, and leading to the arid climate on the west coast of southern Africa (Warren, 1999). Aridity, where precipitation rates are lower than evaporation rates, is a factor associated with evaporite environments in general and hypersaline pan development. Wind speeds are high and seasonal in the Darling and Yzerfontein region, and the area is the site for wind farm development. Wind is also a factor for pan formation, as it serves to both raise evaporation rates, as well as contribute to deflation.

1.4 Pans

Pans, or playas as they are sometimes known, are defined as shallow closed basins or depressions that may be ephemerally flooded. Pans play an important role in the hydrological system in the areas in which they are found. They accumulate elements from their environment such as sediment, water, salts and organic matter. For this reason they can provide information about the surrounding catchment area.

Pans are a common feature in arid environments and the dry regions of southern African are no exception. In South Africa, the Free State, western Mpumalanga and Gauteng, the north-eastern Northern Cape, and the north-eastern Western Cape Province (the study area) are areas high in pan density (Figure 1.3). Most of the pans occur in areas of less than 500 mm mean annual rainfall and more than 1000 mm free surface evaporation loss (Goudie and Wells, 1995). Namibia, with its arid climate, also has a high density of pans. Most well known are the Etosha pans in Northern Namibia, as well as the pans in the southern region in Hereroland to the east of Keetmanshoop (Goudie and Wells, 1995). Pans are also widespread in Mozambique, Botswana, Zambia and Zimbabwe. The reason

for the density of the pans in the southern Africa, as mentioned, is the dry conditions that are associated with the descending Hadley Cells, about 15-45° either side of the equator. Therefore, by the same reasoning, high densities of pans are found in northern Africa, central Asia, western Australia and South America.

Figure 1.3. The distribution of pans in southern Africa (from Goudie and Wells, 1995, Fig. 2)

1.4.1 Pan development

There are a variety of factors involved in pan formation and development, many of them interconnected. Pans may initially form through the disruption of natural drainage (Goudie and Thomas, 1986), such as an estuarine, lagoon, lake or river setting. Drainage disruption may occur as a result of sea-level fall, or faulting that may cause blocking or damming of the existing drainage system. As a result, pans will naturally form in

topographic lows, where water can accumulate. Lunette dunes commonly develop due to the deposition of deflated material on the lee side of seasonally dry river beds (Lawson and Thomas, 2002). The lunette dune then begins to block drainage and contributes to the formation of a pan. With evaporation, salts from coastal rainfall and marine aerosols or from weathering of bedrock may accumulate in a saline lake. Vegetation may become sparse in the area, and as evaporation and desiccation continue, deflation by wind may occur in the dry months. The concentration of salts in the pans leads to the precipitation of evaporite minerals, such as halite, gypsum and carbonate minerals. Marine aerosols and coastal rainfall are common sources of these salts. Capillary action may bring groundwater up to the surface to be evaporated, increasing the amount of ions available for evaporite precipitation. The precipitation of the minerals themselves can also contribute to deflation through a process known as salt weathering. As the evaporite minerals crystallize, they break apart rock and sediments, making them more easily transported by wind, and contributing to deflation. The pan may also be inviting to animals seeking water and salt. Trampling and overgrazing of animals would increase deflation (Goudie and Wells, 1995).

1.4.2 Darlin g and Yzerfontein Pans

The inland hypersaline pans on the West Coast formed during the Holocene (Smith, 2000; Smith and Compton, 2004) and are linearly arranged, trending NE/SW, possibly a relict of a disrupted drainage system. The chemistry of the pans indicates that their chemistry is marine influenced, the ions transported to the pans through coastal rainfall and marine aerosols. There are 2 main types of pans in the study area, coastal and inland pans.

The coastal pans are much larger and more irregular in shape than the inland pans at Darling. The coastal pans are more likely to be the result of a palaeo-lagoon setting, disrupted in the late Pleistocene. As would be expected, the chemistry of the coastal pans is more marine-influenced than the inland pans (Smith, 2000; Smith and Compton, 2004).

The inland pans are smaller and fairly rounded in shape compared to the coastal pans. Some display a lunette dune on their lee side, formed through deflation of the pan. The inland pans can be divided into 2 types by water chemistry, brine-type and brackish-saline. Brine-type pans have high concentrations of dissolved salts, with TDS (Total Dissolved Solids) of 168-379 g/L (Smith, 2000). In the dry season brine pans will form a halite crust, a few centimeters thick on the surface of the pan. The crust forms a barrier between the pan sediments and the environment, limiting their interaction with the atmosphere, protecting them from wind erosion, and also keeping them wet, which allows chemical reactions and bacterial activity to continue in the dry months. Most of the brine-type pans have a black, muddy, sulphate-reduction zone beneath the halite crust (Porter, 2007).

Brackish-saline pans have a lower concentration of salt, between 2 and 64 g/L (Smith, 2000). They do not form a halite crust, and depending on the amount of water available in the dry season, may not remain wet throughout the year. The surface of the brackish saline pans may be vegetated with halophilic plants as a result of their relatively low salinity.

1.4.3 Brine Evolution and Evaporite minerals

Evaporite minerals *are precipitated from a saturated surface or near surface brine in a hydrological system driven by solar evaporation* (Warren, 1996). Evaporative systems include hypersaline pans, such as those in Darling and Yzerfontein, as well as enclosed basins, lagoons or shallow continental shelves. Evaporite minerals form by precipitation during evaporation, and include halite, gypsum, and carbonate minerals, such as calcite and dolomite. Modern evaporite minerals generally form in warm, arid regions, such as sub-tropical deserts.

Depending on the relative concentrations of ions in the pan brines, different sequences of minerals will precipitate. Southern African pans have a wide variety of pan brine composition. Na^{2+}, Cl^{-}, and sulphate dominated brines, such as those of the Namibian Otjamongwa Pan in Namibia, tend to precipitate a suite of minerals dominated by halite and gypsum (Mees, 2003). Ca^{2+} and Mg^{2+}, and carbonate rich brines will result in the precipitation minerals such as calcite, magnesian calcite, and dolomite, such as the Kalahari calcretes (Watts, 1980) and the Namibian palaeo-oasis in the Namib desert (Smith, 1998).

Calcite, however, is usually the first evaporite mineral to form from a natural hypersaline concentrating water (Warren, 1999) because it is the least soluble salt. In seawater it will begin to precipitate after only a 47% loss of water volume by evaporation. Depending on the original brine chemistry, precipitation of calcite may cause a rise in the Mg/Ca ratio in the solution, which may lead to the precipitation of Mg-rich calcite, proto-dolomite

and dolomite. Calcites in the Darling/Yzerfontein pans generally have almost no MgO present, while Mg-calcites have variable molar contents up to 20%. Protodolomite is generally more calcium rich than dolomite, and has between 40 and 45 mol % MgO (Fairbridge et al., 1968), 5 to 10% less than stochiometric dolomite. If carbonate ions concentration is less than sulfate ion concentration, then gypsum may precipitate after calcite with additional evaporation, depending on the amount of calcium available. According to Smith (2000) the inland pans will follow a modified Eugster and Hardie (Hardie and Eugster, 1970) pathway 3: Calcite will precipitate first. This may be followed by the precipitation of gypsum, if the concentration of sulphate ions is high. An Mg – phase will then remove Mg^{2+} ions. Common examples of Mg-phases in pans include the Mg-rich clays palygorskite, and sepiolite, and protodolomite and dolomite (Watts, 1980). The coastal pans may be closer to Eugster and Hardie pathway 2, with calcite precipitation followed directly by gypsum precipitation.

1.4.4 Prec ipitation of Carbonate minerals

Carbonate minerals include calcite and aragonite (polymorphs of $CaCO_3$), and dolomite ($CaMg(CO_3)_2$). Carbonate minerals are forming at present in many different environments, such as shelf deposits, and sabkha-playa coastal settings. Carbonate minerals may precipitate from solution by an increase in temperature because they are less soluble at higher temperatures. pH and the partial pressure of carbon dioxide of the solution also control carbonate precipitation (Fairbridge et al., 1967; Boggs, 2001).

The warm, evaporated waters of the Darling and Yzerfontein hypersaline pans are environments conducive to carbonate mineral precipitation because of their high pH and high concentrations of carbonate ions (Morse, 1993).

High rates of organic productivity are conducive to carbonate precipitation, as organisms play a large role in the precipitation of carbonate minerals. Aragonite is a metastable polymorph of calcite, often found in skeletal structures of organisms. Calcium and carbonate ions may be removed directly from solution by organisms, such as gastropods, brachiopods, corals and calcareous algae to build skeletal structures. When these organisms die, the calcium carbonate may be "recycled" to form precipitated carbonate minerals (Fairbridge et al., 1967; Boggs, 2001). Photosynthesizing plants, such as algae, may also play a role in carbonate mineral formation, by removing carbon dioxide from water through photosynthesis, and thereby increasing solution pH, which is conducive to carbonate precipitation (Boggs, 2001).

Dolomite

Dolomite has an ideal composition of $CaMg(CO_3)_2$, and like calcite, is built of alternating anion and cation layers. Dolomite, however, is distinguished by alternating Ca^{2+} and Mg^{2+} cation layers. It is common for natural dolomite to be far from ideal compositionally (i.e. not stoichiometric), for example containing excess Ca^{2+} ions substituting for Mg^{2+} ions. The degree that the dolomite is said to be ordered, depends on how closely the Ca^{2+} and Mg^{2+} ions are separated into alternating cation layers. Proto-dolomite is often used to describe dolomite that is not ideal stochiometrically or

structurally (Morrow, 1982). Quaternary studies show that dolomite can form under a variety of conditions, chemical and physical, and therefore a series of dolomite models have been proposed, three of which are discussed below (Purser et al., 1994).

Sabkha/evaporite/ hypersaline model

In this model, dolomite forms in pans/playas, salinas or sabkhas, in arid environments where evaporation exceeds precipitation. Excess evaporation causes a concentration of a brine, which is high in salinity, bicarbonate ions, Mg^{2+} and Ca^{2+} ions, resulting in evaporite precipitation. Calcite generally precipitates first, raising the Mg/Ca ratio of the solution/brine. When the Mg/Ca ratio is high, such as 10:1, dolomite formation is favoured. Magnesium-rich water may also flow downward, or Mg^{2+} ions can diffuse along concentration gradients, through calcitic sediment and transform the calcite to dolomite (dolomitize), according to the following reaction (Boggs, 2001; Morrow, 1982):

$2CaCO_3 + Mg^{2+} \rightarrow CaMg(CO_3)_2 + Ca^{2+}$

This model is the closest to the environment and dolomite precipitating conditions of the Darling hypersaline pans.

Organogenic model

The environment of the organogenic model of dolomite precipitation may be more varied than the other models, but it must be one that is high in organic carbon. The organic carbon within the sediment is degraded through fermentation, methanogenesis or sulphate reduction. This process results in the supersaturation of the porewaters with respect to dolomite (Compton, 1988), which may overcome kinetic barriers to dolomite

precipitation. The anoxic, sulphate-free environment that is created by the degradation of organic carbon is also conducive to dolomite precipitation. The Darling Pans may also be influenced by elements of this model.

Mixing zone dolomitization model

This model proposes that dolomite may form in area of mixing of sea and groundwater of meteoric origin. The mixture of waters may modify seawater enough to precipitate dolomite at lower as (low as 1:1) Mg/Ca ratios, possibly as a result of lowered concentrations of sulphate ions. Examples of this model include the dolomite on the Namibian shelf (Compton et al., 2001), the Zebra carbonate palaeo-oases (Smith and Mason, 1998) and the Lower Visean dolomites from northern Belgium (Muchez and Viane, 1994).

2 Methods

2.1 Sample collection

Sampling took place over 3 days in February 2008, during the dry season. Five pans containing biogenic and sedimentary carbonates (Smith, 2000) were chosen for sediment sampling. Yzerfontein Pan, Zwartwater North and South Pans, Rooipan North and South Pans were sampled. The samples were collected by digging a pit approximately half a meter deep, and removing samples from the sediment profile exposed. Biogenic carbonate shells were also sampled if found. The samples were brought back to the laboratory and frozen the same day.

2.2 Sample Preservation and Preparation

Frozen samples were freeze-dried using a VirTis BenchTop Freeze Dryer. Freeze-dried samples were wet sieved into fractions of >63μm, 38-63μm and <38μm. The <38μm fraction was further separated into 2-38 and <2μm fractions. This was achieved by letting the suspended sediment settle in water for 20 minutes. The settled sediment was assumed to be 2-38μm in size, while the sediment that did not settle within this time was assumed to be <2μm in size, based on Stokes settling law which assumes perfect spheres. The suspended sediment was decanted with the supernatant into another beaker. The separated fractions were then dried in an oven at 50°C.

2.3 X-Ray Diffraction Analysis (XRD)

A small amount (less than 1g) of each separated size fraction was finely ground into a powder using an agate mortar and pestle. The powder was mixed with Milli-Q purified

(MQ) water and pipetted onto a glass slide. The sample was allowed to air dry, and then was loaded into the XRD for analysis. The instrument used was a Philips PW 1390 XRD (Department of Geological Sciences, UCT), which uses a Copper K-α X-Ray tube with x-rays wavelength of 1.542 Å. D-spacings, the the distance between atomic layers in mineral crystals are measured using Braggs Law:

$n\lambda=2d\sin\Theta$, where n is an integer, λ is the wavelength of the beam, Θ is the incident angle, and d is the d-spacing of the crystal in Angstroms.

Bragg 2Θ angles between 2 and 50° were used for analysis (except for some the first <2μm size fraction scans that were scanned between 4 and 50°). Peaks in the X-ray patterns corresponding with the d-spacings of minerals were used to identify the minerals present in the samples.

2.4 Scanning Electron Microscope (SEM)

Twenty samples, those identified as containing carbonate minerals, especially dolomite, were chosen for SEM analysis. The fine silt (2-38 μm) fraction was identified by XRD as containing the greatest amounts of carbonate minerals, and was selected for SEM analysis. A small amount of subsample was sprinkled onto stubs with a graphite and glue mix. The samples were left to air dry and then were coated with gold-palladium. They were then loaded into the Leica Stereoscan S440 SEM and viewed, and images were saved.

2.5 Carbonate mineral and organic carbon content and organic carbon $\delta^{13}C$

A total of 11 samples were chosen on the basis of their apparent high organic carbon content, and were all taken from the black, organic-rich surface mud of the pans. Three of the samples, ZNWA, ZNWA/B, and ZNWB were chosen to represent a sediment profile. Approximately 2-2.5 grams of bulk sediment was suspended in approximately 50 ml of MQ water to remove soluble salts, primarily halite. After settling of the suspended sediment the supernatant was decanted and the samples were dried in the oven at 60°C overnight. Approximately 50 ml of 1M HCl was added to the samples to digest the carbonate minerals. The samples were then centrifuged, and rinsed with MQ. This was repeated until the pH of the supernatant was the same as that of the MQ water. The samples were then transferred to beakers and dried at 60°C overnight, and reweighed to calculate the percent of carbonate minerals digested.

A small amount of the bulk, acid digested samples was ground with acetone in an agate mortar and pestle. Approximately 1 mg of ground sediment was weighed with a microbalance into tin cups, which were then squashed to enclose the sample. The samples were combusted using a Flash EA 1112 series elemental analyzer, and a Finnigan Delta Plus XP isotope ratios mass spectrometer was used to analyse the samples for total (organic) carbon and carbon isotope composition (^{12}C and ^{13}C). Standards used were Merck Gel, and New Nasturtium. These standards are calibrated against International Atomic Agency standards. $^{13/12}C$ was used to calculate $\delta^{13}C$ relative, with the use of the standands, to Pee Dee Belemnite (PDB) using the following equation:

$$\delta^{13}C = \{[(^{13}C/^{12}C_{sample}) - (^{13}C/^{12}C_{std})]/(^{13}C/^{12}C_{std})\} \times 1000$$

with $^{13/12}C_{std}$ = 0.0112372 (PDB)

Instrument precision is better than 0.1‰. Standard deviation of standards was 0.058 and 0.108 for Merck Gel and New Nasturtium respectively.

2.6 Carbon and oxygen isotope composition of carbonate minerals

Samples that had high calcite and dolomite contents were analysed for carbon and oxygen isotopes. The isotope analyses were performed on the carbonate minerals in the 2-38 μm size fraction, as this fraction had the highest carbonate percentages. Dolomite was analysed separately in samples that contained both dolomite and calcite. The calcite was removed from these subsamples by digesting the samples in an acetic acid and sodium acetate buffer with a pH of 5. The buffer was prepared by creating a 1M sodium acetate and 0.5M acetic acid solution (about 82 g sodium acetate and 27ml glacial acetic acid in 1L solution) (Jackson, 1969) and adjusting till pH was 5. The subsamples of approximately 0.4 grams were added to the buffer solution, shaken to ensure proper mixing of the sample and solution, and immediately centrifuged for 25 minutes. The samples were then rinsed with MQ water and centrifuged until the solution reached a neutral pH, judged by using blue litmus paper (most samples required 3 rinses). These subsamples were dried in the oven at 50°C and then transferred to an agate mortar and ground until fine with a small amount of acetone. The sample was then dried in the oven at 50°C in glass vials. A small amount of the sample was set aside for XRD analysis to determine if the calcite had been removed and if the dolomite remained in the sample. If so, the sample was analysed for C and O isotope composition of the dolomite. Samples

that contained either calcite or dolomite, but not both, were ground to a fine powder using the agate mortar and pestle with acetone and dried in the oven at 50°C.

Approximately 3 mg of carbonate were required for C and O isotope analysis. Therefore, depending on the approximate percentage of carbonate present in the sample, a sample mass for analysis was calculated, from about 7 mg of sample for the biogenic carbonates and calcretes, to about 40 mg for the sediment samples. The standard used was NM95 (calcite). The weighed out sample was then placed into a reaction vessel, which had a separate side arm into which was placed 100% phosphoric acid. The sample vessel was then degassed under vacuum. Organic matter was removed from the sample by heating the sample, while degassing, with an airgun on a high heat (~450°C) setting. The sample was then placed in a water bath to maintain a constant temperature, and reacted with 100% phosphoric acid. Calcite samples were reacted at 25°C while dolomite samples were reacted at 50°C, both for approximately 20 hours. After reaction the carbon dioxide from the samples was extracted on the carbonate line and analysed for oxygen and carbon isotopes using the Finnigan Delta Plus XP isotope ratios mass spectrometer. $\delta^{13}C$ was calculated for the carbonates after correcting for the water/calcite fractionation factor, 1.01025 for calcite at 25°C, 1.01029 for aragonite at 25°C, and 1.01065 for dolomite at 50°C. Precision for the instruments is ± 0.1‰ for both $\delta^{13}C$ and $\delta^{18}O$. Duplicates of samples were not run, but NM95 standard was run twice for every 6 samples on average. Standard deviation for standards was 0.0383 and 0.0642 for oxygen and carbon respectively.

$$\delta^{18}O = \{[(^{18}O/^{16}O_{sample}) - (^{18}O/^{16}O_{std})]/(^{18}O/^{16}O_{std})\} \times 1000$$

$\delta^{18}O$ was reported relative to SMOW (Standard Mean Ocean Water) and $\delta^{13}C$ are reported relative to PDB, both normalized against the NM95 standard. $\delta^{18}O$ may be converted to the PDB scale using the following equation:

$\delta^{18}O_{PDB} = 0.97002*\delta^{18}O_{SMOW} -29.98$

(Coplen et al., 1983)

2.7 Sr Isotope Analysis

The pan sediments containing more than 20 wt% carbonate minerals were selected for strontium isotope analysis. Calcite and dolomite were assumed to contain 300 and 450 ppm Sr (Smith et al., 2004). One sediment sample was analysed for each pan. The strontium isotope composition of carbonate rich samples was determined in the following steps performed in the isotope clean laboratory at UCT. Approximately 50 mg of finely ground sample was weighed out into centrifuge tubes with one drop of MQ water. Up to 4 ml of 5M doubly distilled (2B) acetic acid was added. The samples were then placed in an ultra-sonic bath for 20 minutes to allow the acid to fully react with the carbonate. The samples were centrifuged for 15 minutes, filtered, and placed into beakers on a hot plate set at 90°C to dry. When dry, 2 ml of concentrated HF was added, and this step was repeated. After drying, 1 ml of 2M HF was added and the sample was transferred to centrifuge tubes and centrifuged for 15 to 20 minutes. A polypropylene column containing a 200 µl Eichrome Sr spec resin bed was used for chromatographic separation of the Sr from other cations in the sample. The resin was conditioned with 2ml 2.0M 2B HNO_3 and 1ml sample (in 2.0 2B HNO_3) was loaded onto the resin bed. The column was washed with 3ml 2.0 HNO_3. The Sr was then eluted with 1ml 0.02M 2B HNO_3. The resin was then cleaned and the samples left to dry on a 90°C hotplate overnight. 1.5 ml 0.2%

2B HNO_3 was added to the dry sample. It was then diluted to the required dilution with 0.2% 2B HNO_3, which in this case was 1 part solution to 3 parts HNO_3. The samples were analysed on a Nu Instrument: Nu-Plasma HR Multi-Collector ICP-MS at the University of Cape Town. The standard used was NIST987, and the precision is ± 0.000038.

3 Results

3.1 Pan Stratigraphy

3.1.1 Sample nomenclature

Pan sediment samples are named as follows: the first two characters indicate the pan from which the sample was taken, and the third character differentiates the pit sampled in each pan (i.e., 1, 2, 3 or N for north pit, S for south pit, C for central pit) (Table 3.1). The fourth character represents the relative depth of the sample, for example, A will indicate the shallowest sample from that sample pit, B the second shallowest and so forth (Table 3.2).

Table 3.1 Pan names, abbreviations, pan type and location

Pan Name	Abbreviation	Pan type	Location of samples
Rooipan South	RS	Inland brine type	33°15'20"S, 18°19'31"E
Zwartwater North Pan	ZN	Inland brine type	33°17'30"S, 18°16'29"E
Zwartwater South Pan	ZS	Inland brine type	33°17'30"S, 18°16'50"E
Rooipan North	RN	Inland brackish-saline type	33°14'54"S, 18°19'52"E
Yzerfontein pan	YZ	Coastal	33°19'26"S, 18°10'56"E

3.1.2 Sampling Localities

3.1.2.1 Brine type inland pans

Rooipan South

Rooipan South Pan is a small, round pan approximately 350 m by 250 m. It had free standing water at the time of sampling. The surface of the pan is covered with a 5 cm thick halite crust. Sediment at the base of the dug pits consists of clean quartz sand, overlain by a mottled green/black mud. Overlying mottled green mud is a dark grey-

green mud about 10 cm thick which grades into a 15-20 cm thick surface sediment layer of black, organic rich, hydrogen sulfide-smelling mud.

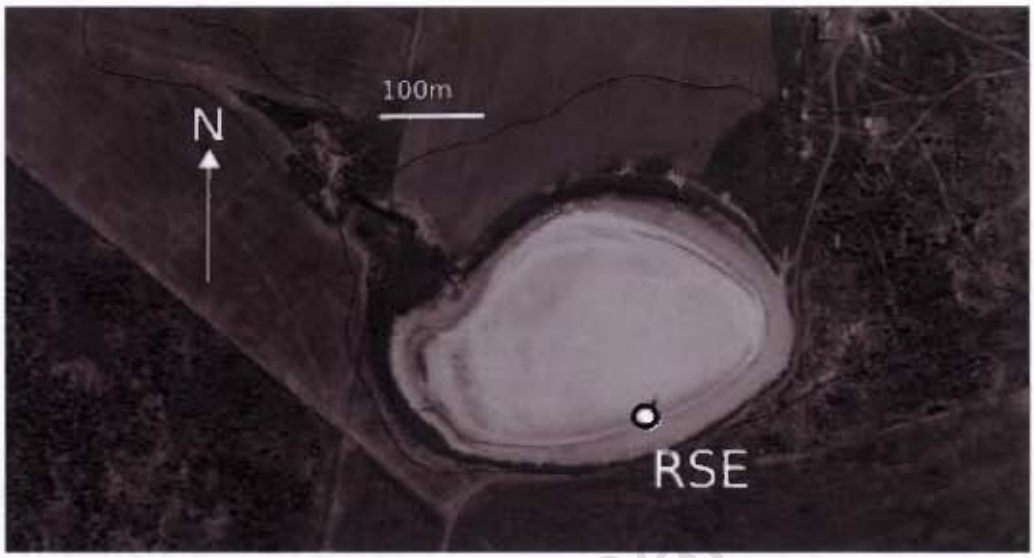

Figure 3.1. Orthophotograph of Rooipan South indicating sample pit (Trigonometric Survey).

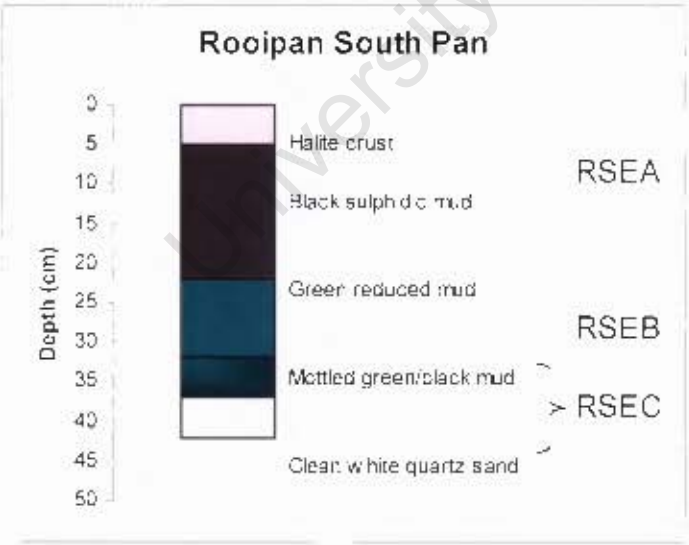

Figure 3.2. Pan stratigraphy of Rooipan South Pan, indicating sample numbers.

Zwartwater North

Zwartwater North is a relatively small, oval pan approximately 410 m long and 200 m wide. At the time of sampling, the area surrounding the pan outer margin was unvegetated and covered by surface soil. The pan had free standing water, and was covered by a 1-5 cm thick pink halite crust. The basal layer of the pan is a pale green/grey carbonate mud, containing calcite nodules up to 15 mm in length. This basal layer is overlain by a gritty orange and green mud, the orange colour suggesting the presence of iron oxides. Dark grey green mud grades upwards into a black sulphidic mud, which is overlain by a halite crust. The organic- rich black mud layer contains small orange shells of the gastropod *Tomichia ventricosa*, none of which appeared to be living.

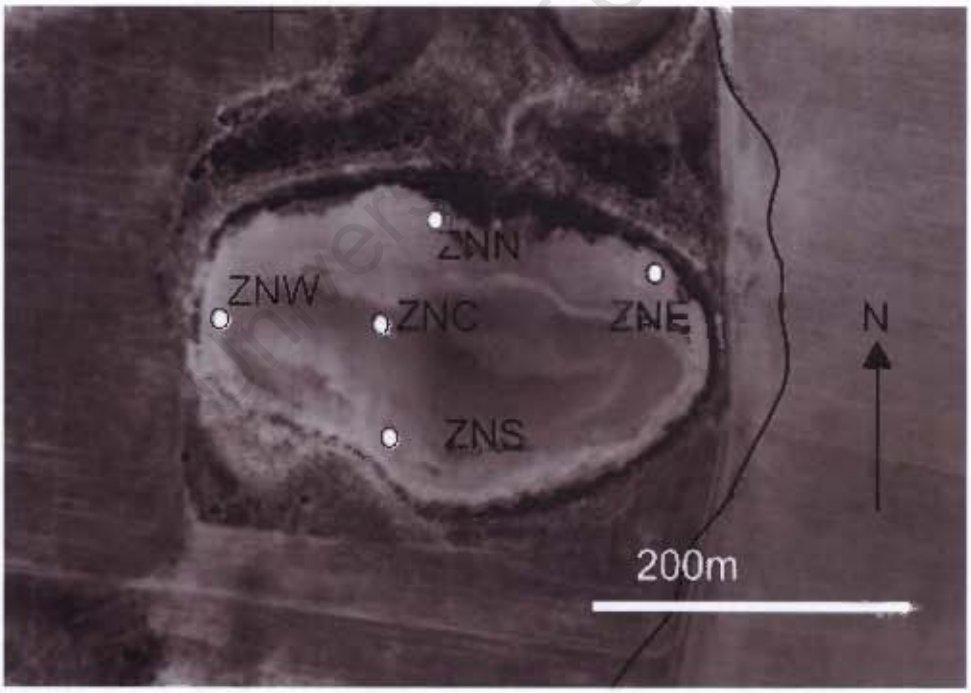

Figure 3.3. Orthophotograph of Zwartwater North Pan indicating sample pits. Note ploughed fields to west, east and south of pan.

Figure 3.4. Pink halite crust, black sulphate reducing mud, and underlying green mud of Zwartwater North Pan, East sampling pit.

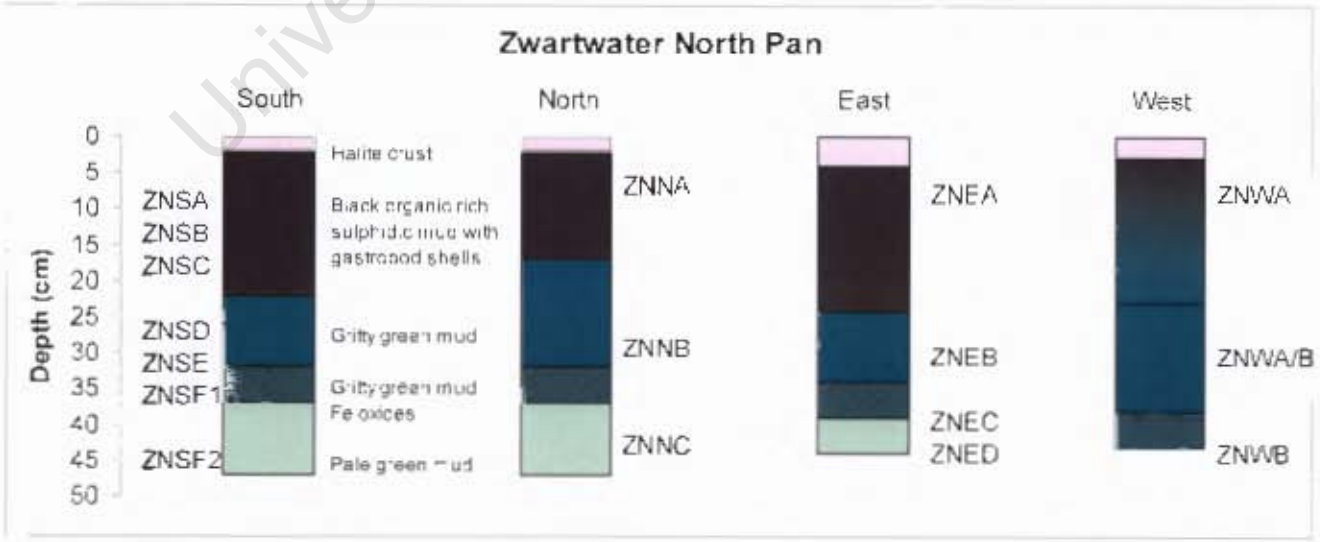

Figure 3.5. Pan stratigraphy of sample pits at Zwartwater North Pan, indicating sample numbers.

Zwartwater South

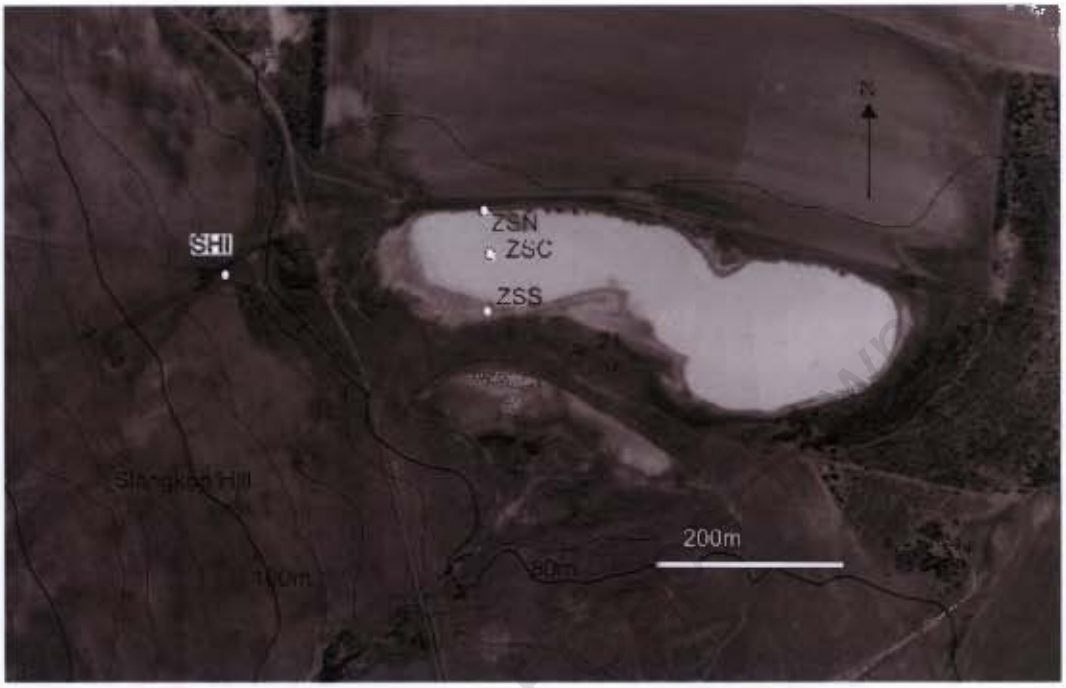

Figure 3.6. Orthophotograph of Zwartwater South Pan and Slangkop hill indicating sample pits at the pan, and sample locality of Slangkop Hill Gully.

Zwartwater South lies about one kilometer south of Zwartwater North and is more elongate in shape, approximately 700 m by 200 m. At the time of sampling the pan had free standing water, especially in the centre, where the sediments were covered by about 20 cm of water. The sediment profile is similar to the other brine type pans. The basal layer is an orange and green mud layer, which contains iron oxide nodules. Above this layer was a green-grey mud grading into black organic-rich mud, overlain by a thin layer of brown sand, and covered by a 5-7cm thick halite crust.

The pan is fed by a gully to the west of the pan, and a seep occurs on the north-western side of the pan (Figure 3.6). The southern side of the pan, which appeared much drier, had a much thinner organic rich layer, had much more distinct sedimentary layers, and contained much more sandy quartz material than the northern side of the pan (Figure 3.7). The northern side was much wetter, and the sediment layers were much less distinct. A sample was also taken of sediments on the edge of the Slangkop Hill gully which runs into Zwartwater South pan from the hill to the east of the pan. The sediments are reddish brown and cream in colour, and appear to be weathered granite, consisting of kaolinite, iron oxides and clay.

Figure 3.7. Pan stratigraphy of Zwartwater South Pan at different sample pits, showing sample numbers.

3.1.2.2 Brackish-saline Pan

Rooipan North lies just under a kilometer north-east of Rooipan South, and is similar in size, approximately 270 m by 180 m in size. At the time of field work, Rooipan North was completely dry. It lies south of a lunette dune, formed by deflation of the basin. The pan has no halite crust, and is vegetated right up to the edge of the pan, suggesting a low salinity relative to the brine-type pans. The pan sediments consist of solid calcrete, overlain by about a 15 cm thick layer of soil, consisting mainly of quartz. Samples were taken from both the centre and northern edge of the pan.

Figure 3.8. Rooipan North Pan showing sample pits RNN and RNC (Google Earth image).

Figure 3.9. View towards southwest of Rooipan North. Note dry surface, the lack of halite crust, and the vegetated pan margin

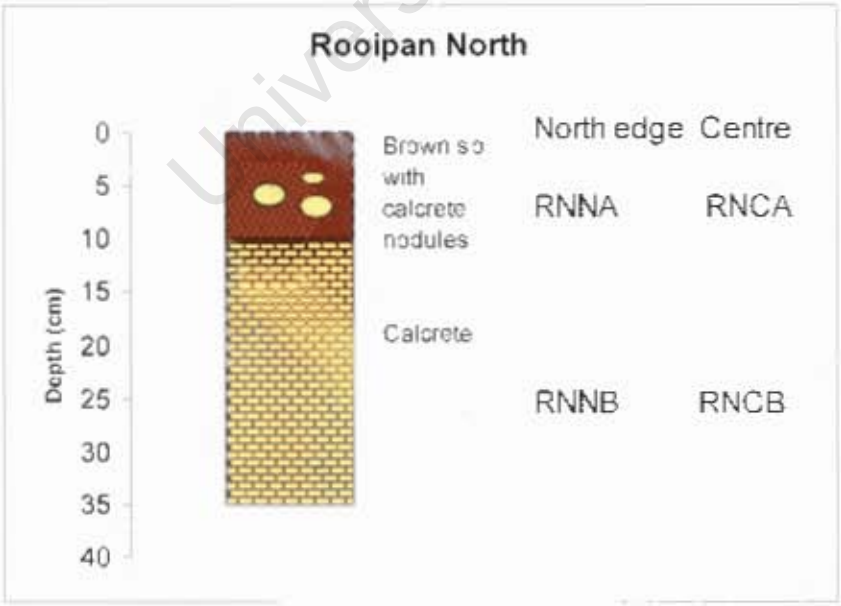

Figure 3.10. Pan stratigraphy of Rooipan North with sample names

3.1.2.3 Coastal Pan

Yzerfontein Pan

Figure. 3.11. View of Yzerfontein Pan looking north.

TheYzerfontein Pan is currently being mined for gypsum. Unlike the brine-type pans it does not have a halite crust, as the halite was mined out by early settlers. It is the only coastal pan in the study, and the largest, at almost 2 km long and 850 m wide. It much more irregular in shape than the inland pans (Figure 3.11, 3.12). The basal layer of the pan is a granular, gypsum layer, overlain by a dark green reducing coarse-grained layer. Above these layers lies a calcitic light grey mud with dark burrows (Figure 3.14). The burrows were formed by the gastropod *Tomichia ventricosa*, the shells of which are found within the overlying dark brown organic rich surface layer. Further towards the centre of the pan, the dark organic rich layer has been partially eroded away, leaving the *T. ventricosa* shells lying above the light grey burrowed mud (Figure 3.13).

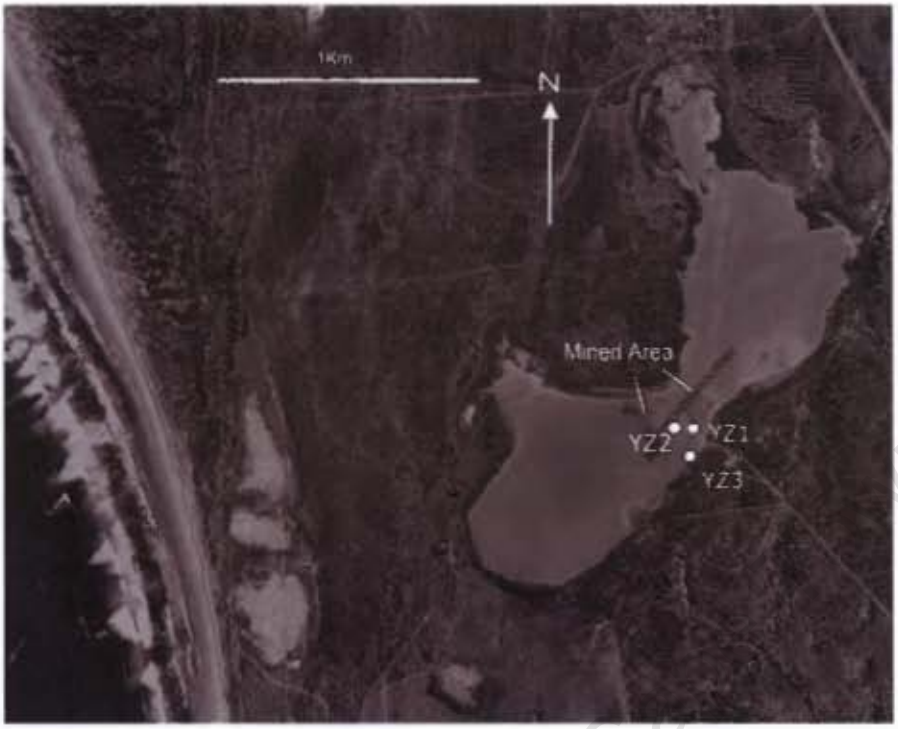

Figure 3.12. Orthophotograph of Yzerfontein pan, showing sample pits, and area mined for gypsum.

Figure 3.13. Pan stratigraphy of Yzerfontein Pan at sample sites, showing sample numbers.

Figure 3.14. Inner margin of Yzerfontein Pan, orange *Tomichia ventricosa* shells, deposited on the surface mud.

Figure 3.15. Sample YZ1A: burrowed calcitic grey mud at inner margin of Yzerfontein Pan. Sediment block ~20 cm wide

Table 3.2 Sample descriptions

Sample name	Description	Approximate Depth
Brine type pans		
Rooipan South		
RSEA	Black, sulphidic, organic rich mud	Surface-20cm
RSEB	Green mud with fine quartz sand	20-30 cm
RSEC	Clean quartz sand mottled with dark green mud	Below 30 cm
Zwartwater North		
ZNNA	Black sulphidic mud with organic matter	Surface to 15 cm
ZNNB	Dark green mud with gravelly quartz sand	15-30m
ZNNC	Very pale green mud with fine grained sand, shells, and calcrete nodules	Below 40 cm
ZNEA	Black sulphidic mud	Surface to 30cm
ZNEA T	*T.ventricosa* shells from ZNEA layer	
ZNEB	Dark green mud with quartz sand and calcrete nodules	30-35 cm
ZNEC	Gritty green mud, with calcrete nodules	35-40 cm
ZNED	Pale green, fine grained mud	Below 40 cm
ZNSA	Black, sulphidic OM rich mud	Surface -10 cm
ZNSB	Dark green mud	10-20 cm
ZNSC	Sandy green mud	20-25 cm
ZNSD	Sandy green mud	25-30 cm
ZNSE	Slightly sandy green mud	30-35 cm
ZNSF1	Green mud with red-stained quartz and feldspar grains	35-40 cm
ZNSF2	Orange -green mud	Below 40 cm
ZNWA	Black, sulphidic, organic rich mud	Surface – 15cm
ZNWA/B	Dark black/green mud	15-35cm
ZNWB	Orange-green tacky layer	Below 35 cm
ZNCA	Sulphidic, OM rich black mud	Surface – 15 cm
ZNCB	Green subsurface mud	Below 15 cm
Zwartwater South		
ZSNA	Black sulphidic OM rich sandy mud	0-5cm
ZSNB	Dark green mud	5-10 cm
ZSNC	Green mud	10-20cm
ZSND	Pale green mud	20-30
ZSNE	Green sandy/gravelly layer	Below 30 cm
ZSSA	Black sulphidic, slightly sandy OM rich mud	Surface to 10 cm
ZSSB	Brownish-grey sandy mud	10-20 cm
ZSSC	Greyish-green sandy mud	20-25 cm
ZSSD	Green sandy mud,	25-30
ZSSE	Green-orange mud with Fe-oxide nodules	Below 35 cm

Table 3.2 continued

Sample name	Description	Approximate Depth
ZSCA	Black sulphidic, OM rich mud	Surface - 10 cm
ZSCB	Black sulphidic, OM rich mud	10-20 cm
ZSCC	Dark green sandy mud,	20-30 cm
ZSCD	Sandy green mud with green stained quartz and feldspar	30-35 cm
ZSCE	Fine grained green mud	35-40 cm
ZSCF1	Orangey stained slightly sandy green mud	40-45 cm
ZSF2	Pale rusty-orange coloured mud	Below 45 cm
Brackish saline type pan		
Rooipan North		
RNNA	Surficial sandy sediments	Surface- 10 cm
RNNB	Solid calcrete from northern pit of pan	Below 10 cm
RNMB	Calcrete from centre of pan	Below 10 cm
Coastal pan		
Yzerfontein Pan		
YZ1T	*T. ventricosa* shells from Yzerfontein Pan	Surface
YZ1A	Grey burrowed mud layer with green and black reduced base	Surface -12cm
YZ1B	Coarse sandy gypsum-rich layer	Below 12 cm
YZ2	Fine dark brown mud, containing *T.ventricosa*	Surface – 10 cm
YZ3A	Dark muddy layer containing *T.ventricosa*	Surface – 10 cm
YZ3B	Grey beige mud burrowed layer	10-22 cm
YZ3C	Dark green sandy layer	22-27 cm
Slangkop Hill Gully		
SH1	Reddish clay-rich weathered sample from Slangkop hill gully	

3.2 Sediment Analysis

3.2.1 Grain size analysis

Most of the samples have the highest weight percentage of sand, moderate to small coarse silt and fine silt fraction, and a high clay (<2 μm) size fraction (Table 3.3). Most samples were classified as clayey sand or sandy clay. The sand (>63um) fractions were not analysed by XRD but were assessed visually by binocular microscope. Depending on the composition of the samples as a whole, the sand fraction contains large pieces of organic material, calcite nodules, and biogenic carbonate (*Tomichia* shells) and quartz and feldspar grains.

Table 3.3: Grain size distribution of sediment samples

Sample name	Grain size distribution (%)				Sediment Classification
	>63μm	38-63 μm	2-38μm	<2μm	
Brine type pans					
Rooipan South					
RSEA	69.37	4.38	0.96	25.29	cS
RSEB	68.59	3.87	0.98	26.56	cS
RSEC	83.14	4.53	0.67	11.66	cS
Zwartwater North					
ZNSA	76.47	4.56	17.81	1.16	zS
ZNSB	88.02	2.65	9.04	0.28	zS
ZNSC	84.32	0.51	2.19	12.98	cS
ZNSD	87.69	0.67	1.12	10.52	cS
ZNSE	36.21	1.29	0.79	61.71	sC
ZNSF1	83.48	0.78	0.60	15.13	cS
ZNSF2	35.70	1.70	4.86	57.74	sC
ZNWA	13.55	13.83	6.04	66.58	zC
ZNWA/B	20.49	4.44	1.95	73.12	sC
ZNWB	23.09	6.91	2.69	67.31	sC
ZNCA	10.19	5.81	5.05	78.95	zC
ZNCB	13.30	1.20	2.09	83.41	sC
ZNNA	74.81	1.93	1.30	21.95	cS
ZNNB	44.54	3.62	2.62	49.22	sC

Table 3.3 continued

Sample name	Grain size distribution (%)				Sediment Classification
	>63µm	38-63 µm	2-38µm	<2µm	
ZNNC	22.04	3.28	3.99	70.68	sC
ZNEA	36.52	4.83	3.46	55.18	sC
ZNEB	46.65	3.58	1.23	48.54	sC
ZNEC	46.43	4.61	1.08	47.88	sC
ZNED	11.73	5.88	1.58	80.82	sC
Zwartwater South					
ZSNA	63.81	3.41	2.07	30.71	cS
ZSNB	62.06	2.28	2.30	33.36	cS
ZSNC	54.20	2.58	5.09	38.13	cS
ZSND	46.68	3.86	6.36	43.10	cS
ZSNE	74.02	1.61	2.60	21.78	cS
ZSSA	81.54	3.60	2.09	12.78	cS
ZSSB	78.11	5.02	2.53	14.34	cS
ZSSC	81.23	1.44	0.87	16.45	cS
ZSSD	81.80	0.55	0.99	16.65	cS
ZSSE	61.55	4.05	2.29	32.12	cS
ZSMA	32.24	5.19	3.40	59.18	sC
ZSMB	6.19	2.78	3.18	87.85	sC
ZSMC	90.85	3.59	1.65	3.91	zS
ZSMD	89.61	1.00	0.92	8.46	cS
ZSME	73.66	2.73	1.16	22.45	cS
ZSMF1	78.00	1.34	1.15	19.51	cS
ZSMF2	43.61	1.84	1.41	53.14	sC
Coastal pan					
Yzerfontein Pan					
YZ1A	55.48	6.18	2.52	35.82	cS
YZ1B	81.53	5.17	3.20	10.10	cS
YZ2	23.79	13.94	1.66	60.62	sC
YZ3A	58.61	1.55	2.00	37.83	cS
YZ3B	70.56	1.33	1.19	26.92	cS
YZ3C	92.46	0.73	1.45	5.36	cS
Slangkop Hill Gully					
SHI	29.79	9.10	8.04	53.07	sC

Sediment Classification : C=clay, Z=silt, S=sand
cS= clayey sand, zS= silty sand, sC= sandy clay, zC= silty clay

3.2.2 Mineralogy (XRD)

The mineralogy of the pan sediments is summarized in Table 3.4. While calcite has the ideal formula $CaCO_3$, cation substitution is common in calcite. A calcite with more than 4 mol% Mg is a high magnesian calcite (Mg-calcite; Mg-cc) (Tucker et al., 1990).

Rooipan South contained the clay minerals illite, kaolinite and smectite, concentrated in the clay (<2um) size fraction, and quartz in the silt and sand size fractions. High-magnesian calcite was the only carbonate mineral found in the pan. It was only found in the uppermost black mud layer and not in the grey-green mud layer (sample RSEB) or sandy layer (sample RSEC) beneath it. Halite was identified, but probably resulted from drying of the porewater.

Zwartwater North contains the clay minerals kaolinite and illite, as well as carbonate minerals, such as calcite, Mg-calcite, and Ca-dolomite and dolomite, in the <2 and 2-38μm fractions, with the coarse silt and sand fractions containing mostly quartz and feldspar. XRD peaks indicate both a high magnesian calcite and low magnesian calcite, often in the same sample. Ca-rich dolomite and a more stoichiometric dolomite were also identified, but generally not together in the same sample. The nodules in the east pit (sample: ZNED cc nodule) are predominantly calcite, but also contain dolomite, quartz, and clay minerals.

Zwartwater South was similar in mineralogy to Zwartwater North. It too contains illite and kaolinite, and calcite and dolomite in the clay and fine silt fractions, and quartz and feldspar in the coarser size fractions. As for Zwartwater North, carbonate minerals

include calcite and Mg-calcite, and Ca-dolomite and more stoichiometric dolomite. Carbonate minerals are less abundant than in the Zwartwater North Pan. The northern pit on the seep-side of the Zwartwater South pan contains more carbonate minerals than the rest of the pan, while the southern pit contains the least. Only the surficial samples from the southern sample pit, ZSSA, ZSSB and ZSSC, representing black reducing surface mud, contain the carbonate minerals Mg-calcite, dolomite and calcite. The green colour of some of the brine-type pan sediments can probably be attributed to glauconite. Glauconite has been included under "illite" in the results table due to their similarity and difficulty in distinguishing the two minerals by XRD.

3.2.2.1 Brackish saline inland pans

Calcrete from the Rooipan North pan is predominantly calcite with minor amounts of quartz, illite/mica and kaolinite. The upper soil layer was dominated by quartz, with calcite nodules. It did not contain dolomite.

3.2.2.2 Coastal Pan

Yzerfontein was the only pan to contain significant amounts of gypsum, which is currently being mined for application to potato fields. Samples from the inner margin of the pan (pit YZ1), close to the mined area, contain primarily low-magnesian calcite and gypsum, with the larger size fractions containing comparatively more gypsum. Samples from the outer edge of the pan (pit YZ3) only contain small amounts of gypsum, and contain mostly calcite, and minor amounts of quartz, and the clay minerals kaolinite, illite and smectite. None of the Yzerfontein samples contained dolomite. *Tomichia ventricosa* shells (YZ1-T) are composed of aragonite.

Table 3.4. Mineralogy of pan sediments obtained by X-Ray Diffractometry (patterns presented in Appendix) ordered in relative decreasing abundance. Results shown for each separate size fractions: 38-63 μm coarse silt fraction, 2-38 μm fine silt fraction and <2 μm clay fraction. Qtz=quartz, K-fsp = K-feldspar, kao= kaolinite, cc = calcite, Mg-cc=magnesian calcite, dol=dolomite, ill=illite, hal=halite, gyps = gypsum, goe=goethite, smec=smectite, ?=unidentified peak.

	XRD Mineralogy		
Sample name	**38-63μm coarse silt fraction**	**2-38μm fine silt fraction**	**<2μm clay fraction**
Brine type pans			
Rooipan South			
RSEA	qtz, Mg-cc,k-fsp	qtz, Mg-cc, hal,k-fsp,plag	qtz, Mg-cc, plag ,kao, ill
RSEB	qtz, kao, smec	qtz, smec, kao	smec, kao, qtz, ill, Mg-cc
RSEC	qtz, smec	qtz, kao, clay? smec, ill	qtz,smec,clay?kao,ill
Zwartwater North			
ZNNA	qtz, cc, Mg-cc, Ca-dol, kao	qtz, kao, ill,cc, Ca-dol, Mg-cc	qtz, kao, Ca-dol, cc, Mg-cc, ill
ZNNB	qtz, cc, hal, k-fsp	qtz, cc, Ca-dol, kao	qtz, kao, cc, Ca-dol, ill,hal
ZNNC	qtz, dol, hal, qtz, k-fsp, cc	hal, dol, qtz, kao, k-fsp, cc	Hal, dol, qtz, kao, cc
ZNEA	qtz, cc, kao, Mg-cc, dol ,K-fsp, plag	qtz, kao, cc, Mg-cc, dol, ill, k-fsp	qtz, kao, ill, cc, Mg-cc, dol
ZNEB	qtz, cc, dol, k-fsp, kao	kao, cc, qtz, dol, k-fsp, kao	cc,qtz, dol, kao, mica, hal
ZNEC	qtz,cc,dol,kao,k-fsp	cc,qtz,dol,kao,ill	cc, qtz, dol, hal, kao,I ll
ZNED	qtz,cc,dol,k-fsp	cc, dol, qtz,kao, ill	cc, dol, qtz, kao
ZNED cc nodule	Cc, qtz, dol		
ZNSA	qtz ,cc, kao, k-fsp	qtz, Mg-cc, cc, hal, Ca-dol, kao	
ZNSB	qtz, cc, Mg-cc,kao, dol, clay?	kao, qtz, Mg-cc, cc, dol, hal, ill, clay?	
ZNSC	qtz,k-fsp, kao	kao, ill, qtz, hal,	kao, ill, qtz
ZNSD	qtz,k-fsp,plag	qtz, kao, ill, k-fsp	kao, qtz, ill
ZNSE	qtz,plag	qtz, kao, ill, hal,	qtz,kao, ill
ZNSF1	qtz , k-fsp, plag	Ill , kao,qtz	Ill , kao
ZNSF2	qtz, k-fsp	qtz, ill, kao	kao ,ill, qtz , hal
ZNWA	qtz, k-fsp, Mg-cc,	qtz,hal, kao,cc, Mgcc	kao, qtz, ill, hal, cc, Ca-dol, dol
ZNWA/B	qtz, cc, kao, Ca-dol	qtz,kao, hal, dol, cc, ill	kao, qtz hal, dol, Mg-cc, cc, ill
ZNWB	kao, qtz	kao,qtz	kao,hal, qtz, ill
ZNCA	qtz, Mg-cc, cc, kao, dol	hal,qtz,mg-cc,cc,kao	qtz,Mg-cc, kao, ill, dol, cc
ZNCB	qtz, dol, cc	Ca-dol, qtz, kao, cc	dol, kao, qtz, ill, cc

Table 3.4. Continued

Sample name	XRD Mineralogy 38-63µm coarse silt fraction	2-38µm fine silt fraction	<2µm clay fraction
Zwartwater South			
ZSNA	qtz, cc, kao, k-fsp, plag	qtz, kao, Mg-cc, dol, ill, k-fsp, plag	kao, qtz, Mg-cc, dol, ill, plag, k-fsp
ZSNB	qtz, Mg-cc, kao, ill, plag, k-fsp, dol	qtz,dol,Mg-cc,kao,mica	Kao, Mg-cc, dol, ill, qtz
ZSNC	qtz, cc, Mg-cc, dol, k-fsp, ill, kao, plag	qtz,dol,Mg-cc,cc,kao,ill	Kao, Mg-cc, dol, cc, ill, qtz
ZSND	qtz, cc, Mg-cc, hal, dol, k-fsp	qtz,dol,Mg-cc,cc,kao,ill	dol, qtz, Mg-cc, cc, ill, kao
ZSNE	qtz, k-fsp, Mg-cc, plag, ill, dol	qtz, dol, kao, ill, k-fsp, Mg-cc	dol, kao, qtz, ill, Mg-cc
ZSSA	qtz,Mg-cc, cc, k-fsp, kao, ill	qtz, hal, Mg-cc, kao, cc, k-fsp, ill, dol	kao, qtz, k-fsp, ill, Mg-cc, cc, dol
ZSSB	qtz, Mg-cc, k-fsp, plag	qtz, hal, k-fsp, Mg-cc, kao, plag, ill	kao, qtz, illite, Mg-cc
ZSSC	qtz, k-fsp, Mg-cc, ill, kao	qtz, k-fsp, kao, ill, Mg-cc	kao, ill, qtz,
ZSSD	qtz, kao, ill, k-fsp	qtz, kao, ill, k-fsp	kao, ill, clay?
ZSSE	qtz, kao, ill, smec	kao, qtz, ill, smec, k-fsp	kao, ill, smec, qtz
ZSMA	qtz, cc, k-fsp, dol, ill,?	qtz, cc, kao, dol, k-fsp,?	kao, qtz, cc. ill
ZSMB	qtz, k-fsp, dol, cc,??, ill	qtz, hal, dol, kao, ill	qtz, hal, Ca-dol, cc, kao, ill
ZSMC	qtz, dol, k-fsp, plag, cc, kao, ill	qtz, Ca-dol, kao, ill, cc	kao, ill, qtz, cc
ZSMD	qtz, kao, ill, k-fsp	qtz, plag, kfsp, kao, ill	kao, ill,
ZSME	qtz, plag, kao, ill	qtz,kao,ill	qtz, kao, ill
ZSMF1	qtz, kao, ill, k-fsp, plag	qtz, kao, ill, k-fsp, plag	kao, ill, qtz
ZSMF2	qtz, k-fsp, plag	qtz, kao, Ca-dol, ill	kao, ill, Ca-dol
Brackish saline type pan			
Rooipan North			
RNMB	BULK		cc,qtz, clay?
RNNA			
RNNB	BULK		cc, qtz, clay?
Coastal pan			
Yzerfontein Pan			
YZ1A	gyps, cc,qtz	gyps, cc, qtz	cc, gyps
YZ1B	gyps, cc, qtz,	gyps, cc, qtz?	cc, gyps
YZ2	gyps, cc, qtz, kao, ill	gyps, cc, qtz, kao, ill	cc, gyps, kao, ill
YZ3A	qtz, cc, k-fsp	cc, gyps, qtz, kao, ill, k-fsp	cc, gyps, kao, qtz, ill
YZ3B	cc, qtz, k-fsp	cc, qtz,	cc, kao, k-fsp, qtz, smec?
YZ3C	qtz, cc, fsp?	qtz, cc, kfsp?	cc, smec, mica, kao
YZ1-T	Aragonite		
Slangkop Hill Gully			
SHI	qtz, kao, goe	kao, qtz, goe, ill	kao, qtz, goe, ill

3.2.3 Sediment texture (SEM)

SEM images show the presence of organic matter in Zwartwater North and South pans, as well as fine fragments of biogenic carbonate (shell). Calcite and dolomite had a knobby and anhedral texture, especially Zwartwater North and South pans relative to the coastal Yzerfontein pan. The Yzerfontein pan displayed euhedral platey gypsum crystals and rhombohedral calcite crystals (see Discussion section for images).

3.2.4 Organic Carbon and $\delta^{13}C$

The OC content ranges from 0.85 to 3.90 wt%. The OC content decreases down profile in the pit on the western edge of the Zwartwater North pan. The $\delta^{13}C$ value of the organic matter ranges from -19.1‰ at Rooipan South to -24.1‰ at Zwartwater North. Approximate carbonate mineral (calcite + dolomite) percentage, calculated by mass difference of sample after acid digestion, ranged from 2 to 53%.

Table 3.5. Organic carbon (OC) content and carbon isotope composition of bulk pan sediment samples.

Sample no.	OC (wt%)	δ13C (‰) of OC	Approx. wt% calcite+dolomite
RSEA	2.26	-19.13	20
ZNNA	2.61	-21.52	34
ZNCA	3.9	-21.73	53
ZNEA	3.05	-22.72	34
ZNSA	0.85	-21.70	5
ZNWA	2.74	-24.07	16
ZNWA/B	1.56	-21.37	20
ZNWB	0.637	-22.56	2
ZSSA	1.81	-20.72	12
ZSCA	2.01	-21.05	27
YZ2	2.30	-20.38	44

3.2.5 Stable and Radiogenic Isotopes

The $\delta^{13}C_{PDB}$ values range from -8.85 to -1.54‰ and $\delta^{18}O_{PDB}$ range from -2.41 to 5.56‰. $^{87}Sr/^{86}Sr$ values range from 0.710313 at Rooipan North to 0.711591 at Zwartwater South Pan (Table 3.6).

Table 3.6. Carbon, oxygen and strontium isotope analyses of pan calcite and dolomite.

Sample	$\delta^{13}C$ (‰) $_{PDB}$	$\delta^{18}O$ (‰) $_{PDB}$	$\delta^{18}O$ (‰) $_{SMOW}$	$^{87}Sr/^{86}Sr$
RSEA	-1.54	3.15	34.11	0.710797
ZNNA calcite	-4.93	4.27	35.26	
ZNNA dolomite	-6.22	4.22	35.21	
ZNNC calcite	-6.21	4.88	35.90	
ZNNC calcite+ dolomite				0.711253
ZNEA –T (aragonite)	-6.32	5.27	36.29	
ZNED calcite	-7.68	-0.01	30.86	
ZNED dolomite	-6.31	4.01	35.00	
ZNED calcite nodule	-8.85	-2.41	28.37	
ZNWA/B calcite	-4.53	5.09	36.11	
ZNWA/B dolomite	-5.78	3.07	34.03	
ZNMB dolomite	-6.01	5.07	36.09	
ZSND calcite	-5.54	3.66	34.64	
ZSND dolomite	-6.31	5.56	36.60	
ZSND calcite+ dolomite				0.711591
ZSNE dolomite	-7.02	4.39	35.39	
ZSSB calcite	-4.13	2.40	33.34	
ZSMB dolomite	-7.03	4.30	35.30	
ZSMF2 dolomite	-7.50	2.57	33.52	
RNNB	-6.12	3.45	34.43	0.710313
YZ 1-T (aragonite)	-4.20	4.60	35.61	
YZ1A	-2.23	0.72	31.61	
Y23A	-1.87	0.93	31.83	0.710997

4 Discussion

4.1 Origin of carbonate minerals

In this study the origin of the carbonate minerals in the Yzerfontein and Darling Pans was determined from their oxygen, carbon and strontium isotope compositions as well as their sedimentology and mineral textures.

4.1.1 Oxygen isotope evidence for the extent of evaporation during carbonate mineral precipitation

The $\delta^{18}O$ value of carbonate minerals in arid regions is often most indicative of the amount of evaporation the precipitating solution has undergone. It will, however, also be influenced by the temperature and the $\delta^{18}O$ composition of the source waters (rainwater and groundwater) before they underwent evaporation. ^{18}O is enriched in water that has undergone evaporation which preferentially removes ^{16}O. A $\delta^{18}O_{PDB}$ value for carbonate minerals that is close to zero for marine sediment, or close to the $\delta^{18}O$ of the groundwater (after correcting for the calcite-water fractionation factor) of terrestrial systems, suggests that it precipitated from a solution in which little evaporation has occurred. Carbonate precipitated from a evaporated solution will have a higher than expected $\delta^{18}O_{PDB}$ value. Rainwater collected at the University of Cape Town (80 km south of the study area) had $\delta^{18}O_{SMOW}$ values between -8.1‰ and -0.4‰, and a weighted mean of -3.74‰ over the two year period of 1996 and 1997 (Diamond and Harris, 1997). Groundwater in the Atlantis region (approximately 25 km south of Darling) had a $\delta^{18}O_{SMOW}$ value of -3.6‰ in 1997 (Harris et al., 1999).

Almost all of the Darling and Yzerfontein pan carbonates display high $\delta^{18}O$ values. The water-calcite fractionation factor will decrease at higher temperatures, between 2 and 3 ‰ for every 10°C between 0 and 30°C. The values are at least 3 to 13 ‰ higher than would be expected with respect to the rain and groundwaters, indicating that they precipitated from highly evaporated rain and ground waters (Figure 4.1). The exception is the disseminated calcite (Sample ZNED) and calcite nodules (Sample ZNED cc nod) in the basal layer of Zwartwater North pan, which have the most lowest $\delta^{18}O_{PDB}$ values of -2.41 and -0.01, respectively. The dolomite from the same sediment layer (Sample ZNED) has a $\delta^{18}O_{PDB}$ value of 4.01. The difference in oxygen isotope composition indicates that the dolomite may have precipitated from more evaporative waters than the calcite nodule and disseminated calcite, precipitated from less evaporated water during an earlier stage of pan development. For most samples containing calcite and dolomite, the dolomite $\delta^{18}O_{PDB}$ values are higher than the calcite, indicating that dolomite precipitated from more evaporated water than the calcite. This may also be as a result of the dolomite-water-calcite fractionation factor, which would result in dolomite $\delta^{18}O$ values 3 - 4 ‰ higher than the calcite values (Vasconcelos et al., 2005).

Biogenic carbonate tends to have similar or higher $\delta^{18}O$ values (4.60‰ and 5.27‰ for biogenic aragonite at Yzerfontein and Zwartwater Pans respectively) compared to the precipitated carbonate minerals from their respective pans. The higher $\delta^{18}O$ values of the *T. ventricosa* shells indicate that the organisms lived during the early stages of pan development when evaporation rates were high, but salinities of pan waters were still low enough (<130‰) to allow these gastropods to survive (Brown, 1994).

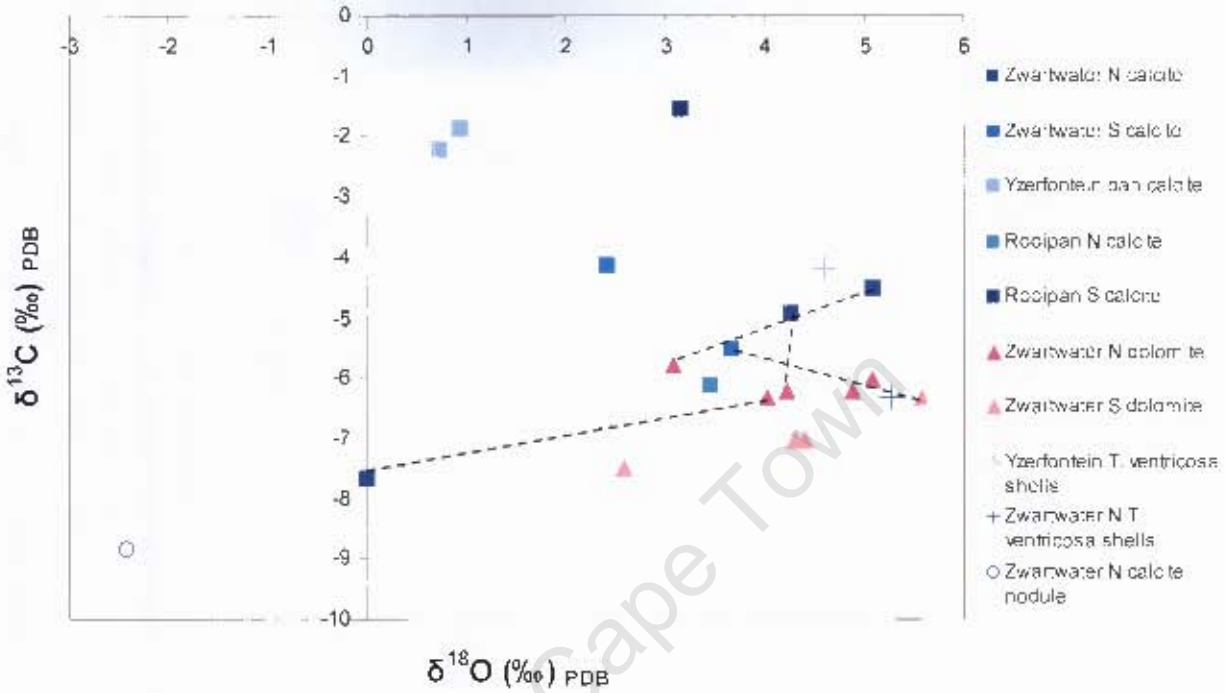

Figure 4.1. Plot of $\delta^{13}C$ versus $\delta^{18}O$ isotope values for the disseminated pan dolomite, calcite, calcite nodule, and biogenic carbonate. Dotted lines join calcite and dolomite from the same sample.

4.1.2 Source of carbonate ions

4.1.2.1 Carbon isotopes of carbonate minerals

The source of the carbonate ions in precipitated carbonate minerals, whether originating from seawater, organic material or bedrock, can be inferred from their $\delta^{13}C$ values. A $\delta^{13}C_{PDB}$ value that is close to zero or slightly positive (Mazzullo, 2000; Wacey et al., 2007) suggests that the mineral precipitated from porewater unaltered by the degradation of organic matter. An either strongly positive or negative value may indicate bacterial degradation of organic carbon, altering the carbon isotopic signature of the precipitating

solution. Organic carbon has variable, but generally low $\delta^{13}C$ values. Sulphate reduction and methanogenesis are two common microbial processes that utilize organic carbon and can alter the carbon isotope composition of dissolved carbonate ions. The rapid increase in carbonate alkalinity associated with organic matter degradation may also increase the degree of supersaturation with respect to dolomite, and overcome kinetic barriers to the precipitation of dolomite (Compton, 1988). During methanogenesis, the production of methane, carbon isotope fractionation takes place between CO_2 and CH_4, with ^{12}C enrichment in the CH_4, and ^{13}C enrichment in the remaining CO_2. (Mazzulo, 2000). Carbonate minerals that precipitate in methane rich environments will have positive $\delta^{13}C$ values. Sulphate reduction oxidizes organic matter, resulting in a precipitation of carbonate minerals with a negative $\delta^{13}C$. If microbial degradation of organic carbon is the predominant source of carbonate ion, then the $\delta^{13}C_{PDB}$ values may be as low as -20‰ (Vasconcelos and McKenzie, 1997).

The $\delta^{13}C$ values of the carbonate minerals from the Darling and Yzerfontein pans are negative, between -1.54 to -8.85 (Figure 4.1, 4.2). Soils outside the pan in the region are not particularly high in organic matter and are unlikely to influence the $\delta^{13}C$ value of surface or throughflow waters draining into the pan sediments. The relatively light carbon isotope composition indicates that the source of the carbonate ion in the carbonate minerals must be, at least partly, organic matter buried and microbially degraded in the pan sediments. The carbonate is likely made available through degradation of organic matter by sulphate reducing bacteria (Porter, 2007). Similar $\delta^{13}C$ values are found for other carbonate minerals associated with sulphate reduction, such as Lagoa Brazil

Lagoon (Vasconcelos and McKenzie, 1997), East Salina in the British West Indies (Perkins et al., 1994), and the sulphate reducing zone within the Monterey Formation in California (Burns and Baker, 1987) (Figure 4.2). The $\delta^{13}C$ values are too low for the carbonate minerals to be associated with methanogenesis, such as the methanogenesis zone within the Monterey Formation, California (Burns and Baker, 1987) (Figure 4.2) or the Gulf of California (Kelts and McKenzie, 1982). The $\delta^{13}C$ values of the pan carbonates are also too low for precipitation of carbonates from unaltered seawater. These would have $\delta^{13}C$ values of ~ 0‰, as do the Tertiary Romanche Fracture Zone pelagic limestones (Bernoulli et al., 2004) and Pleistocene dolomite from the Namibian shelf (Compton et al., 2001). The $\delta^{13}C$ values are not low enough for the source of the carbonate to be pure organic matter (i.e. ~-20‰). This suggests that the source of the carbonate is a mixture of organic carbon and carbonate derived from chemical (carbonic acid) weathering of silicate bedrock (i.e. Cape Granite).

In the paired dolomite and calcite samples, the dolomite usually has a more negative $\delta^{13}C$ value than the calcite (Figure 4.1). This suggests that the dolomite requires, or tends to form in, a more sulphate reducing environment than the calcite. Zwartwater North and South pans show a decrease in $\delta^{13}C$ value with depth, indicating higher amounts of contribution of carbonate from organic matter at depth. While the black organic-rich layer is at the surface of the pan at present, the carbonate minerals in these deeper layers may have formed in the sulphate reduction zone before burial. At deeper burial levels in the pan sulphate reduction would have slowed down or ceased. Porter (2007) found that at the Darling pans, sulphate reduction rates were greatest close to the sediment surface.

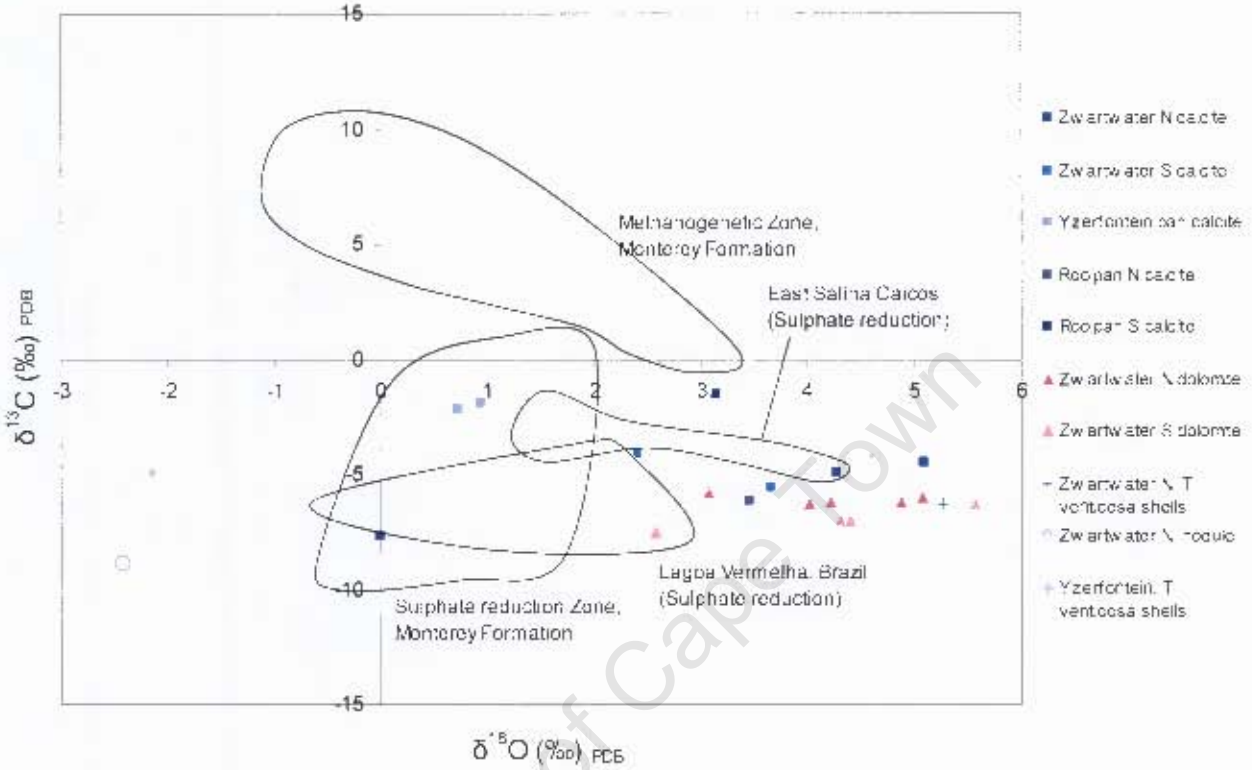

Figure 4.2. Plot of $\delta^{13}C$ versus $\delta^{18}O$ values for carbonate minerals in the pans compared to carbonate minerals from other studies precipitated in sulphate reduction and methanogenesis zones, such as East Salina Caicos (Perkins et al., 1994), Monterey Formation (Burns and Baker, 1987) and Lagoa Vermelha (Vasconcelos and McKenzie, 1997)

Yzerfontein Pan however, has higher $\delta^{13}C$ values than the other pans, suggesting that the calcite had not been as greatly influenced by bacterial degradation of organic carbon, but had precipitated from close-to-unmodified seawater/groundwater. The $\delta^{13}C$ value increases with sediment depth in the Yzerfontein pan. It appears that any contribution from organic carbon is restricted to the near surface, from the organic brown surface layer

(YZ2, Y3A), and that the carbonate from the pale calcitic mud (YZ1A) had little of its carbonate sourced from organic carbon.

Organic Carbon

The $\delta^{13}C$ values of the bulk organic carbon from the pan sediments range from -19.1‰ to -24.1‰ (Figure 4.3) and reflect the photosynthesis reaction which is accompanied by carbon isotope fractionation. Plants preferentially use lighter carbon isotopes during photosynthesis, resulting in their low $\delta^{13}C$ values. The $\delta^{13}C$ values indicate that the organic matter is mostly algal; however the more negative $\delta^{13}C$ values indicate a mixture of algal matter and C3 plants, such as Zwartwater North and South (Smith and Epstein, 1971). C3 plants discriminate against ^{13}C more than C4 plants, and therefore have lower $\delta^{13}C$ values. The C3 plant contribution could be indigenous vegetation, alien vegetation (*Acacia cyclops*) and the wheat that is farmed in the area. There is no indication of a contribution of C4 grasses, which would have $\delta^{13}C$ values of ~12‰.

The positive correlation between the abundance of organic carbon and carbonate minerals in the samples (Figure 4.4) suggests that microbial degradation of organic carbon is important in carbonate precipitation. Sample YZ2 from the dark brown surface mud at Yzerfontein displays a higher than expected carbonate mineral (i.e calcite + dolomite) content relative to its organic carbon content (Figure 4.4), which suggests that most of the carbonate ions were not from an organic carbon source, consistent with the less negative $\delta^{13}C$ of the calcite in this sample.

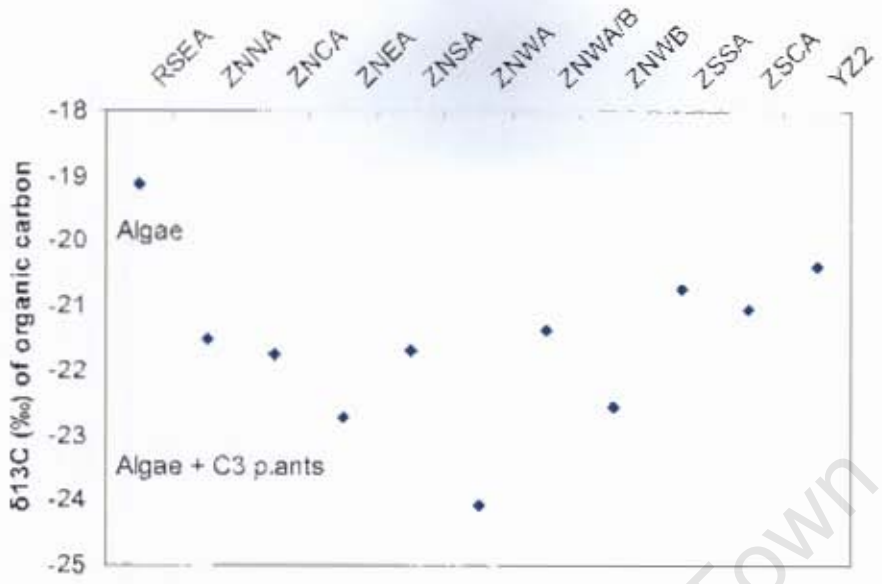

Figure 4.3. Plot showing the distribution of $\delta^{13}C$ values of the bulk organic carbon in pan sediment samples. The organic carbon in the pan sediment is interpreted to be a mixture of algal (-19 to -21‰) and woody C3 plants (-25 to -27‰).

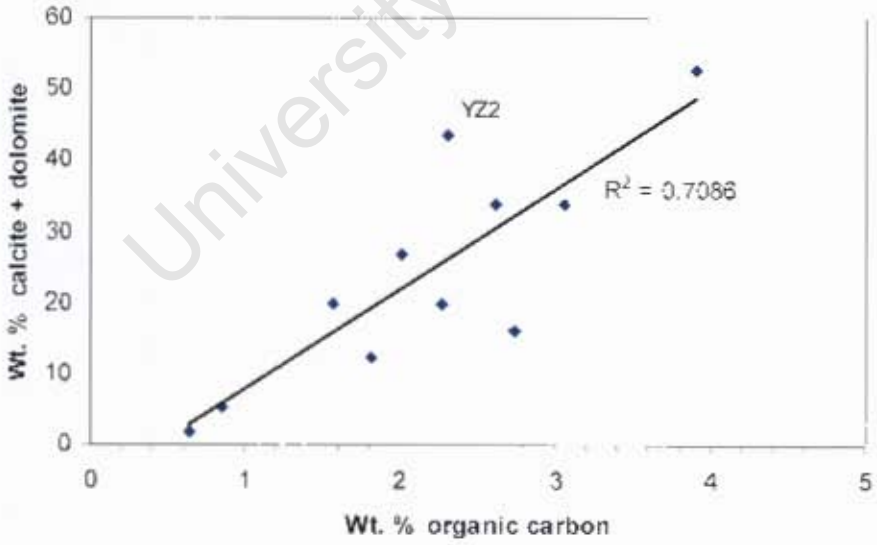

Figure 4.4. The weight percent of organic carbon versus weight percent calcite + dolomite of samples, mostly from black surface mud layers, shows a positive correlation (R^2 = 0.71). YZ2 sample is from the Yzerfontein coastal pan.

Sulphate reducing bacteria (SRB)

Dissimilatory sulphate reduction and methanogenesis are the most common means of organic matter degradation in anaerobic environments. Sulphate reduction, however, is usually dominant in sulphate rich environments, such as marine environments or marine derived brines (Fauque, 1999). Sulphate reduction is used by sulphate reducing bacteria as a means of respiration. Sulphate reducing bacteria (SRB) use SO_4^{2-} as a terminal electron acceptor to oxidise organic matter and produce carbonate ions as a waste product (Mazzulo, 2000):

$2CH_2O$ (organic matter) + $SO_4^{2-} \rightarrow 2HCO_3^- + H_2S$

The presence of sulphate reducing bacteria in the Darling pans, and specifically in the brine type pans, was confirmed in this study by the organic-rich, black, sulphidic smelling mud found in their surficial sediments. Since sulphate reduction is comparatively lower in energy yield than oxygen respiration and oxygen is toxic to the SR bacteria, sulphate reduction occurs mostly in anoxic or partially anoxic environments. Sediment in saline environments, salt marsh, saltpan or marine environments easily becomes anoxic and prone to sulphate respiration. This is a result of the solubility of oxygen decreasing in saline waters. Porter (2007) reported that sulphate reduction takes place in the Darling pans at rates ranging from 27 to 3685 nmol cm^{-3} day^{-1}, which are extremely high and comparable to the Great Salt Lake (USA), as well as highly productive saltmarsh and benthic microbial mat environments (Porter et al., 2007). Brine-type pans Zwartwater South, Zwartwater North, and Rooipan South respectively had the highest sulphate reduction rates of all the pans. Porter (2007) found that the high salt contents of the pans did not hinder the bacteria, but rather that higher salinities resulted in

a short term rise in the sulphate reduction rate, possibly a shock response as the organisms become stressed. However at salinities above 272 to 311%, bacterial cells become de-energised, and rates begin to drop. The concentration of sulphate ions in the pan brine waters is generally high (Table 4.1) and it is the availability of organic matter rather than sulphate ions that appears to limit sulphate reduction.

Table 4.1. Major ion chemistry of pan water samples (concentrations in mmol/kg) from Smith, 2000, Table 4.2) and molar Mg/Ca ratio

Pan	Mg^{2+}	Ca^{2+}	Alkalinity	SO_4^{2-}	Molar Mg/Ca
Seawater (Faure, 1992)	52	10	2.3	27	5.2
Rooipan South	141	10.2	0.62	350	13.82
Zwartwater North	166	13	1.45	373	12.77
Zwartwater South	186	10.2	2.1	275	18.24
Rooipan North	0.3	0.1	5.06	1	3.00
Yzerfontein pan	160	37	0.97	186	4.32

By producing carbonate ions, and increasing carbonate alkalinity, the sulphate reducing bacteria provide an environment highly favourable to carbonate mineral precipitation, especially dolomite. Sulphate reducing bacteria have been associated with the precipitation of dolomite in evaporite and marine environments (Vasconcelos and McKenzie, 1997). The bacteria are thought to be able to mediate kinetic obstacles that hinder low-temperature dolomite precipitation (Warthmann et al., 2005). SRB have been found in dolomite precipitation environments (Vasconcelos and McKenzie, 1997) and have been used to mediate dolomite precipitation in the laboratory under low temperature (i.e. under 80°C) conditions (Warthmann et al., 2005). The bicarbonate ions that are

produced by the sulphate reducing bacteria may react with Mg^{2+} and Ca^{2+} ions to produce dolomite, shown by the following equation:

$2HCO_3^- + Mg^{2+} + Ca^{2+} \leftrightarrow CaMg(CO_3)_2 + 2H^+$

SRB also enhance dolomite precipitation by reducing sulphate ions which may inhibit dolomite nucleation and precipitation (Baker and Kastner, 1981). Sulphate ions form an ionic pair with Mg^{2+}, making Mg^{2+} unavailable for dolomite precipitation. The SRB also secrete excess Mg^{2+} that they use for physiological functions, and together with the carbonate ions that they produce, a surrounding micro-environment favourable to dolomite precipitation is created (Vasconcelos and McKenzie, 1997).

Aside from mediating dolomite precipitation, sulphate reducing bacteria are involved in many other chemical reactions, such as the methylation of mercury, and the precipitation of heavy metal sulphides (Barton and Tomei, 1995). The sulphide may react with iron-rich sediments or metal ions in solution to form monosulphides, pyrite and other metal sulphides. The hydrogen sulphide smell of the Darling saltpans indicate that monosulphides have been precipitated in the black surficial layer of the pans, but this was not confirmed by XRD. Either the percentage of monosulphides is too low or they are too amorphous to be identified by XRD.

SRB are thought to be one of the oldest and most enduring life forms, emerging in the Early Archaean. Some of the earliest evidence of SRB is variations in $\delta^{34}S$ values in 3.4 billion year old pyrite from Barberton, South Africa (Ohmoto et al., 1993). In this case the $\delta^{34}S$ signature is characteristic of low temperature fractionation, indicating biological

sulphate reduction. It is likely that the SRB were dominant in the oceans of the Precambrian, during which lower-than-modern oxygen levels in the atmosphere existed and predators, such as metazoa, had not evolved yet (Wacey et al., 2007). If SRB were indeed dominant in the past, oceans would have been more conducive to dolomite precipitation than at present, and this process could at least partially explain the great dolomite platforms in the rock record.

4.1.2.2 Carbonate mineral textures

SEM allows observation of sediment textures on micro and nano- meter scales. Such fine textures are useful to determine growth morphology of precipitated minerals, such as carbonates minerals. It is also useful to determine sites of nucleation of these precipitates, and other factors involved in their precipitation, such as organic matter. SEM images reveal that the carbonate minerals of the inland Darling pans are anhedral in shape, lacking the characteristic euhedral rhombohedral crystal habit of calcite and dolomite (Figure 4.5, 4.6). The calcite and dolomite appear knobby in shape, without any recognizable crystal faces. Sample ZNED, from Zwartwater North, displays dolomite in what is possibly the inter-locking dumbbell shape (Figure 4.6 B) characteristic of microbial influence of sulphate reducers on dolomite (Vasconcelos and McKenzie, 1997). The knobby shape, and more specifically, the interlocking dumbbell shape, may be caused by dolomite nucleation around the sulphate bacteria themselves (Vasconcelos and McKenzie, 1997). The bacteria excrete both carbonate and Mg^{2+} ions, creating a micro-environment conducive to dolomite precipitation in their immediate surroundings. The bacterial "bodies" then act as nuclei for dolomite precipitation and become covered by nanocrystals of dolomite. The bacterial cells finally become enclosed by the dolomite

crystals (Vasconcelos and McKenzie, 1997) which precipitate as knobby and subspherical structures. The calcite and dolomite crystals also develop on the surface of sedimentary particles, such as quartz grains, and organic material (Figure 4.5). After the dolomite has nucleated, it may begin to precipitate more euhedral crystal faces, over the original knobby shaped dolomite. Therefore the knobby shape of the dolomite in Zwartwater North indicates that the dolomite has not "aged" yet, to form a more euhedral and stoichiometric dolomite.

The calcite found in Yzerfontein coastal pan had smooth crystal faces, unlike the knobby textured carbonate minerals found in the inland pans (Figure 4.6A). As mentioned previously, the Yzerfontein pan calcite is not mediated by the SRB to the same extent as are the carbonate minerals of inland pans. The Yzerfontein calcite appears to be precipitated by inorganic means from porewater unaltered by SRB, resulting in the smoother, less knobby texture of the calcite.

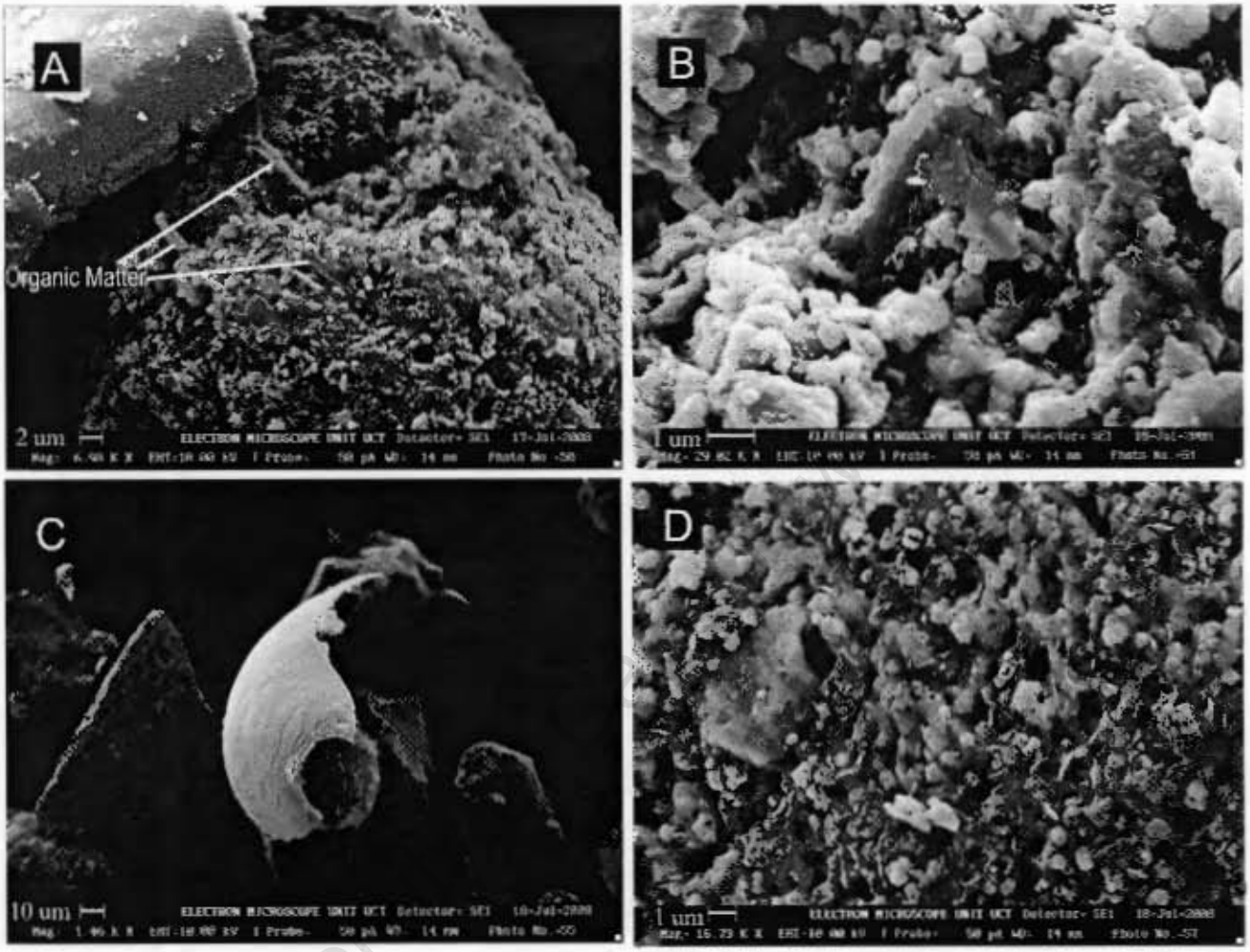

Figure 4.5 A) SEM images of fine silt fraction of sample ZNMA (from Zwartwater North) showing quartz grains and small laths of organic matter B) Fine silt fraction of sample ZNMB (Zwartwater North) showing carbonate mineral coating on organic matter C) Biogenic carbonate - aragonitic *T. ventricosa* shell fragment from coarse silt fraction of sample ZNMB (Zwartwater North) D) Organic matter (small irregular fragments) and carbonate mineral precipitate in fine silt fraction of sample ZNMB (from Zwartwater North).

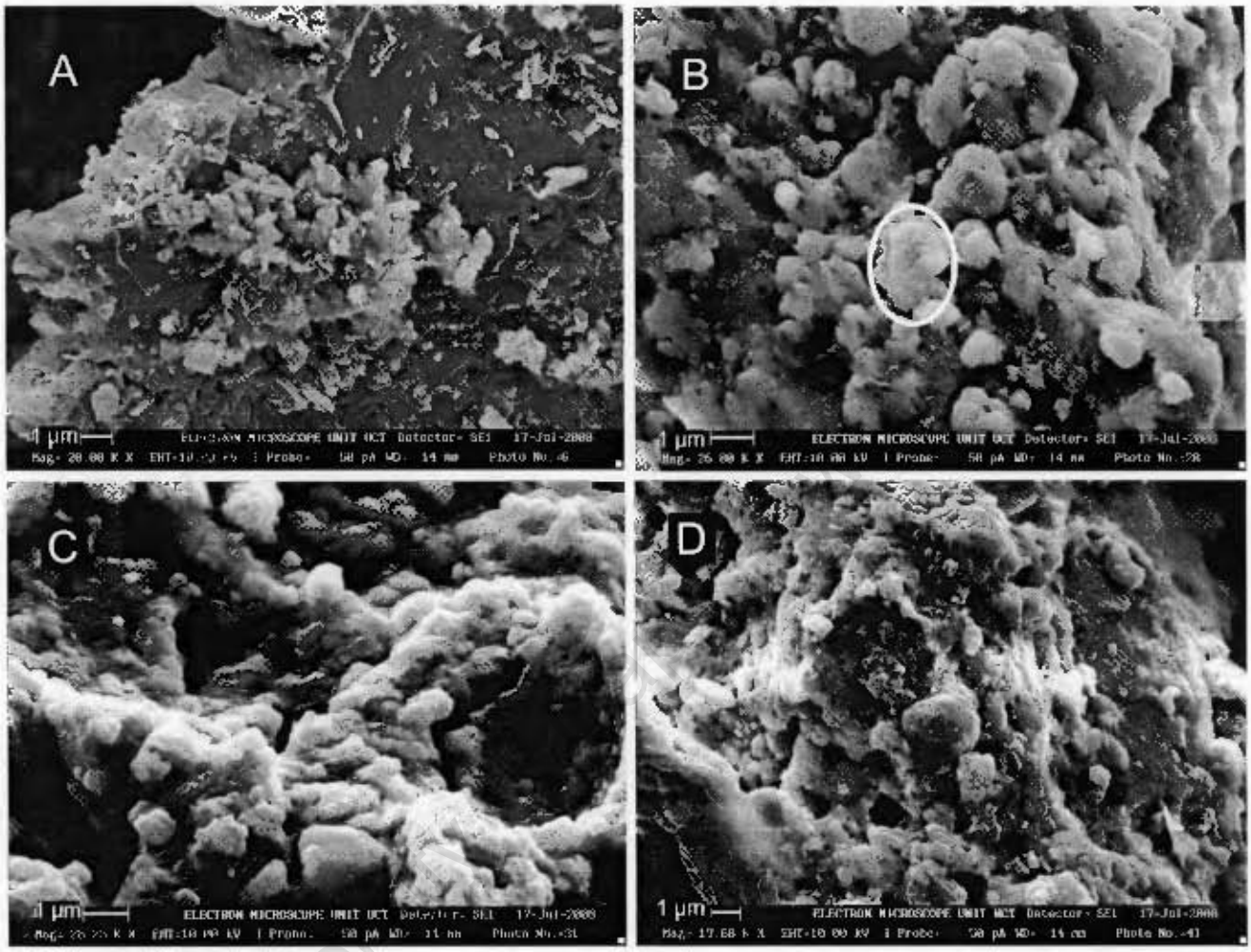

Figure 4.6. SEM images from A)Yzerfontein pan (sample YZ1A) gypsum and calcite crystals (note smooth crystal faces of calcite and small platey gypsum crystals), B) Dolomite with possible interlocking dumbbell structure in silt fraction of sediment from Zwartwater North pan (sample ZNED), C) Knobby anhedral carbonate mineral possibly coating nanobacteria from Zwartwater North pan (sample ZNNC) D) knobby texture of carbonate minerals in fine silt fraction of sediment from Zwartwater South (sample ZSNC). XRD indicates that these are a mixture of calcite and dolomite. These are interpreted to be dolomite.

4.1.3 Sourc e of Ca^{2+} and Mg^{2+} ions

Calcium and magnesium ions are likely to have been transported to the pans from two main sources. Firstly, the ions may come from the weathering of the bedrock in the area. The Cape Granite Suite bedrock may be the source of the Ca^{2+} ions, as may the Malmesbury Group metasediments. In the Cape Granite, plagioclase is a source of Ca^{2+} ions, and biotite and cordierite are a source of Mg^{2+} ion. The Darling granites have a molar Mg/Ca ratio of 0.707 to 1.04 (Scheepers, 2000), so weathering of the granite provides slightly more to equal amounts of calcium as magnesium. The Malmesbury Group consists largely of metamorphosed continental margin terrigenous shale and siltstone. While the Mg/Ca ratio of the Malmesbury Group Tygerberg terrane in the study area is unknown, the Mg/Ca ratio is probably significantly greater than one, because rocks of the adjacent Boland terrane of the Malmesbury Group have Mg/Ca molar ratios of up to 32 (Frimmel et al., 2001). MgO and CaO contents are between 0.32 and 3.78 and 0.0 and 5.65 weight percent respectively. Therefore, chemical weathering of the Cape Granite and Malmesbury Group basement rocks is a potential source of both calcium and magnesium to the pans. All of the inland pans appear to be surrounded by the Cape Granite, however the Brak river, with its source in the Malmesbury Group, does drain into the area close to the Zwartwater pans.

A second source of the Ca^{2+} and Mg^{2+} ions in the pans is seawater, which has an Mg/Ca molar ratio of 5:1. The coastal Yzerfontein pan was in episodic contact with the sea at least during its early development, and the pan would therefore have a dominant seawater influence. The inland pans also have a marine influence, as a result of washout of marine

aerosols from the coast. The rainwater along the western coast is dominated by marine derived Na^{+}, Cl^{-}, Mg^{2+} and sulphate ions (Soderberg and Compton, 2007).

Since strontium often substitutes for calcium, strontium isotopes have been used as a proxy to identify the source of calcium. The Sr isotope technique has been used in previous studies on the origin of carbonate sediments (Chiquet et al., 1999; Naiman et al., 2000; Compton et al., 2001). If the sole source of the calcium is seawater, then carbonate minerals would be expected to have a seawater $^{87}Sr/^{86}Sr$ ratio. The seawater $^{87}Sr/^{86}Sr$ ratio ranges from 0.7090 to 0.70915 during the Quaternary. The modern seawater $^{87}Sr/^{86}Sr$ ratio is 0.70915 and the seawater Sr ratio has increased since the Eocene, such that recrystallization or replacement of older marine carbonate, should give a lower than modern seawater Sr isotope ratio. Most marine carbonate on the West Coast is Quaternary coastal calcrete (e.g. Langebaan Formation) or wind blown calcite shell sand grains whose $^{87}Sr/^{86}Sr$ values are similar to that of modern seawater.

The carbonate minerals from the five pans studied displayed a higher than seawater $^{87}Sr/^{86}Sr$ ratio. The source of the Ca^{2+} and Mg^{2+} therefore must be a mixture of seawater and bedrock influenced-meteoric water, since the bedrock has $^{87}Sr/^{86}Sr$ ratios higher than seawater. The Malmesbury Group has an average $^{87}Sr/^{86}Sr$ ratio of approximately 0.75, and the Cape Granite $^{87}Sr/^{86}Sr$ ratio ranges from 0.73 to 0.94 (Allsop and Kolbe, 1965). The high $^{87}Sr/^{86}Sr$ ratios of the bedrock indicate that the amount of Sr in the carbonates derived from bedrock is low relative to marine sources. Based on the $^{87}Sr/^{86}Sr$ ratios of the bedrock, the $^{87}Sr/^{86}Sr$ ratio of the carbonate minerals from the pans suggest that very

little of the strontium was derived from bedrock sources. Therefore, the Ca^{2+} and Mg^{2+} ions are of predominantly marine origin, which is consistent with the rainout of marine aerosols along the coast. A dominant seawater strontium source suggests that marine aerosols play a large part in the delivery of ions to the pans. Strontium is a heavy element so it is more likely that the strontium was carried inland by wind blown aerosols and sea spray, than that it was evaporated at the coast and brought inland via water vapour. Coastal rainwater has molar Mg/Ca ratios of about 2.4, lower in the rainwater (Soderberg and Compton, 2007) than the sea (~5). Since Mg/Ca ratios above that of seawater are conducive to dolomite precipitation, it is likely that there is extra input of Mg^{2+} from groundwater (Table 4.2) into the pans that have precipitated dolomite (Zwartwater North and South). Since the Malmesbury Group has high Mg/Ca ratios this is the most likely source of extra Mg^{2+} in the groundwater.

Table 4.2. Regional groundwater borehole data from the DWAF geohydrological database (concentrations in mmol/kg) (from Smith, 2000, Table 4.8.) and Mg/Ca ratio

Region	Mg^{2+}	Ca^{2+}	Alkalinity	SO_4^{2-}	Molar Mg/Ca
Rooipan North and South	1.3	0.7	0.7	0.3	1.86
Zwartwater North and South Pans	12.3	0.1	1.5	4	123
Yzerfontein	1.3	1.3	2	0.3	1.00

Carbonate minerals from the brackish saline Rooipan North and coastal Yzerfontein have $^{87}Sr/^{86}Sr$ ratios similar to the modern seawater ratio. Yzerfontein pan is closest to the sea, and would have the most marine influence of all the pans studied. The source of Ca^{2+} in the Rooipan North carbonate nodules is possibly from weathering of Quaternary calcrete in the area, such as the Langebaan Formation, or marine aerosols, but the two are indistinguishable using strontium isotope ratios. Zwartwater North and South have the

highest $^{87}Sr/^{86}Sr$ ratio, indicating the largest bedrock/meteoric water influence, probably through runoff from the adjacent granite hills, such as Slangkop Hill, or recharge from the deeper Malmesbury Group metasediments. Recharge from the Malmesbury Group is probably the cause of the high Mg/Ca ratio of the groundwater from the Zwartwater pan region (Table 4.2).

4.2 Evolution of pans

4.2.1 Brine type pans

The brine-type pans appear to have evolved by following a sequence of mineral formation, leading to the present mineralogy of the pans. During the formation of a pan from an established drainage system, an intermediate brackish-saline pond may develop as climate becomes more arid or during a particularly dry season. Since the nascent pan is within a drainage system, such as a river channel, the pan would accumulate ions from surface runoff and throughflow in the catchment during the wet, winter season and concentrate salts during the dry, summer season. During the early phase of pan formation, there is input of ions into the system from the sea as well as chemical weathering of rocks in the catchment (Figure 4.7 A). Marine salt input may be achieved either through rainout of marine aerosols or by sea spray which may be brought in from the coast by the wind. Marine salts would be washed out of the atmosphere by rainwater or rinsed from the surface and brought into the pan. Surface runoff as well as wind carries eroded soil into the pan which includes both soil minerals and organic matter. The rainfall and marine aerosols contribute Ca^{2+}, Mg^{2+}, SO_4^{2-}, and HCO_3^- to the system. The chemical weathering of bedrock produces Ca^{2+}, Mg^{2+}, and HCO_3^- ions, which would be transported to the pan by runoff or throughflow.

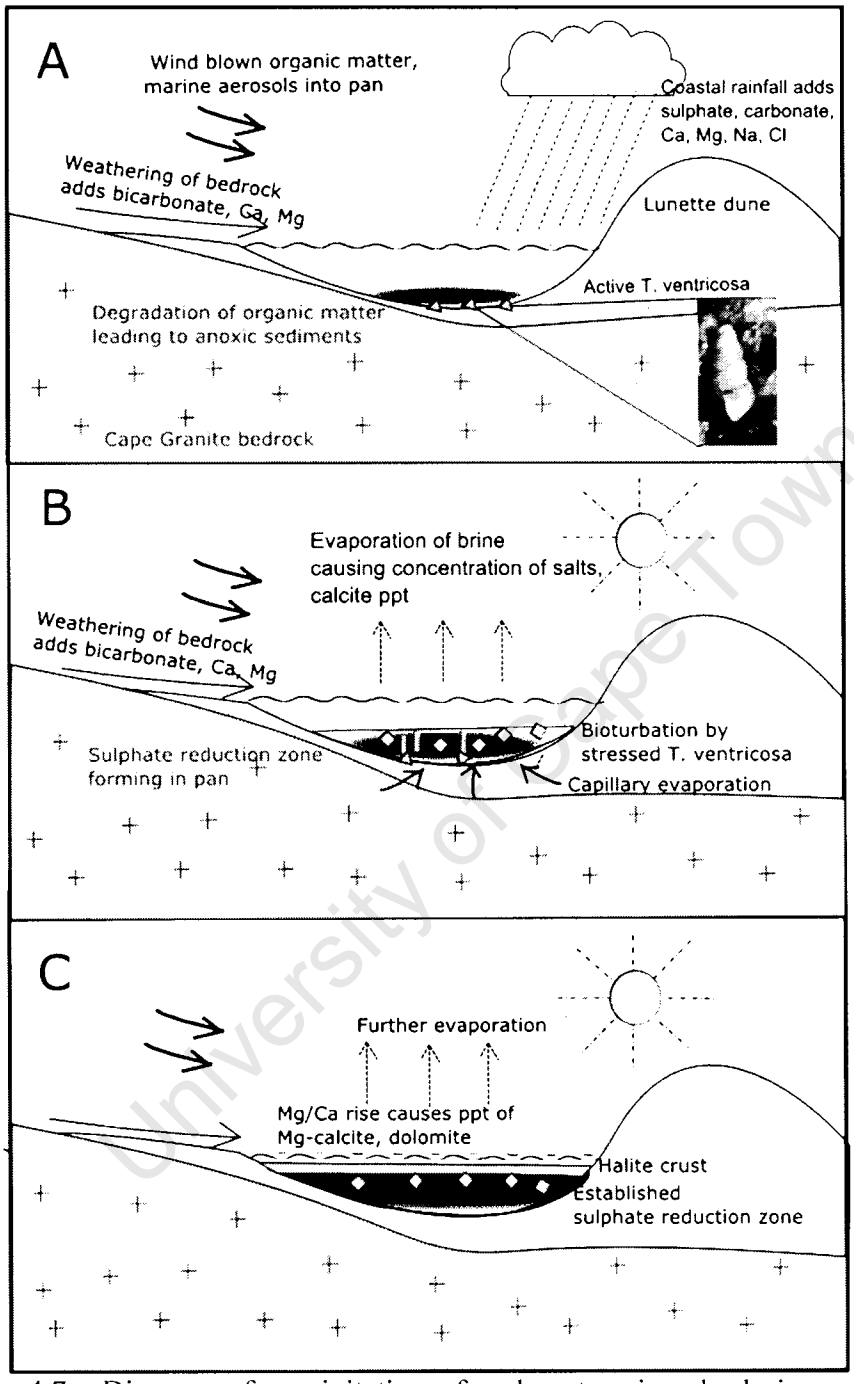

Figure 4.7. Diagram of precipitation of carbonate minerals during pan evolution. A) brackish-saline stage with active *T. ventricosa*; B) saline pan with moderate salt and calcite precipitation during early stages of evaporation, and C) hypersaline pan with well developed halite crust in summer Mg/Ca ratio rise and sulphate reduction leading to dolomite precipitation.

Over time, salts accumulate in the pans and salinities increase. As climate, or the season, becomes slightly more arid, evaporation of the pan waters increases, concentrating the ions even further. Calcite is the least soluble of the major salts in pan collected waters and is likely to precipitate early during evaporation. Salinity remains low at the stage of initial calcite precipitation, and relatively low salinities allow organisms such as the gastropod *Tomichia ventricosa* to survive. These gastropods are adapted to variable and stressful conditions, such as the high salinities that exist in brackish saline pans. As time passes, salt accumulates in the pan and the salinity of pan waters increases, forcing *T. ventricosa* to burrow downwards into pan sediments to survive the summer desiccation (Figure 4.7B). Those that survive the dry season will emerge during the following rainy season to reproduce (Brown, 1994). *T. ventricosa* is no longer active once salinities rise above 130‰ (Brown, 1994). Therefore, if the pans have reached a point in their development where high salinities are maintained throughout the year, because summer halite crusts dissolve in winter rainwater input, then *T. ventricosa* can no longer survive even in the wet months. Rooipan South has very high salinities (Smith, 2000) which explains the lack of *T. ventricosa* shells in this pan. Sulphate reduction starts to dominate in the pan as oxygen levels decrease as a result of increased salinity, which when high enough will prevent ventiliation by burrowing gastropods. Precipitation of low magnesian calcite continues, probably causing a rise in the Mg/Ca ion ratio of pan waters. The increase in the Mg/Ca ratio results in the precipitation of Mg-calcite, as indicated by the broad Mg-calcite XRD peaks of the sediments (Figure 4.8, 4.9, 4.10)

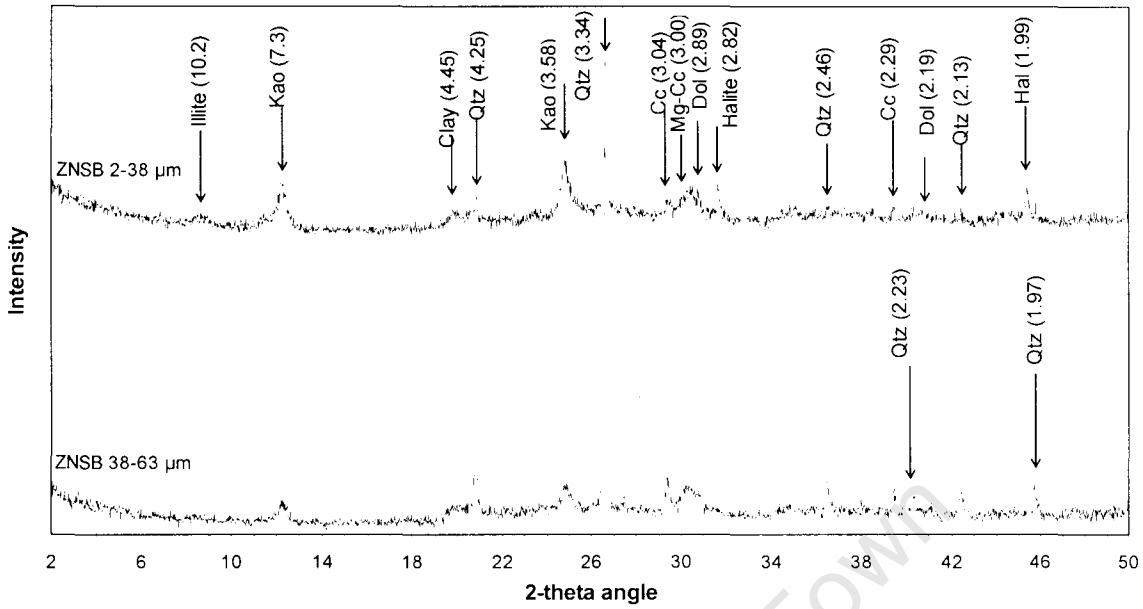

Figure 4.8. XRD scan of sample ZNSB, showing mineralogy of 2-38 µm and 38-63 µm size fractions. Kao=kaolinite, Qtz=quartz, Cc=calcite, Mg-cc=magnesian calcite, Dol=dolomite, Hal=halite

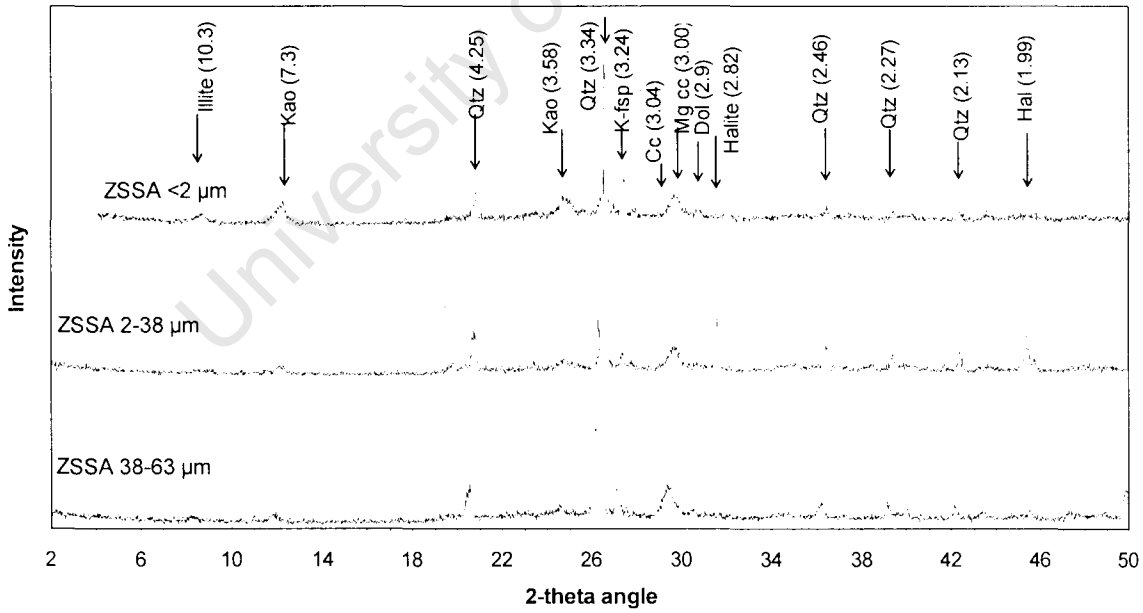

Figure 4.9. XRD scan of sample ZSSA, showing mineralogy of 2-38 µm and 38-63 µm size fractions. Kao=kaolinite, Qtz=quartz, Cc=calcite, Mg-cc=magnesian calcite, Dol=dolomite, Hal=halite

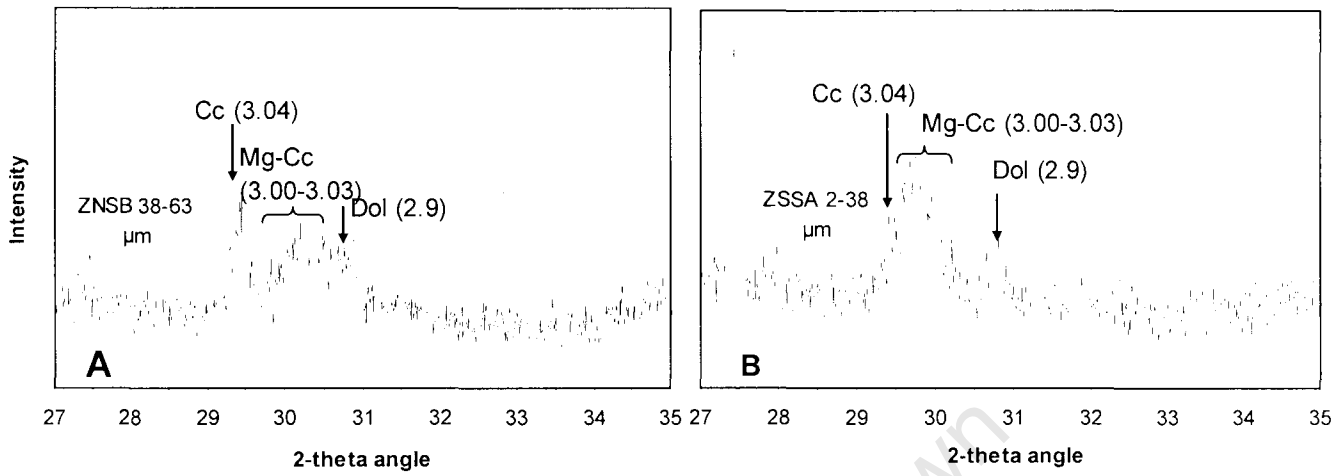

Figure 4.10. Cropped XRD scans of sample A) ZNSB and B) ZSSA, showing main low magnesian calcite (cc), high magnesian calcite (Mg-cc) and dolomite (dol) peaks. Note the broad magnesian calcite peaks, indicating the range of magnesium content.

As the Mg/Ca ion ratio of subsurface porewaters rises further, precipitation of Ca-rich proto-dolomite and dolomite may begin (Figure 4.7C) as in the case of the Zwartwater pans (Figure 4.10). Mg-rich evaporative brine water may flow downwards, or may diffuse along a concentration gradient, allowing dolomitization of previously precipitated calcite minerals in the sediments. Eventually the build up of marine salts in the pan leads to the precipitation of a halite crust, as can be seen on the Rooipan South and the Zwartwater pans. A halite crust slows evaporation of pan sediment porewaters, and promotes sulphate reduction in subsurface organic-rich mud by limiting atmospheric exchange with the sediment. The sulphate reduction zone becomes buried, and a new sulphate reduction zone forms in the subsurface sediments. With burial, proto-dolomite may recrystallize over time to form a properly structured, stoichiometric dolomite. Brine type pan Rooipan South has not precipitated dolomite. Like the Zwartwater pans, it

obtained salt through input of coastal rainfall, marine aerosols and weathering of bedrock. Calcite precipitated first, however low carbonate ion concentrations (Table 4.2) limit the amount of calcite precipitation other than in the black organic-rich surface mud where carbonate produced from the degradation of organic matter allowed more calcite to form.

4.2.2 Brack ish-saline Pan

The brackish-saline Rooipan North pan contains evaporative calcite, but calcite precipitation was limited by calcium (Table 4.1). Rooipan North has a low salinity relative to the other pans, and did not precipitate a halite crust, leaving the pan to dry out for at least half of each year.

4.2.3 Coas tal Yzerfontein Pan

Yzerfontein pan is different from the inland pans because of a more direct marine influence. Yzerfontein pan was probably episodically in contact with the sea, as a lagoon, for much of its development (Figure 4.11). While evaporation of the lagoon would have concentrated salts, exchange with the sea would have periodically lowered salinities, allowing *T. ventricosa* gastropods to survive. The gastropods probably burrowed downwards during periods of high salinities and remerged during times when the salinity dropped (reflooding of the pan by seawater or runoff of fresh water during winter months). Repeated flooding and evaporation formed the relatively thick deposit of gypsum along with some calcite. The piles of mined gypsum at Yzerfontein contain black mussel *(Choromytilus meridionalis)* shell fragments. These shells have discoloured from purple to orange and indicate a late Pleistocene age, most likely the previous interglacial (Eemian; 120-130 ka) (Compton and Franceschini, 2004). The black mussels indicate that

the pan at that time was adjacent to rocky shoreline environments, before sea level rise modified it to a lagoonal setting. Continued progradation of the beach and build up of sand dunes would have led to the formation of the pan we see today. Progradation of the coastline would have caused isolation of the pan from the sea by the formation of large sand dunes. Isolation from the sea resulted in a final evaporation and deposition of a salt crust since completely mined out by early settlers (Figure 4.11).

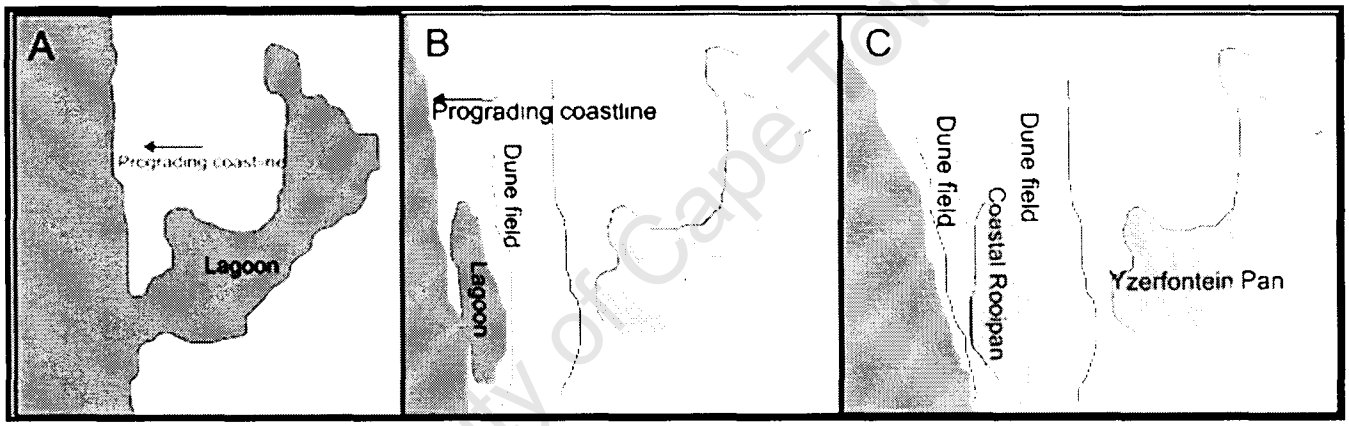

Figure 4.11. Schematic diagram showing the sequential progradation of the Yzerfontein coastline, leading to the formation of Coastal Rooipan (not in the study) and Yzerfontein pans. A) Last interglacial highstand of the sea (Eemian), 120-130 ka, B) Progradation of beach and build up of dunes as sea level fell during the early stages of the last glaciation. C) Present-day abandoned lagoons transformed into salt pans. The lagoon would have been intermittently connected to the sea between stages A and B related to sea-level fluctuations and build up of beach and dune sand deposits.

4.3 Factors enhancing carbonate mineral precipitation

Waters with high carbonate alkalinity, high pH, and warm temperatures are conducive to carbonate mineral precipitation. In the case of calcite, a high Ca^{2+} concentration will enhance precipitation. Mg^{2+} ions, however, inhibit calcite precipitation (Morse, 1983) and low Mg/Ca ratios in solution are required to precipitate calcite rather than aragonite or dolomite. Sulphate and phosphate ions are also calcite inhibitors (Morse, 1983).

The scarcity of dolomite in present day environments may be explained by kinetic factors that inhibit dolomite precipitation. One of these factors is the hydration differences between Ca^{2+} and Mg^{2+} ions, as Mg^{2+} is surrounded by a strong hydration shell. Therefore calcite is more easily precipitated than dolomite, and high concentrations of Mg^{2+} relative to Ca^{2+} will enhance dolomite precipitation. The occurrence of Mg-rich clay minerals sepiolite and palygorskite, often found in carbonate precipitating pans, could make Mg^{2+} even more unavailable for Mg-carbonate precipitation (Watts, 1980). However sepiolite and palgorskite were not identified in the pan sediments of this study.

Another kinetic factor is the amount of ordering required in the structure of dolomite, which may prevent it from precipitating. While supersaturated brines may contain high concentrations of Mg^{2+}, rapid crystallization may result in the precipitation of an Mg-carbonate with a disordered structure, without the alternating cation layers present in dolomite (Morrow, 1982). High concentrations of sulphate ion in supersaturated brines may also inhibit dolomite nucleation (Morrow, 1982; Baker and Kastner, 1981). For dolomite to precipitate, these factors must be overcome. These kinetic factors can be overcome at high temperatures, as shown by the synthesis of dolomite under laboratory

conditions at temperatures above 100° C, but not at temperatures easily achieved on Earth surface environments. The pans probably reach temperatures of 30°C, which while warm, is not warm enough. Other factors may help to reach supersaturation of dolomite and overcome the kinetic inhibitors. Unlike calcite, high Mg/Ca ratios enhance dolomite precipitation to overcome the higher hydration energy of the Mg^{2+} ion, relative to the Ca^{2+} ion. While dolomite may be precipitated at Mg/Ca ratios below 1.5 at temperatures above 200°C, a molar ratio above 10 may be required to precipitate dolomite in the type of environments seen in the pans (Baker and Kastner, 1981). Even low sulphate ion concentrations inhibit dolomite nucleation. As mentioned previously, the sulphate reducing bacteria decrease the concentration of sulphate ions, as well as increase the carbonate alkalinity in the solution, and in their excretion of Mg^{2+} ions, provide an ideal microenvironment for dolomite to nucleate. High amounts of organic carbon are necessary for bacteria metabolism. Organic carbon also creates an anoxic environment, with a low Eh favourable to the SR bacteria, which cannot survive in oxic environments.

4.4 Regional differences in pan carbonate minerals

The Darling area pans have salinities that range between 2-379g/L (TDS) (Smith, 2000). Sulphate ion concentrations of pan waters of this study are high for the most part, but are also variable, and range between 1 mmol/kg to 373 mmol/kg. Magnesium ion concentrations in the studied pans range from 0.3 to 186 mmol/kg (Table 4.1). The waters of all the pans are neutral to alkaline (Smith, 2000). Regional differences in the pans of carbonate minerals are likely to be caused by differences in pore water and groundwater chemistry (Table 4.2), amount of organic matter, and SRB activity.

Zwartwater North and South pans both contain calcite, Mg-calcite, Ca-dolomite/proto-dolomite and stoichiometric dolomite. Both pans according to Smith (2000) have high carbonate alkalinity concentrations (Table 4.1) which enhance the precipitation of the carbonate minerals. These two pans also have all the factors necessary to precipitate dolomite. Firstly, the Mg/Ca ratios of the pan waters are high (Table 4.1). The groundwater has high Mg^{2+} concentrations and very high Mg/Ca ratios (Table 4.2) and is an important source of Mg^{2+} to the pans. Sr isotopes are the highest (most radiogenic) of all the pans, indicating that these pans have the highest bedrock contributions of Ca^{2+} and Mg^{2+}. Without significant contributions of Mg^{2+} from weathering bedrock (specifically the Malmesbury Group), the Mg/Ca ratios of the other pans would probably remain too low to precipitate dolomite. Secondly, sulphate reducing bacteria are very active in these pans, especially in the thick black hydrogen-sulphide smelling surface mud (Porter, 2007). Thirdly, a relatively high organic carbon content is available to the bacteria and the bacterial degradation of this organic carbon contributes to the large amounts of total calcite and dolomite precipitation (Figure 4.4). Carbonate minerals, especially dolomite, are mostly precipitated in the northern and eastern sides of the pans. This is probably as a result of the deposition of terrigenous sediments from the Slangkop and surrounding hills on the western and southern areas of the pans, which inhibit the precipitation of carbonate minerals by dilution of organic matter and burial of the sulphate reduction zone. The northern side was much wetter, and the sediment layers were much less distinct, probably a result of pan water circulation mixing the sediment layers on this side of the pan. Sulphate reduction and the precipitation of carbonate minerals tend to coincide with areas

of low sedimentation rate. The carbonate minerals also tend to form in the wet areas of the pans, which in the case of the Zwartwater Pans, is the northern side. A possible reason for this is that bacterial activity is probably much higher in the wet areas of the pan. Circulation of Mg^{2+} by water through sediments is also conducive to dolomitization of calcitic sediments.

Rooipan South only has precipitates of calcite in the thick black sulphidic mud layer, and no dolomite. It might not have high enough carbonate ions to precipitate large amounts of carbonate minerals, although organic carbon content is similar to the Zwartwater pans. Another possible explanation for why Rooipan South has no dolomite is that the sediment pore water Mg/Ca ratio is too low to precipitate dolomite. Rooipan South is the only pan in the study with sediments containing significant amounts of the clay mineral smectite (Table 3.4). It is possible that the smectite is removing Mg^{2+} from solution through cation exchange (Deer et al., 1992) making the Mg^{2+} unavailable for dolomite precipitation.

Brackish-saline Rooipan North, which contains only calcite, does not show sulphate reduction taking place at present, which may be the reason for the lack of dolomite precipitation. Mg/Ca ratios are also relatively low for dolomite precipitation (Table 4.1).

Coastal Yzerfontein pan contains low-magnesian calcite, but does not contain dolomite. The pan, while having high Mg^{2+} concentrations, also has high Ca^{2+} concentrations, and therefore has an Mg/Ca (Table 4.1) ratio too low for dolomite precipitation. Sulphate concentrations are high evidenced by gypsum precipitation. Sulphate reduction is not as

active at Yzerfontein pan as it is at the inland brine-type pans, such as Zwartwater North and South pans. The low levels of sulphate reduction is consistent with the generally low organic matter content of the surficial mud layer, which has been extensively burrowed by *T. ventricosa*. The bioturbation will cause oxidation of the sediments, which is not favourable for sulphate reducing bacteria. High concentrations of sulphate in solution are sustained without bacterial sulphate reduction and will inhibit dolomite formation.

4.5 Comparison to pans within southern Africa

Evaporative systems that precipitate carbonate minerals, such as playas, sabkhas and saline lakes, including hypersaline pans, such as the Darling Pans, are common in southern Africa as a result of the arid climate. In some cases, the system no longer exists, but due to the formation calcrete and dolomite rock sediments, a palaeo-lake or -playa can be identified.

4.5.1 Pres ent-day pan environments

Etosha Pan in northern Namibia contains sediments with calcite and dolomite as well as clay minerals. These pans, unlike the brine type Darling pans, do not have a thick halite crust, do not currently contain water, or evidence of sulphate reduction. The drainage basin consists of the dolomitic Otavi mountains, so the dolomitic sediments are probably a result of weathered bedrock (Buch and Rose, 1996).

Lebatse Pan in Botswana also has a similar mineralogy to that of the Darling Pans, with quartz, calcite, dolomite and halite dominated sediments. The source of the carbonate is

thought to be groundwater, and since organic content of the sediments is low (less than 1%) in most sediment samples, organic carbon is probably not the main contributor to carbonate ions in the calcite and dolomite (Holmgren and Shaw, 1997).

These present day pans do have elements in common with the Darling and Yzerfontein pans. The mineralogy is similar; however, the modes of calcite and dolomite precipitation are different. While organic matter appears to be important in the precipitation of dolomite and calcite in the Darling pans, many present day southern African pans appear to source most of their carbonate ions from bedrock.

4.5.2 Pal aeo-lake and palaeo- playa environments

The Makgadikgadi basin is a large complex in Northwestern Botswana interpreted as a palaeolake setting, about 2 million years old. Like the Darling and Yzerfontein pans, especially brackish saline Rooipan North, the sediments are calcrete grading up to a more siliceous sediment and silcrete. Unlike the Darling brine-type pans the Makgadikgadi basin does not seem to have had an established sulphate reduction zone. The calcite however, does appear to be associated with both plant matter and bacteria, as it has precipitated around plant roots and stems in marshy environments, forming stem casts. Like the Darling pans, bacteria also seem to be involved in calcite precipitation, but in this case it is the *Dilococcus* bacteria that are involved (Ringrose et al., 1999).

The Zebra Pan-type carbonates of the Central Namib Desert Region are thick dish shaped lenses of dolomitic limestone. These lenses are interpreted to have been vegetated paleao playa lakes (i.e. oases) which formed during a "wet desert phase". Algal filaments mats,

cyanophytes, and calcareous algae are present. The outer most lenses are interpreted as a mixing zone between saline evaporated waters within the pan, and fresh groundwater on the outside, leading to the precipitation of dolomite. Organic matter does seem to have facilitated the precipitation of the carbonate minerals in these palaeo environments (Smith and Mason, 1998).

These palaeo environments suggest that that in the past, during wetter periods, organic matter, such as marsh vegetation, and algae, and bacterial activity may have played a larger role in the precipitation of carbonate minerals in lakes and playas in southern Africa. These settings may have been similar to those seen in the Darling pans with more organic matter, but with less of a marine influence as the distance from the sea is too great.

5 Summary and Conclusions

This aim of the study was to investigate carbonate minerals of the Darling and Yzerfontein pans, in terms of mineralogy and isotopic composition in order to understand their origin. All pans studied contain carbonate minerals, concentrated in the silt and clay size fractions. The brine-type Zwartwater pans were the only two pans in the study that contain dolomite and/or Ca-dolomite. All of the pans, except Rooipan South, contain low magnesian calcite, and all of the brine-type inland pans contained high magnesian calcites. The coastal Yzerfontein pan contains calcite, together with large amounts of gypsum.

$\delta^{18}O$ values of the carbonate minerals were positive, indicating that the carbonate minerals precipitated from evaporative waters. Negative $\delta^{13}C$ values of the carbonate minerals suggest that the source of the carbonate ions was at least partially organic carbon, oxidized by sulphate reducing bacteria. The weathering of Cape Granite bedrock is probably an additional source of carbonate ions. The coastal Yzerfontein pan calcite was found to have the smallest contribution of carbonate ions from organic carbon, most of the carbonate having groundwater/bedrock source.

SEM photomicrographs show that carbonate minerals are small, sub-spherical and knobby, consistent with mediation by sulphate reducing bacteria. The bacteria provide a microenvironment conducive to carbonate mineral, especially dolomite, precipitation, by excreting Mg^{2+}, producing carbonate ions, and reducing sulphate ions.

The source of the Ca^{2+} and Mg^{2+} ions in the carbonate minerals was identified using strontium isotope ratios. Higher-than-seawater $^{87}Sr/^{86}Sr$ ratios indicate that the source of the Ca^{2+} and Mg^{2+} ions is a mixture of seawater and the Cape Granite and Malmesbury Group bedrock. However, seawater provides the majority of the ions through coastal rainfall and marine aerosols. Zwartwater North and South carbonate minerals have the highest $^{87}Sr/^{86}Sr$ ratios, indicating that their source was more influenced by bedrock than the other pans.

The evolution of the brine type pans was as follows: Calcite precipitates first from the pans, creating a higher Mg/Ca ratio in the brine. Calcite with increasing magnesium content then precipitate as the Mg/Ca ratio rises from calcite precipitation. When the Mg/Ca ratio is high enough, the precipitation of Ca-dolomite or protodolomite is enhanced. Over time, a disordered dolomite may recrystallize to a stoichiometric dolomite. The coastal Yzerfontein pan first precipitated calcite, which was followed by large amounts of gypsum precipitation. The gastropod *T. ventricosa* with an aragonitic shell was active during periods of low salinity in the Zwartwater North and coastal Yzerfontein pans.

The most important factors that seem to have an effect on the precipitation of dolomite are sulphate reduction, and therefore high amounts of organic carbon, and high Mg/Ca ratios (above ~5). These factors are interlinked, and control the regional distribution of dolomite in the pans.

The Darling Pans are somewhat similar to palaeo-pans and –lakes in southern Africa, such as the Makgadikgadi basin in Botswana (Ringrose et al., 1999) and the Zebra carbonates in Namibia (Smith and Mason, 1998) where organic matter may have played a large role in the precipitation of carbonate minerals. While the mineralogy of the Darling and Yzerfontein pans may be similar to other present day pans in Southern Africa, the mode of formation and origin of the carbonate mineral are often different, as in the case of Etosha (Buch and Rose, 1996) and Lebatse Pans (Holmgren and Shaw, 1997).

6 References

Allsop. H.L., P. Kolbe. 1965. Isotopic age determinations on the Cape Granite and intruded Malmesbury sediments, Cape Peninsula, South Africa. *Geochimica et Cosmochimica Acta* **29:** 1115-1130.

Baker, P.A., M. Kastner.1981. Constraints on the Formation of Sedimentary Dolomite. *Science*, **213:** 214-216.

Barton, L.L., F.A. Tomei. 1995. Characteristics and Activities of Sulfate Reducing Bacteria. In: *Sulfate-Reducing Bacteria* (Ed. Barton, L.L.) Plenum Press, NewYork, pp. 217-235.

Bernoulli, D., L. Gasperini, E. Bonatti, P. Stiller. 2004. Dolomite formation in pelagic limestone and diatomite, Romanche Fracture Zone, Equatorial Atlantic. *Journal of Sedimentary Research*, **74**: 924-932.

Boggs, S. 2001. *Principles of Sedimentology and Stratigraphy. Third Edition.* Prentice Hall, New Jersey. 726 pp.

Brown, D.S. 1994. *Freshwater snails of Africa and their Medical Importance.* CRC press.

Buch, M.W., D. Rose. 1996. Mineralogy and geochemistry of the sediments of the Etosha Pan Region in northern Namibia: a reconstruction of the depositional environment. *Journal of African Earth Sciences* **22:** 355-378.

Burns, S.J., P.A. Baker. 1987. A geochemical study of dolomite in the Monterey Formation, California. *Journal of Sedimentary Petrology* **57:** 128-139.

Chiquet, A., A. Michard, B Hamelin. 1999. Atmospheric input vs. in situ weathering in the genesis of calcretes: An Sr isotope study at Galvez (Central Spain). *Geochimica et Cosmochimica Acta* **63:** 311-323.

Compton, J. 1988. Degree of supersaturation and precipitation of organogenic dolomite. *Geology* **16:** 318-321.

Compton, J., G. Franceschini. 2005. Holocene geoarchaeology of the Sixteen Mile Beach barrier dunes in the Western Cape, South Africa. *Quaternary Research* **63:** 99– 107.

Compton, J., C. Harris, S. Thompson. 2001. Pleistocene dolomite from the Namibian Shelf: High $^{87}Sr/^{86}Sr$ and $\delta^{18}O$ values indicate an evaporative, mixed-water origin. *Journal of Sedimentary Research* **71:** 800-808.

Coplen, T.B., C. Kendall, J. Hopple. 1983. Comparison of stable isotope reference samples. *Nature* **302**: 236–238.

Da Silva, L.C., P.G. Gresse, R. Scheepers, N.J mc Naughton, L.A. Hartmann, I. Fletcher. 2000. U-Pb SHRIMP and Sm-Nd age constraints on the timing and sources of the Pan-African Cape Granite Suite, South Africa. *Journal of African Earth Sciences*, **30:** 795-815.

Deer, W.A., R.A. Howie, J. Zussman. 1992. *An Introduction to Rock-Forming Minerals, Second Edition.* Prentice Hall, London. 696 pp.

Diamond, R.E., C. Harris. 1997. Oxygen and hydrogen isotope composition of Western Cape meteroic water (Research Letter). *South African Journal of Science*, **93:** 371-374.

Fairbridge, R.W., G.V. Chilingar, H.J. Bissel. 1967. *Carbonate Rocks 9A*. Elsevier, Amsterdam, 471pp.

Fauque, G.D.1995. Ecology of sulfate-reducing bacteria. In: *Sulfate-Reducing Bacteria* (Ed. Barton, L.L.). Plenum Press, New York, pp. 217-235.

Faure, G.1992. *Principles and Applications of Inorganic Geochemistry*, MacMillan Publishers, New York.

Frimmel, H.E., P.G. Fölling, R. Diamond. 2001. Metamorphism of the Permo-Triassic Cape Fold Belt and its basement, South Africa. *Mineralogy and Petrology* **73:** 325-346.

Goudie, A.S., G.L. Wells.1995. The nature, distribution and formation of pans in arid zones. *Earth-Science reviews* **38:** 1-69.

Goudie, A.S., D.S.G. Thomas. 1986. Lunette dunes in southern Africa. *Journal of Arid Environments* **10:** 1-12.

Hardie, L.A., H.P. Eugster. 1970. The evolution of closed basin brines. *Mineralogical Society of America Special Publication* **3:** 273-290.

Harris, C., B.M. Oom, R.E. Diamond. 1999. A preliminary investigation of the oxygen and hydrogen isotope hydrology of the greater Cape Town area and an assessment of the potential for using stable isotopes as tracers. *Water SA* **25:** 15-24.

Harris, C., R.E. Diamond. 1997. Oxygen and hydrogen isotopecomposition of Western Cape meteoric water. *South African Journal of Science* **93**: 371-374.

Holmgren, K., P. Shaw. 1997. Palaeoenvironmental Reconstruction from Near-Surface Pan Sediments: An Example from Lebatse Pan, Southeast Kalahari, Botswana. *Physical Geography* **79:** 83-93.

Jackson, M.L. 1958. *Soil Chemical Analysis.* New Jersey, Prentice Hall. 489 pp.

Kelts, K., J.A. McKenzie. 1982. Diagenetic dolomite formation in Quaternary anoxic diatomaceous muds of DSDP Leg 64, Gulf of California. *Initial Reports of the Deep Sea Drilling Project,* **64:** 553–569.

Lambrechts, J.J.N.1981. Soils of the coastal lowlands of the Western Cape, in *Proceedings of a Symposium on Coastal Lowlands of the Western Cape,* (Ed. Mol, E.) University of the Western Cape, Cape Town.

Lawson, M.P., D.S.G. Thomas. 2002. Late Quaternary lunette dune sedimentation in the southwestern Kalahari desert, South Africa: luminescence based chronologies of aeolian activity. *Quaternary Science Reviews* **21:** 825–836.

Mazzullo, S.J. 2000. Organogenic dolomitization in peritidal to deep-sea sediments *Journal of Sedimentary Research*, **70**: 10-23.

Mees, F. 2003. Salt mineral distribution patterns in soils of the Otjomongwa pan, Namibia. *Catena* **54:** 425-437.

Morrow, D.W. 1982. Diagenesis 1.Dolomite 1: The Chemistry of Dolomitization and Dolomite Precipitation. *Geoscience Canada* **9:** 5-13.

Morse, J. W. 1983. The kinetics of calcium carbonate dissolution and precipitation. In: *Carbonates: Mineralogy and Chemistry* (Ed. Reeder, R.J.). Mineralogical Society of America, pp. 227–264.

Muchez, P., W. Viane.1994. Dolomitization caused by water circulation near the mixing zone: an example from the Lower Visean of the Campine Basin (northern Belgium). In: *Sulfate-Reducing Bacteria* (Ed. Barton, L.L.) Plenum Press, New York, pp. 155-166.

Naiman, Z., J. Quade, P.J. Patchelli. 2000. Isotopic evidence for eolian recycling of pedogenic carbonate and variations in carbonate dust sources throughout the Southwest United States. *Geochimica et Cosmochimica Acta* **64:** 3099-3109.

Ohmoto, H., T. Kakegawa, D.R. Lowe. 1993. 3.4-Billion-Year-Old Biogenic Pyrites from Barberton, South Africa: Sulfur Isotope Evidence. *Science* **262:** 555-557.

Perkins, R.D., G.S. Dwyer, D.B Roshoff, J. Fuller, P.A. Baker, R.M. Loyd.1994. Salina sedimentation and diagenesis: West Caicos Island, British West Indies. In: *Dolomites: A volume in honour of Dolomieu* (Ed. Purser, B.H., M.E. Tucker, D.H. Zenger) Blackwell Scientific Publications, Oxford, pp 37-54.

Porter, D., A. Roychoudhury, D. Cowan. 2007. Dissimilatory sulphate reduction in hypersaline coastal pans: activity across a salinity gradient. *Geochimica et Cosmochimica Acta* **71:** 5102-5116.

Porter, D.A. 2007. *An integrated geochemical and microbiological investigation of sulphate reduction in hypersaline pans*, PhD thesis, University of Cape Town.

Purser, B.H., M.E. Tucker, D.H. Zenger. 1994. Problems, progress and future research concerning dolomites and dolomitization. In: *Dolomites: A volume in honour of Dolomieu* (Ed. Purser, B.H., M.E. Tucker, D.H. Zenger) Blackwell Scientific Publications, Oxford, pp. 3-28.

Ringrose, S., B. Downey, D. Genecke, F. Sefe, B. Vink. 1999. Nature of sedimentary deposits in the western Makgadikgadi basin, Botswana *Journal of Arid Environments* **43:** 375–397.

Ronov, A.B. 1983. *Earth's Sedimentary Shell.* Amer Geological Institute.

Scheepers, R. 2000. Granites of the Saldania mobile belt, South Africa: radioelements and P as discriminators applied to metallogeny. *Journal of Geochemical Exploration* **68:** 69-86.

Schoch, A.E. 1976. The Darling Granite Batholith. Ann. Univ. Stellenbosch. Pp 1-104

Smith, B.N., S. Epstein. 1971. Two categories of $^{13}C/^{12}C$ ratios for higher plants. *Plant Physiology*. **47**: 380-384.

Smith, M. 2000. *A geochemical investigation of Darling and Yzerfontein saline pans, Western Cape, South Africa.* MSc thesis, University of Cape Town, Cape Town.

Smith, M., J. Compton. 2004. Origin and evolution of major salts in the Darling pans, Western Cape, South Africa. *Applied Geochemistry* **19:** 645-664.

Smith, R.M.H., T.R. Mason. 1998. Sedimentary Environments and Trace Fossils of Tertiary Oasis Deposits in the Central Namib Desert, Namibia. *Palaios* **13:** 547-559.

Soderberg, K., J.S. Compton. 2007. Dust as a Nutrient Source for Fynbos Ecosystems, South Africa. *Ecosystems* **10:** 550–561.

South African Weather Service website: www.weathersa.co.za. Accessed 20 Dec. 2008.

Vasconcelos, C., J.A. McKenzie, R. Warthmann, S.M. Bernasconi. 2005. Calibration of the $\delta^{18}O$ paleothermometer in microbial cultures. *Geology* **33:** 317-320.

Vasconcelos, C., J.A. McKenzie.1997. Microbial mediation of modern dolomite precipitation and diagenesis under anoxic conditions (Lagoa Vermelha, Rio De Janeiro, Brazil). *Journal of Sedimentary Research* **67**: 378-390.

Wacey, D., D.T. Wright, A.J. Boyce. 2007. A stable isotope study of microbial dolomite formation in the Coorong Region, South Australia. *Chemical Geology* **244:** 155-174.

Warren, J. 1996. Evaporite, brines, base metals: What is an evaporite? Defining the rock matrix. *Australian Journal of Earth Sciences* **43:** 115-132.

Warren, J. 1999. *Evaporites: Their Evolution and Economics.* Blackwell Science, Oxford, 437 pp.

Warthmann, R., C.Vasconcelos, H. Sass, J.A. McKenzie. 2005 Desulfovibrio brasiliensissp. nov., a moderate halophilic sulfate-reducing bacterium from Lagoa Vermelha (Brazil) mediating dolomite formation. *Extremophiles* **9**: 255-261.

Watts, N.L. 1980. Quaternary pedogenic calcretes from the Kalahari: mineralogy, genesis and diagenesis. *Sedimentology* **27:** 661-686.

Appendix: XRD Scans

Mineralogy of different size fractions of pan sediments (separated into coarse silt (38-63 µm), fine silt (2-38µm) and clay (<2µm).

Arag=aragonite, Ca-dol=Calcian dolomite, cc=calcite, Dol=dolomite, Goe=goehtite, Gyps=gypsum, Hal=halite, Ill=illite, Kao=kaolinite,K-fsp= K-feldspar, Mg-cc=magnesian calcite, Plag=plagioclase feldspar, Qtz=quartz, Smec=smectite ?=unknown.

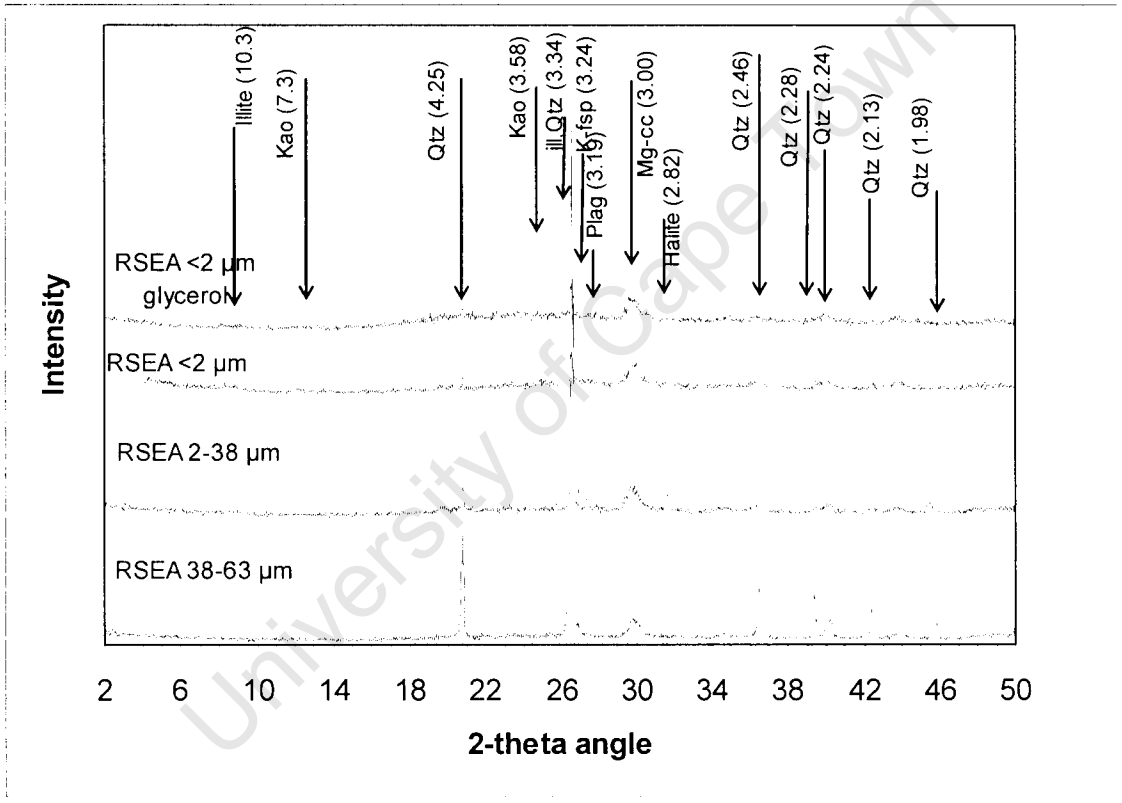

Figure 1. XRD scans showing mineralogy of size fractions of sediment sample RSEA, from Rooipan South.

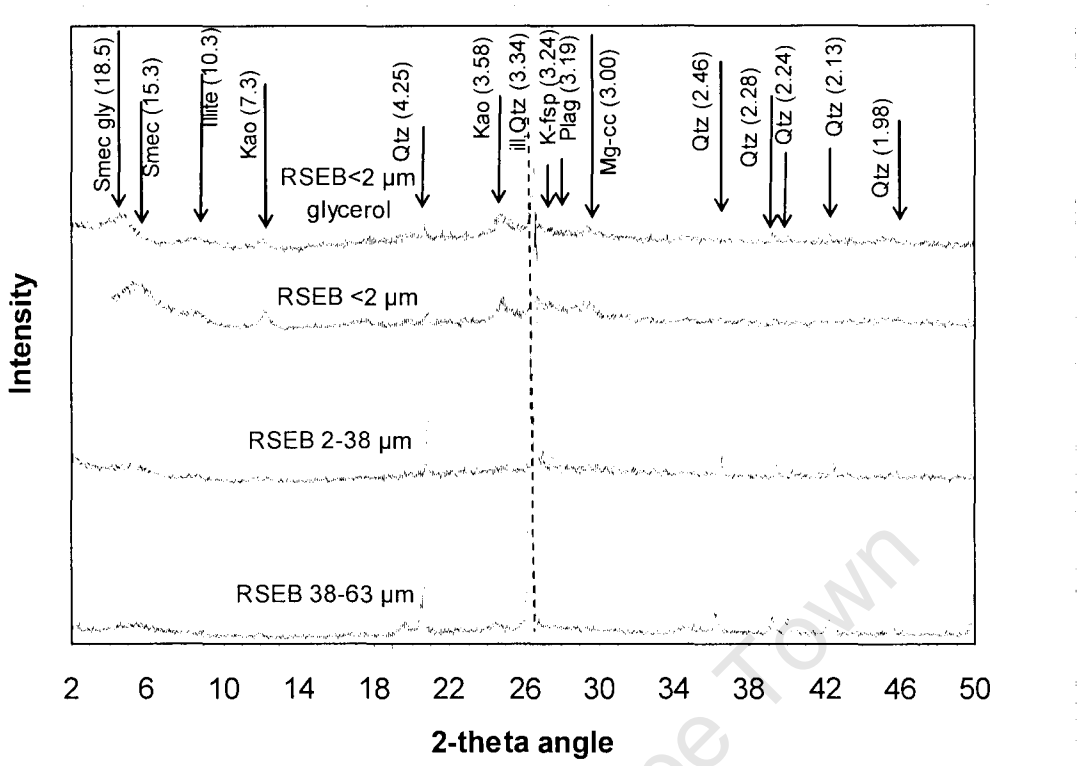

Figure 2. XRD scan showing mineralogy of sample RSEB

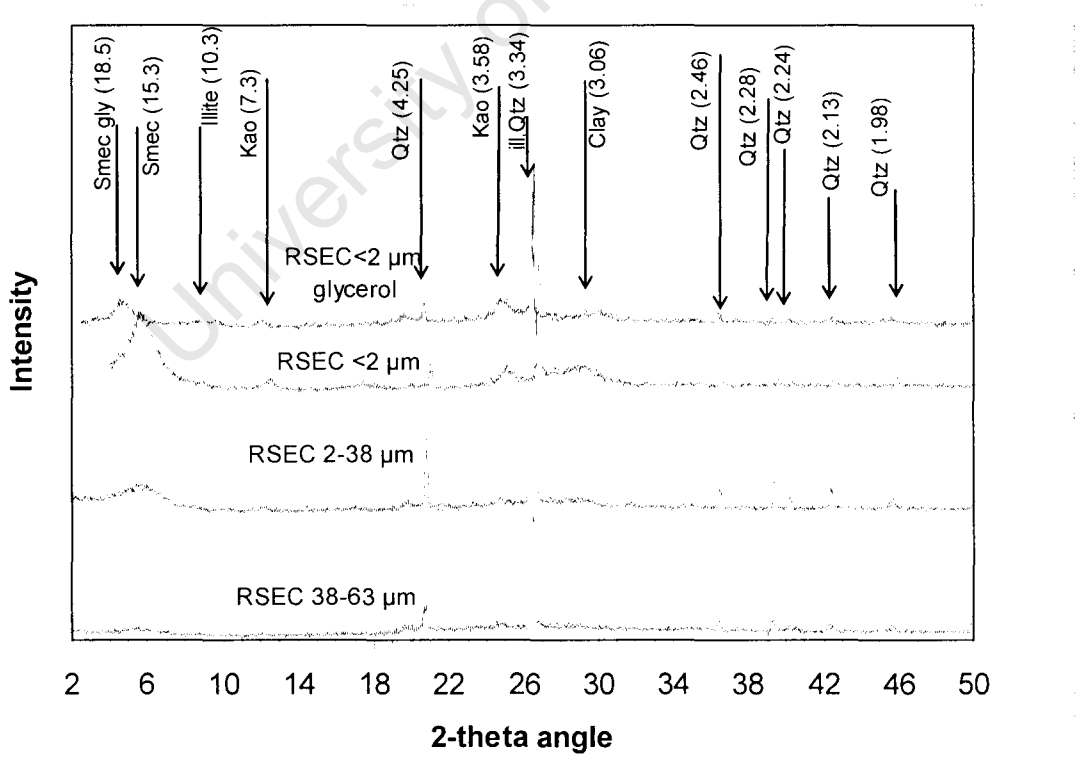

Figure 3. XRD scan showing mineralogy of sample RSEC

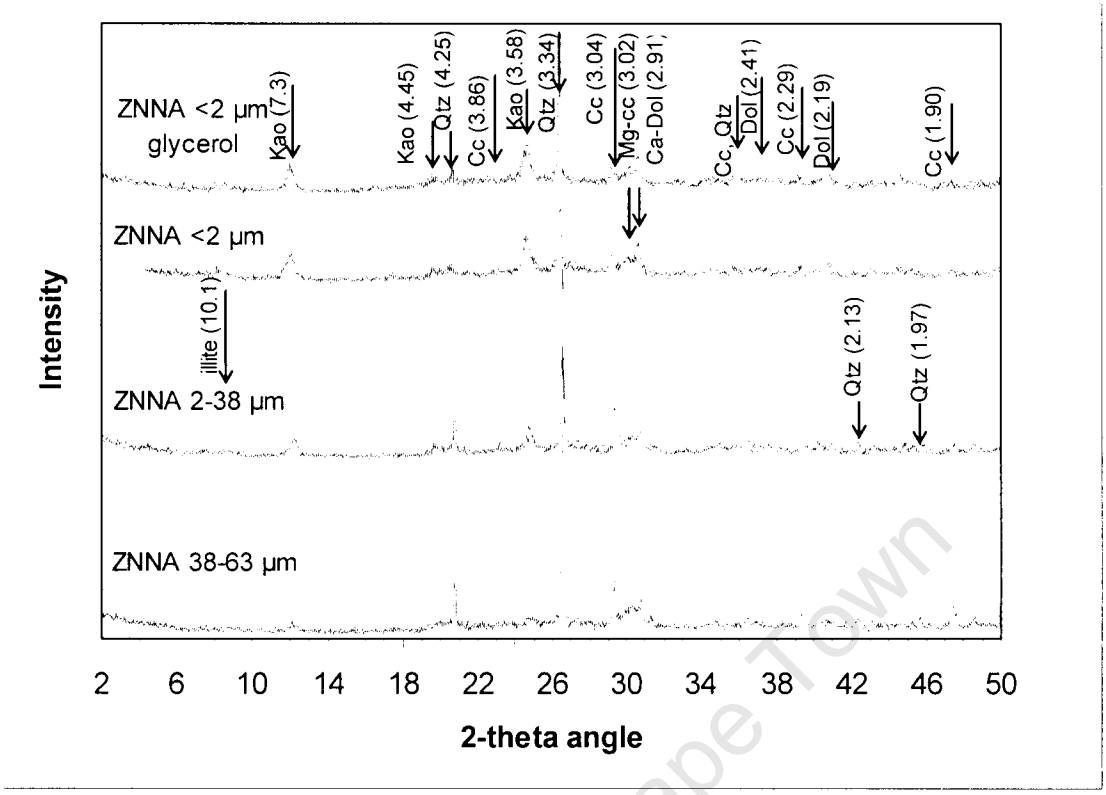

Figure 4. XRD scan showing mineralogy of sample ZNNA

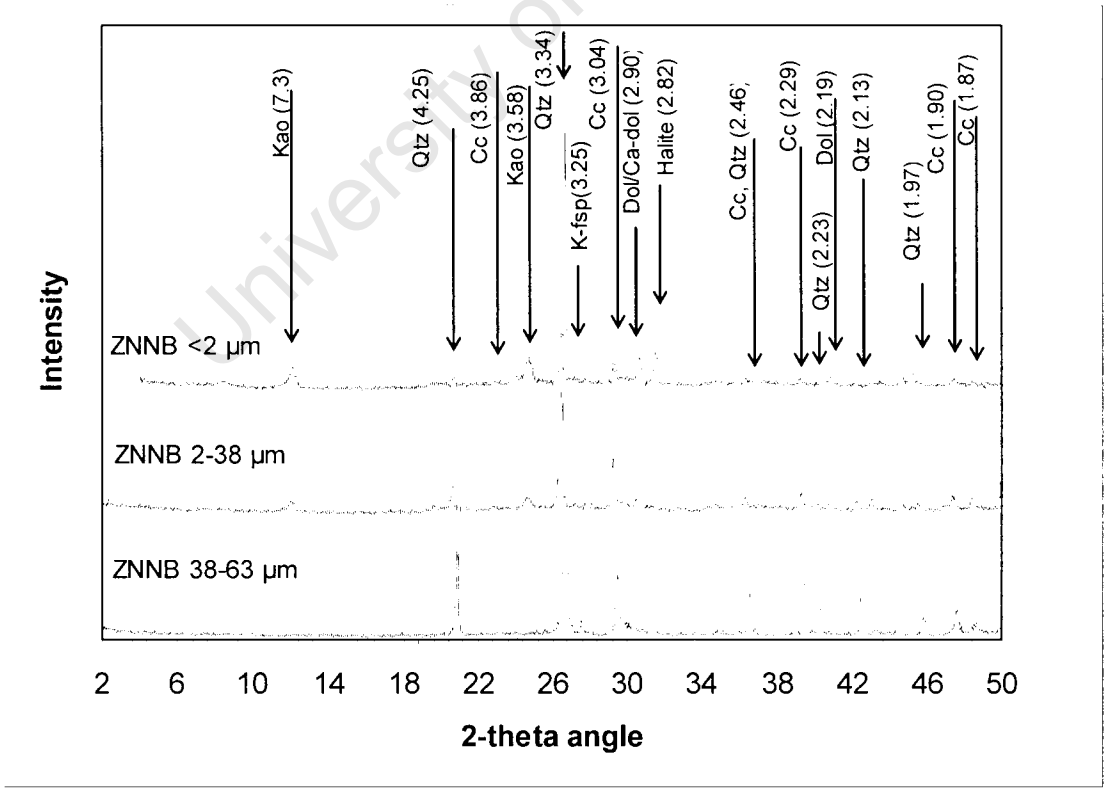

Figure 5:XRD scan showing mineralogy of sample ZNNB

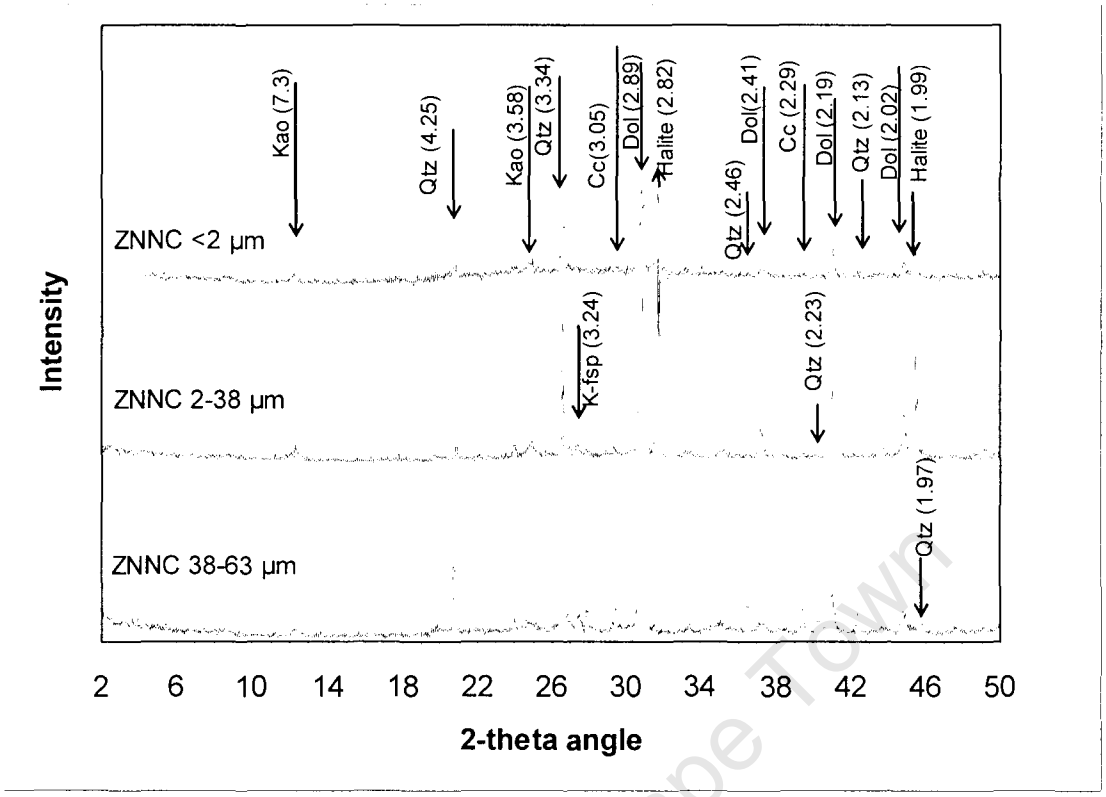

Figure 6: XRD scan showing mineralogy of sample ZNNC

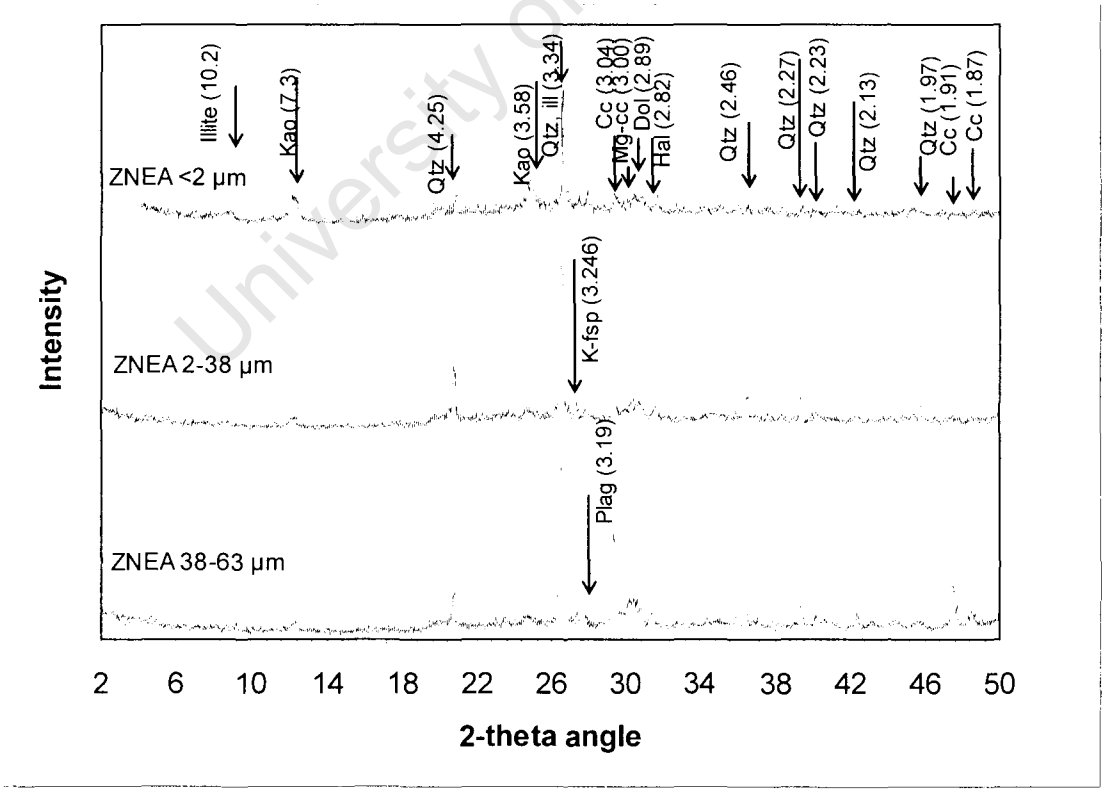

Figure 7 XRD scan showing mineralogy of sample ZNEA

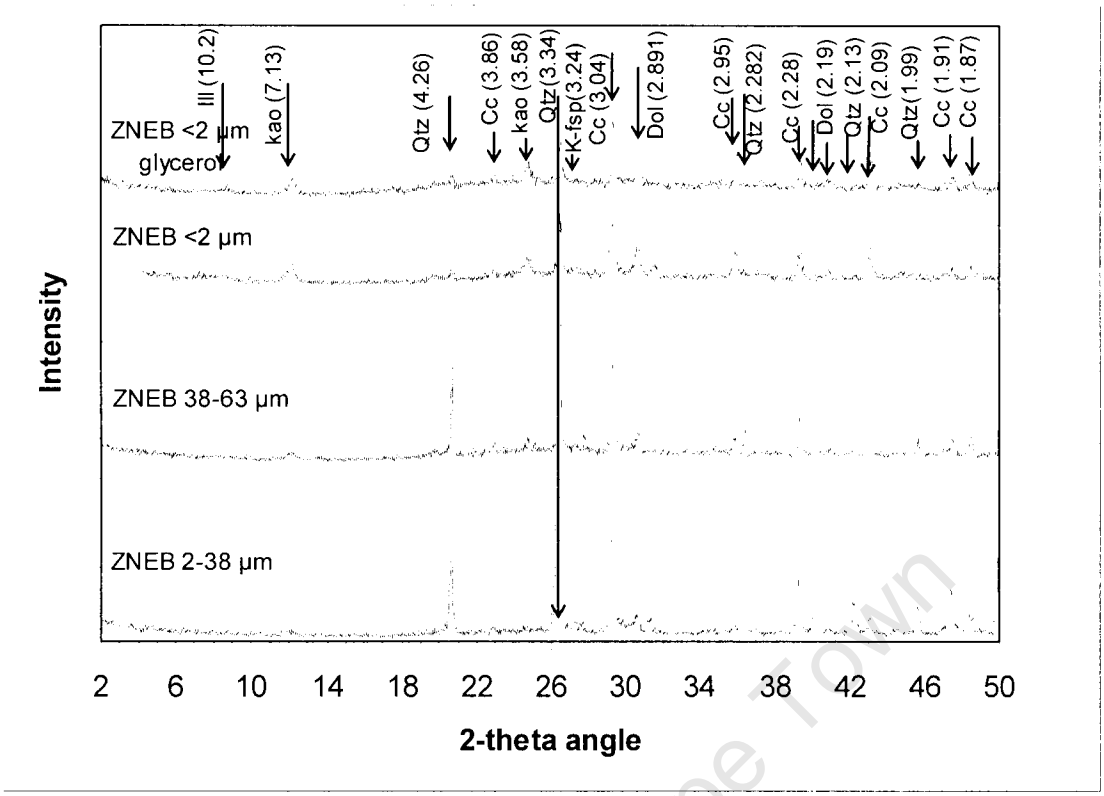

Figure 8. XRD scan showing mineralogy of sample ZNEB

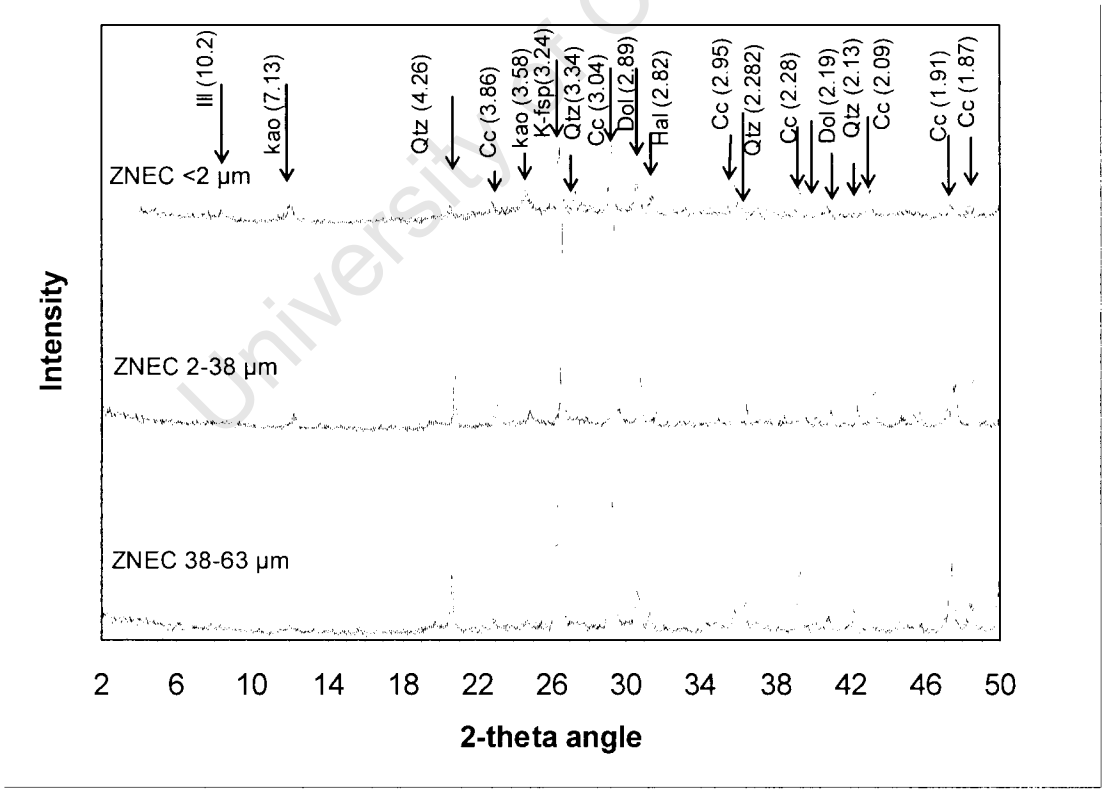

Figure 9. XRD scan showing mineralogy of sample ZNEC

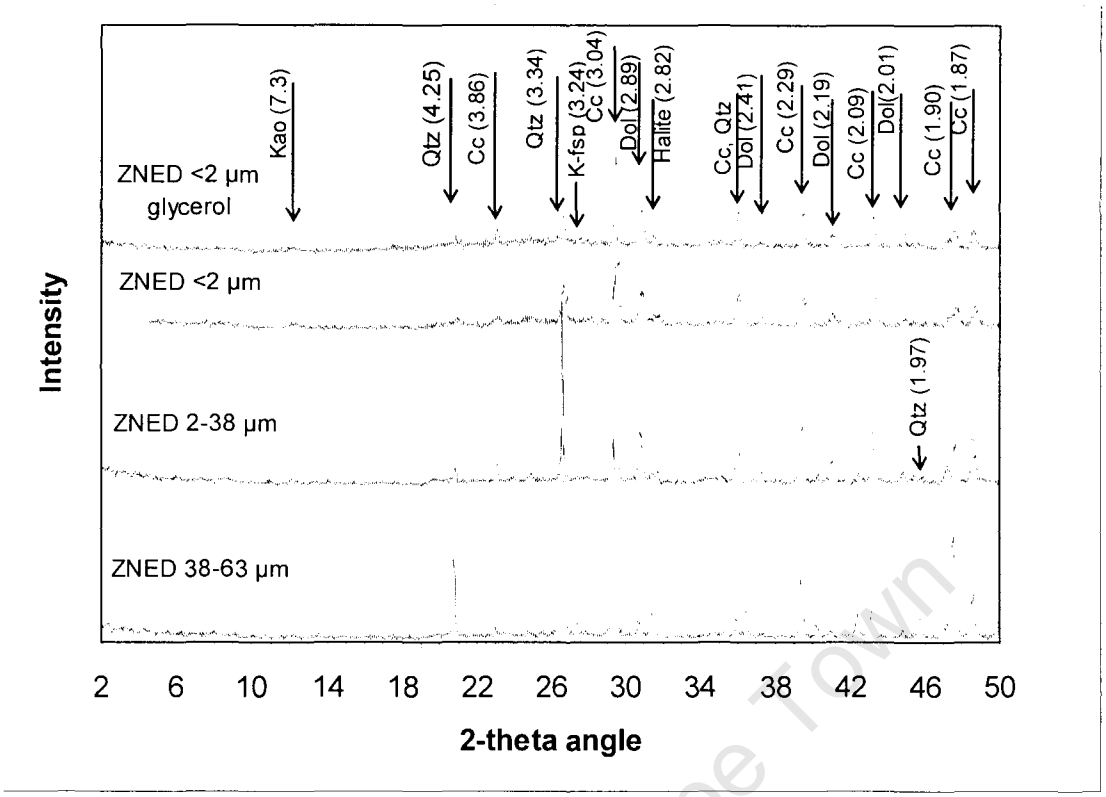

Figure 10. XRD scan showing mineralogy of sample ZNED

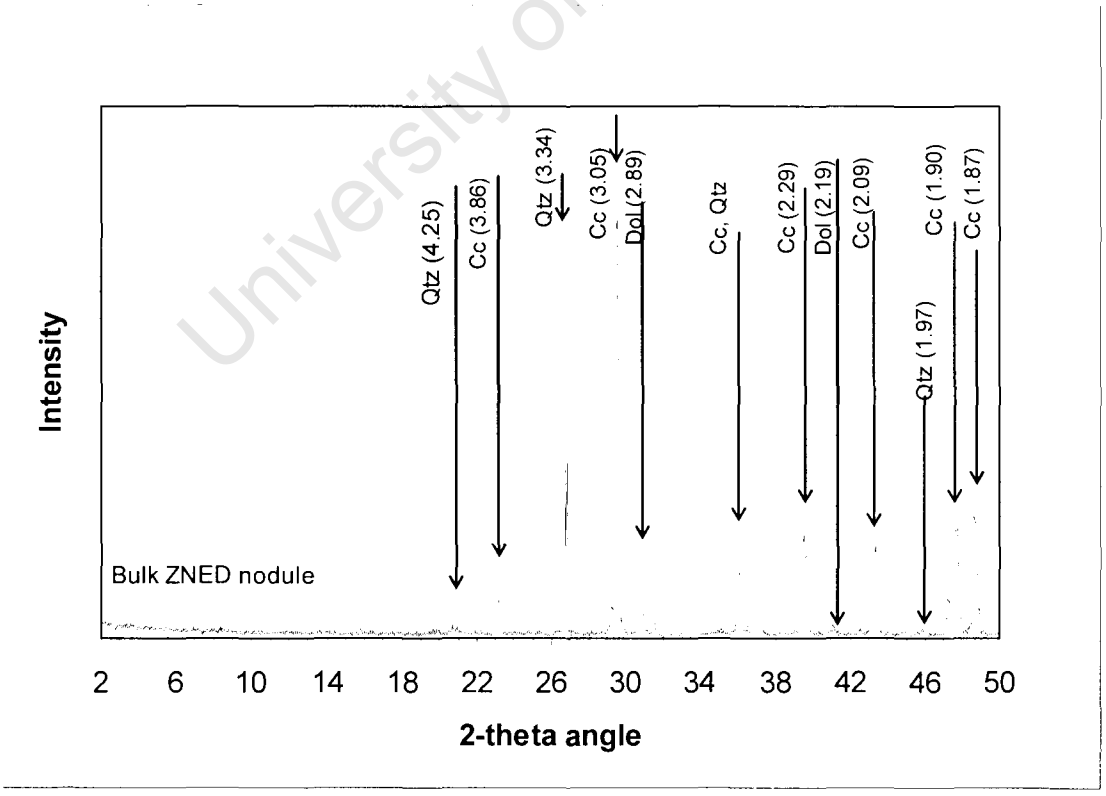

Figure 11. XRD scan showing mineralogy of sample ZNED cc nodule

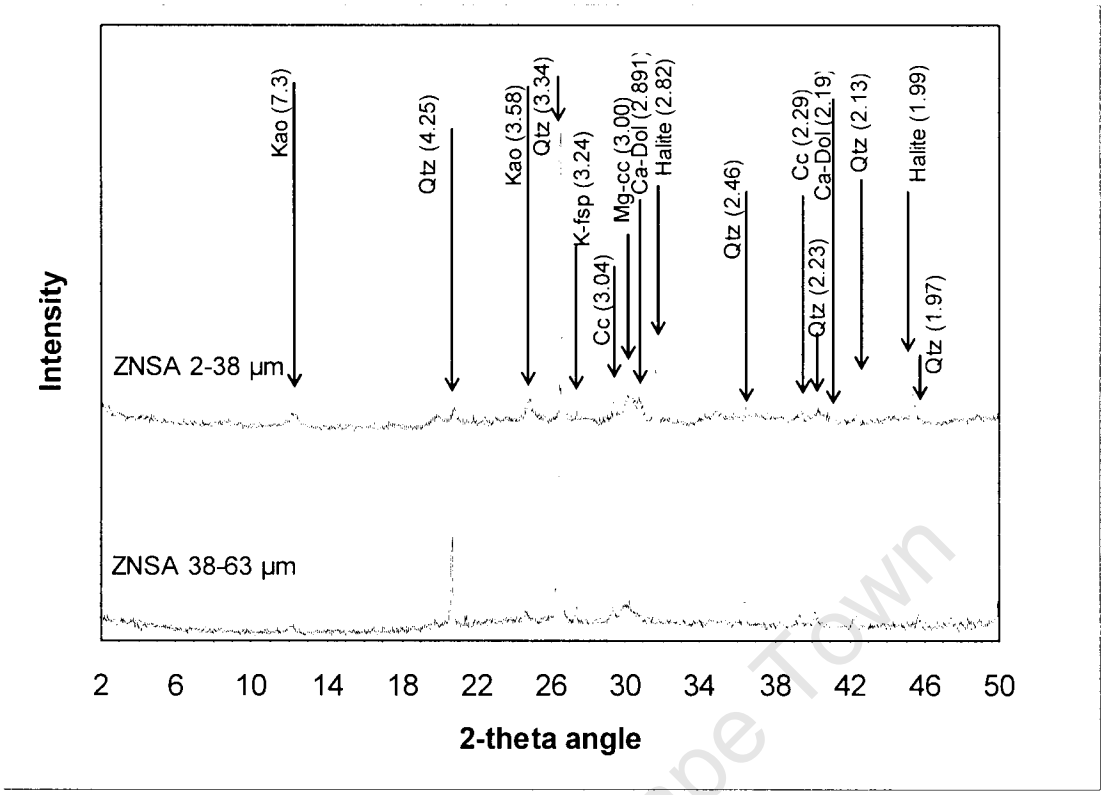

Figure 12. XRD scan showing mineralogy of sample ZNSA

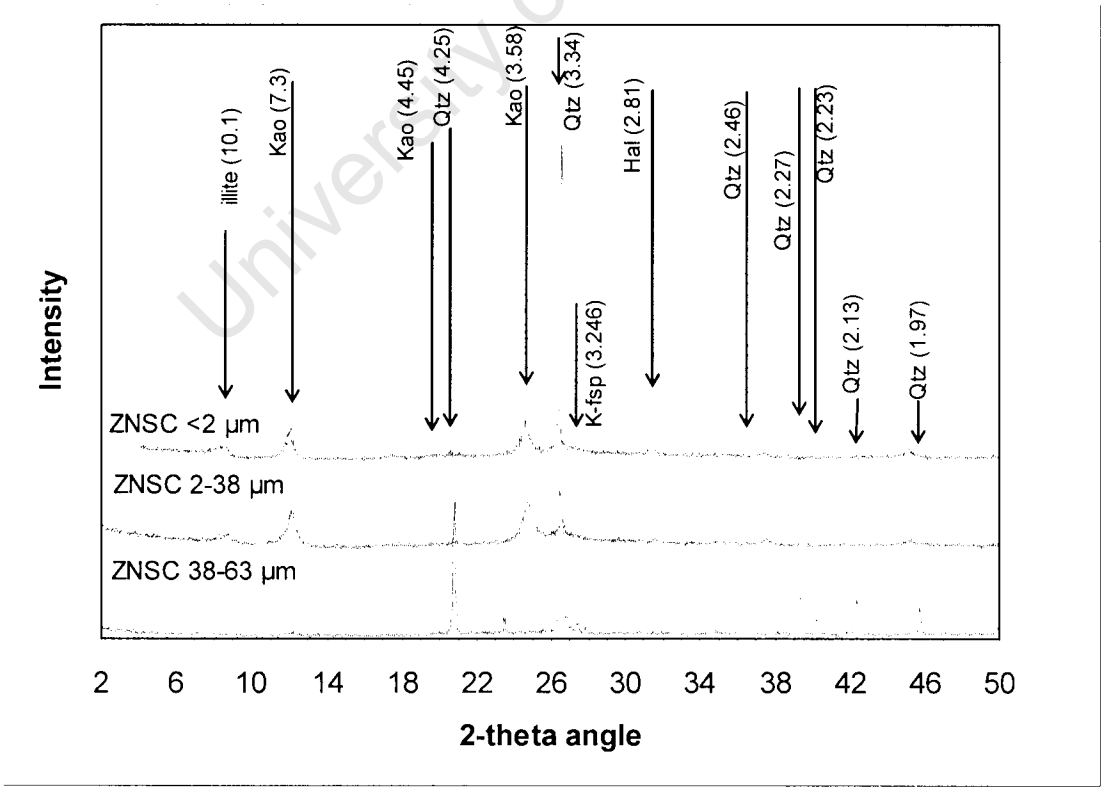

Figure 13. XRD scan showing mineralogy of sample ZNSC

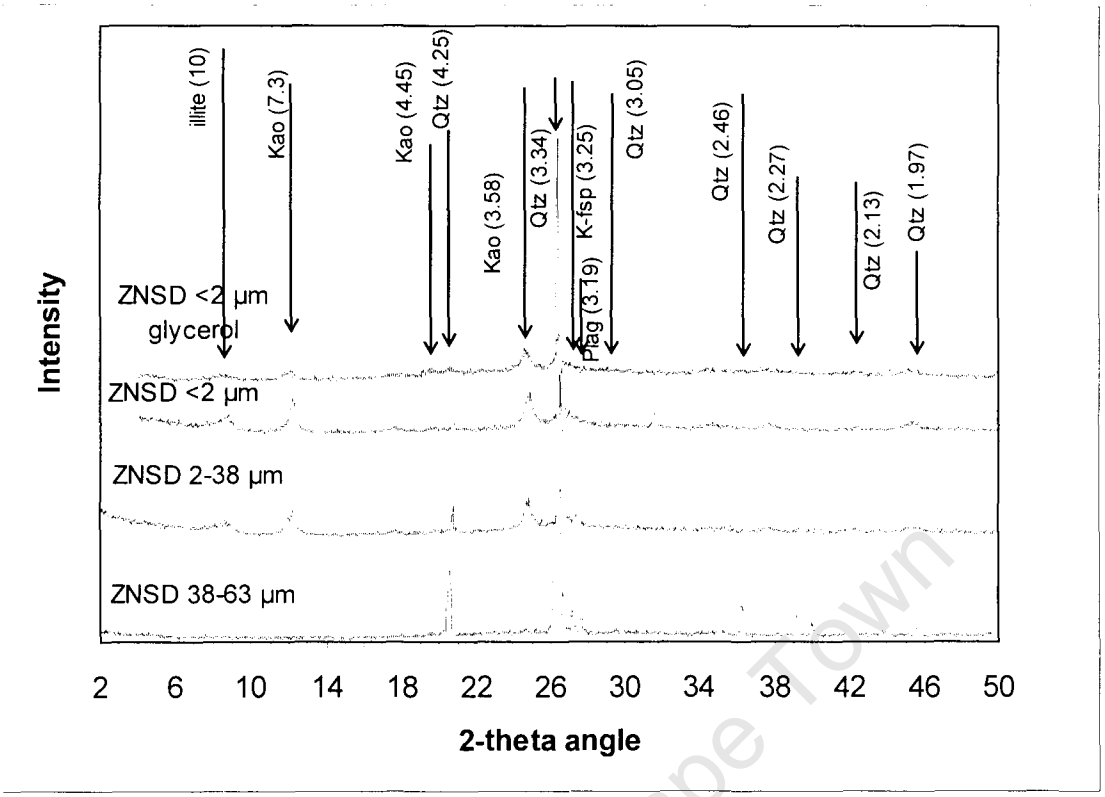

Figure 14. XRD scan showing mineralogy of sample ZNSD

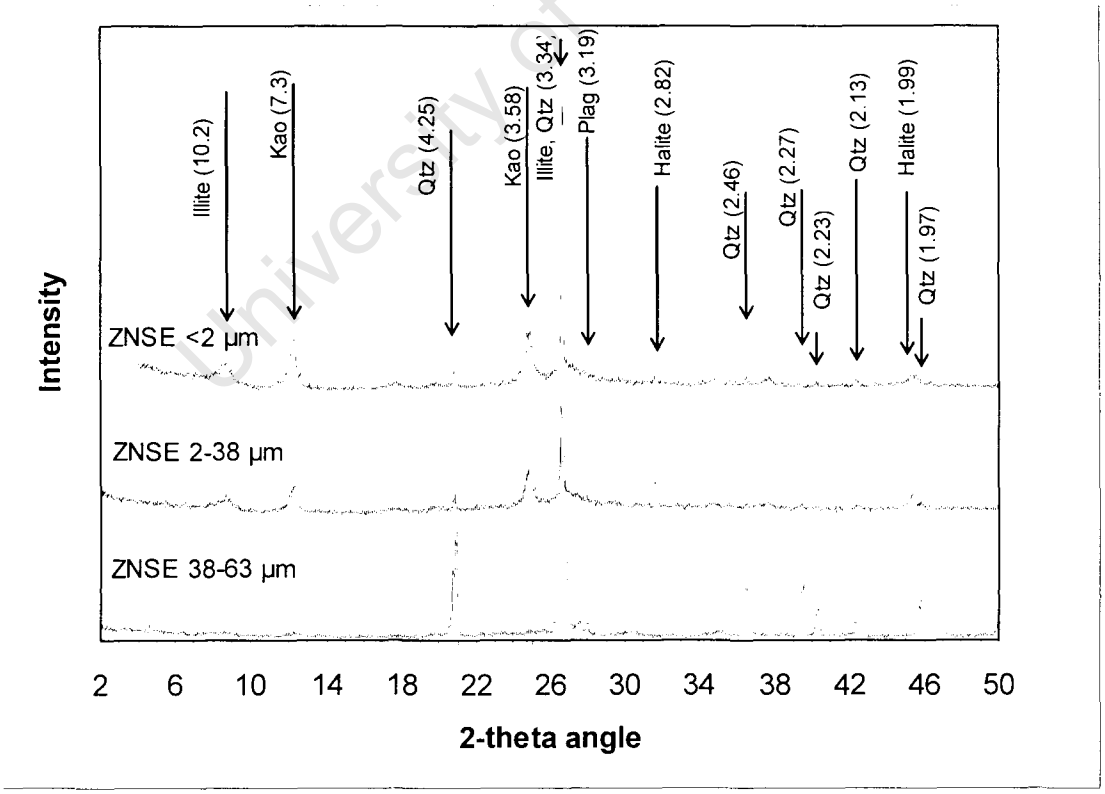

Figure 15. XRD scan showing mineralogy of sample ZNSE

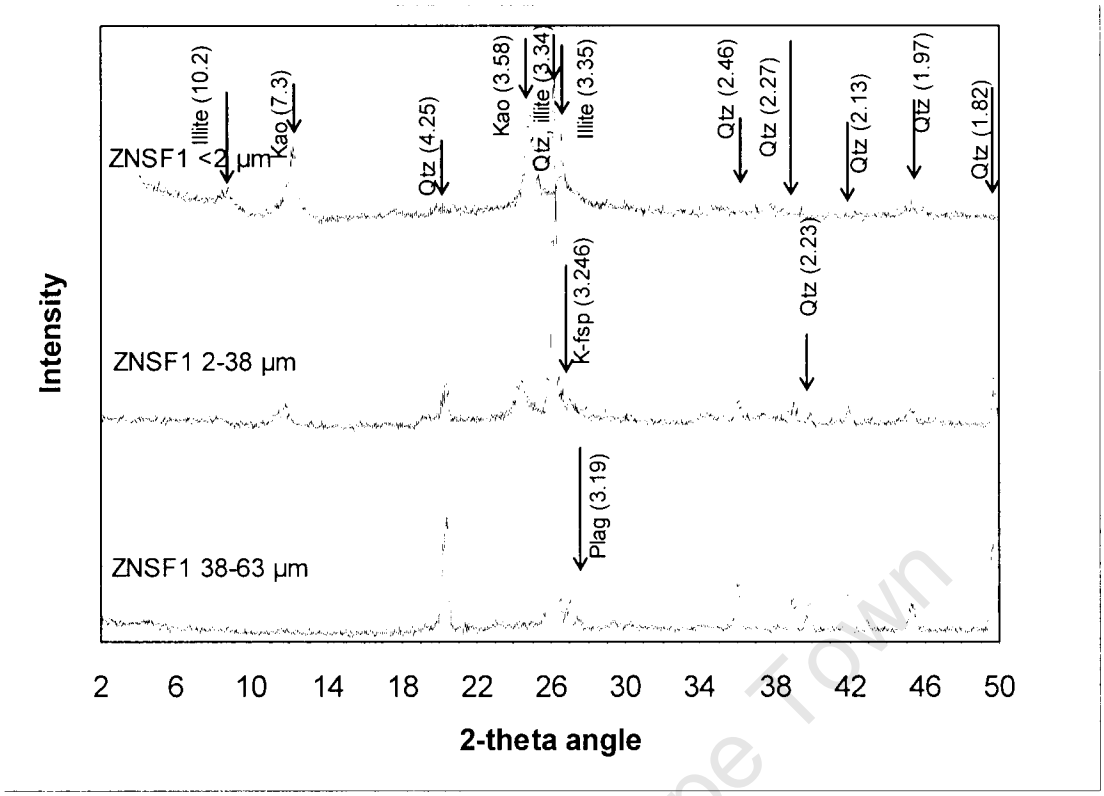

Figure 16. XRD scan showing mineralogy of sample ZNSF1

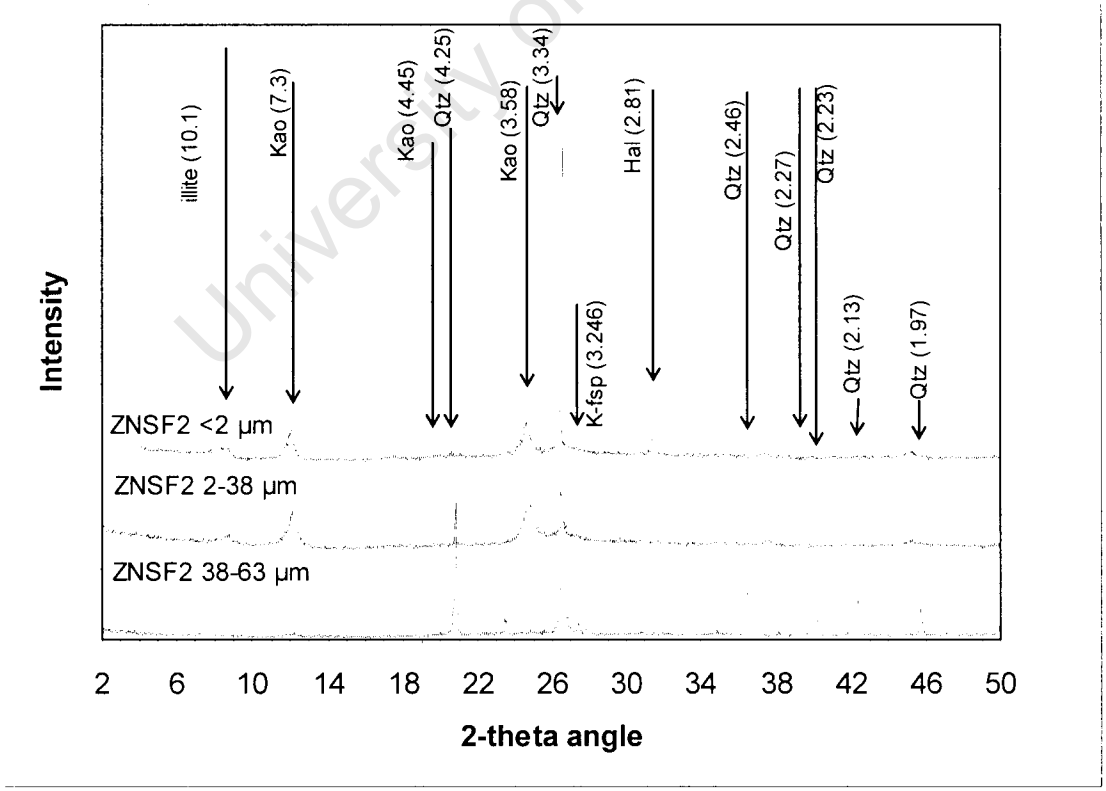

Figure 17. XRD scan showing mineralogy of sample ZNSF2

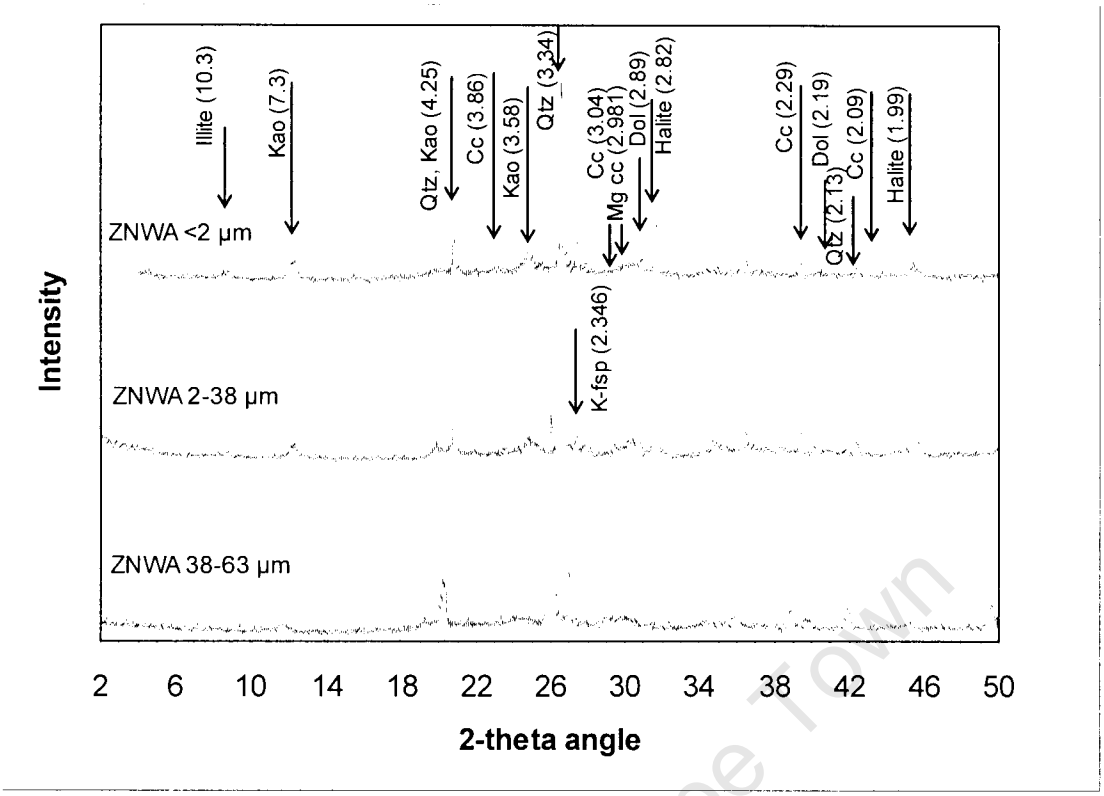

Figure 18. XRD scan showing mineralogy of sample ZNWA

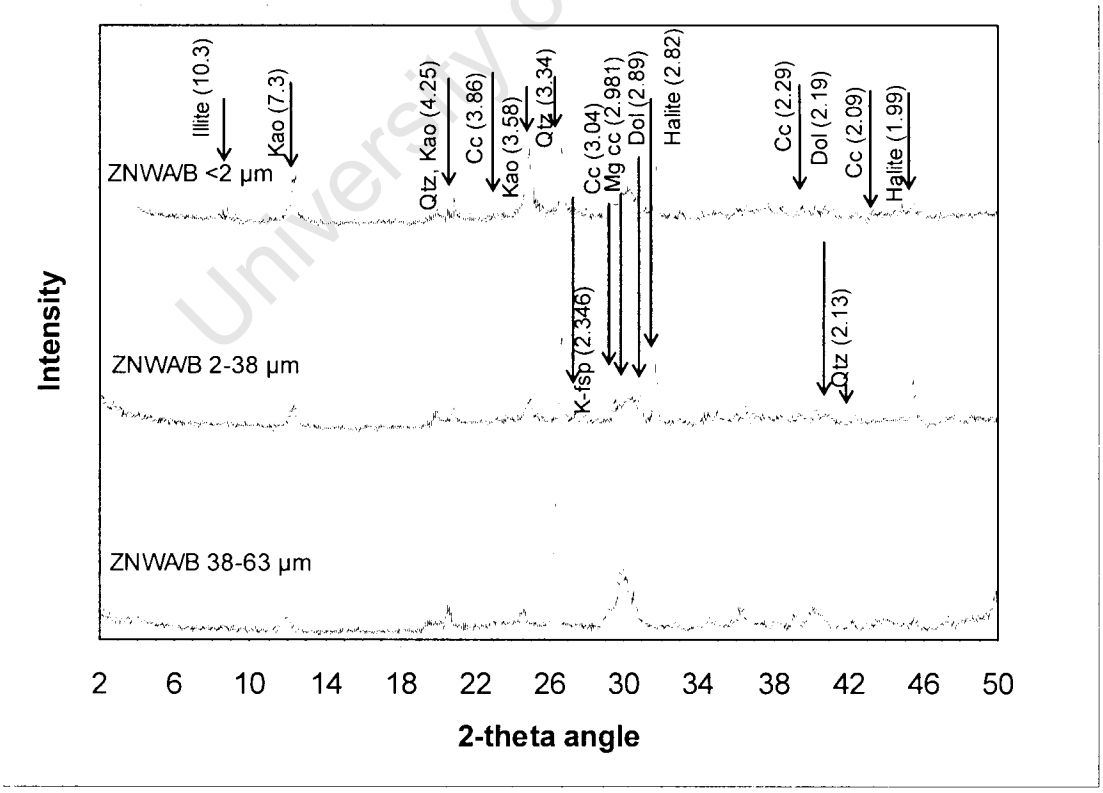

Figure 19. XRD scan showing mineralogy of sample ZNWA/B

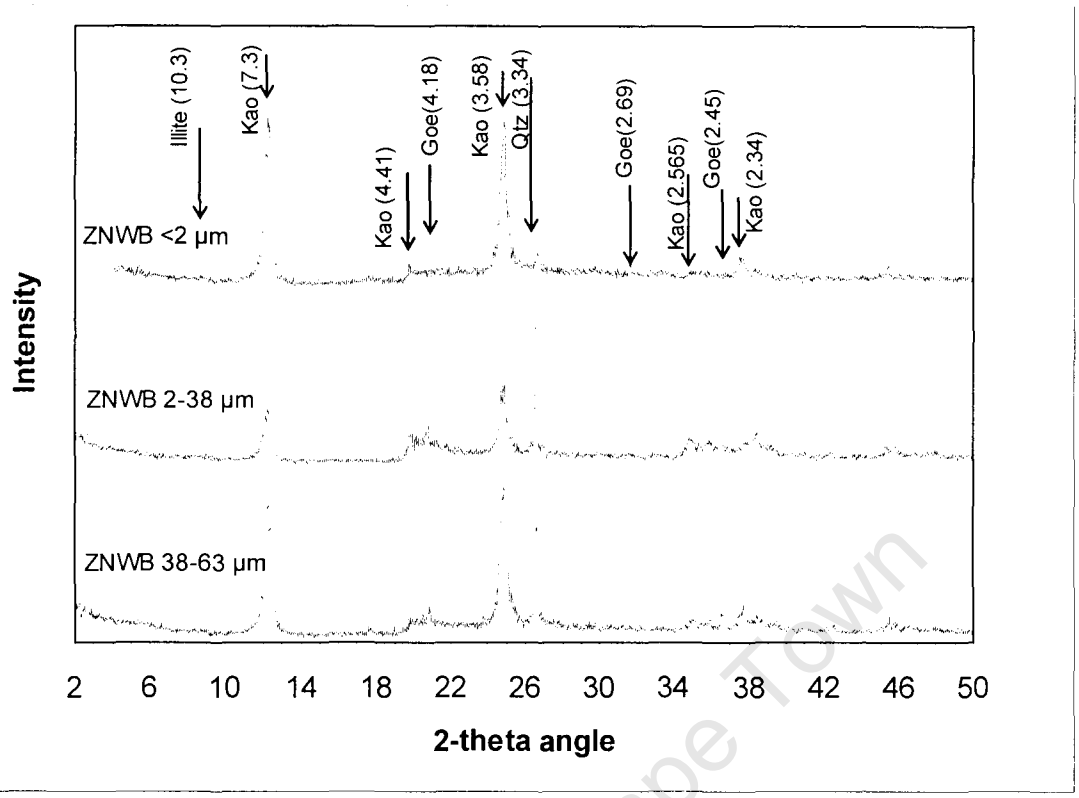

Figure 20. XRD scan showing mineralogy of sample ZNWB

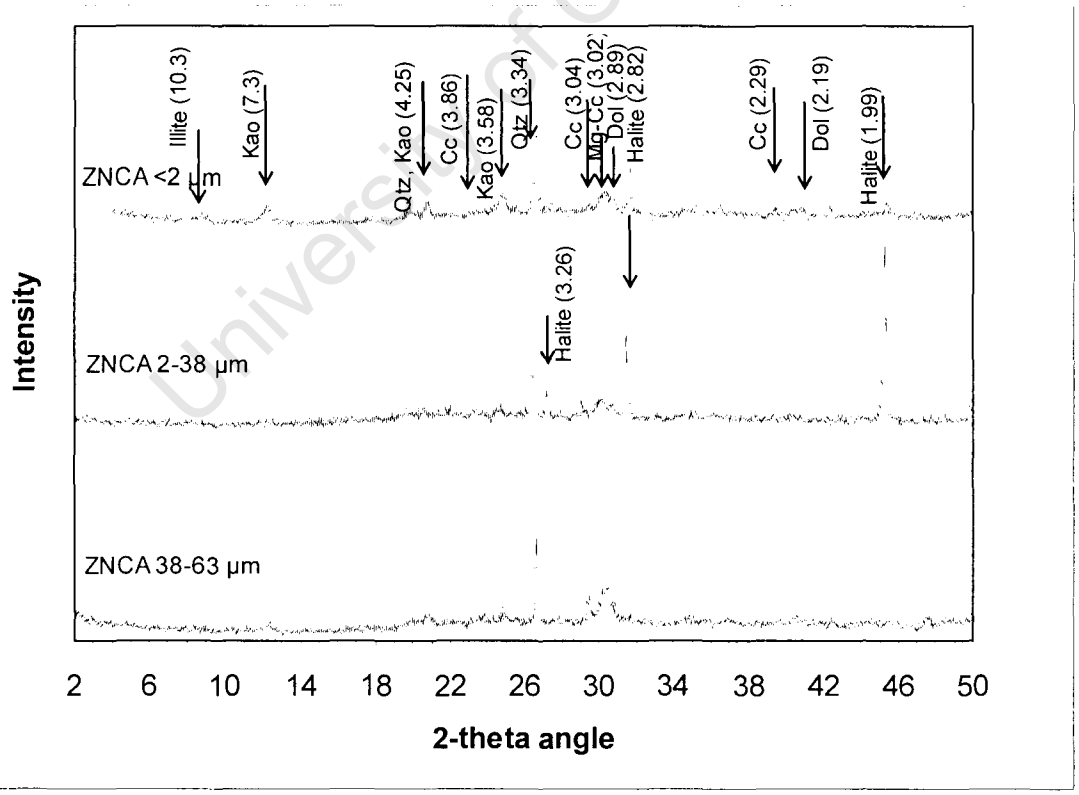

Figure 21. XRD scan showing mineralogy of sample ZNCA

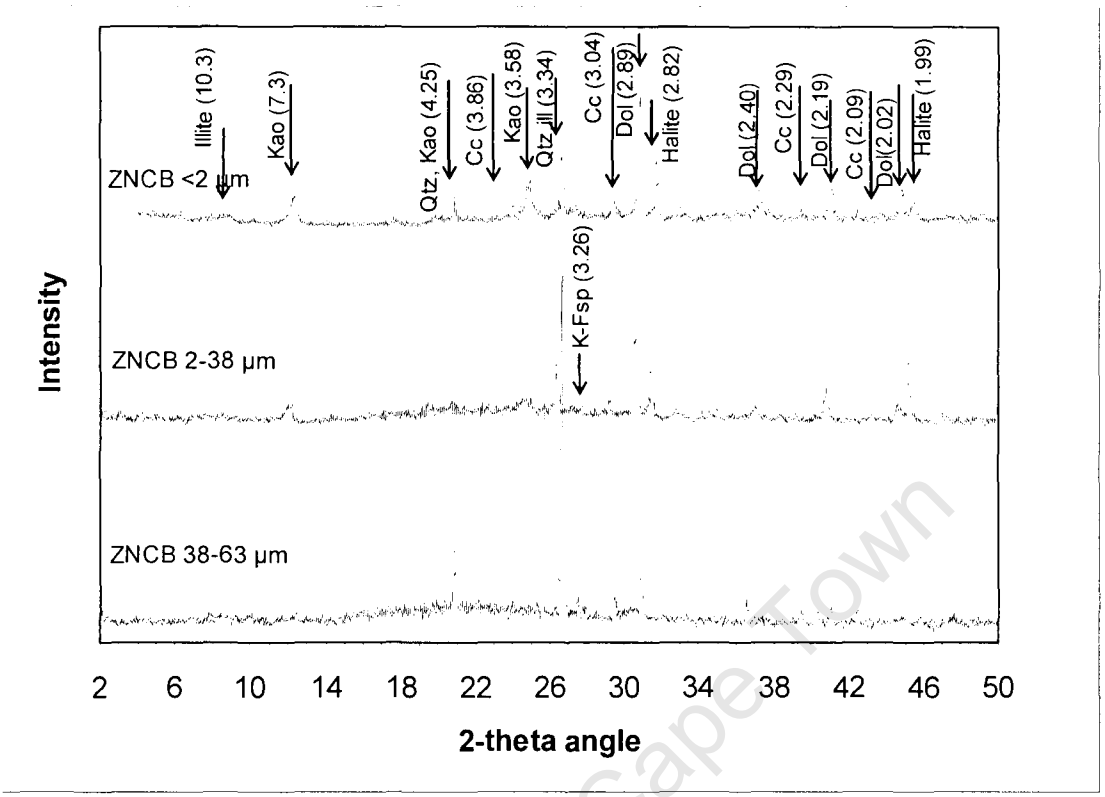

Figure 22. XRD scan showing mineralogy of sample ZNCB

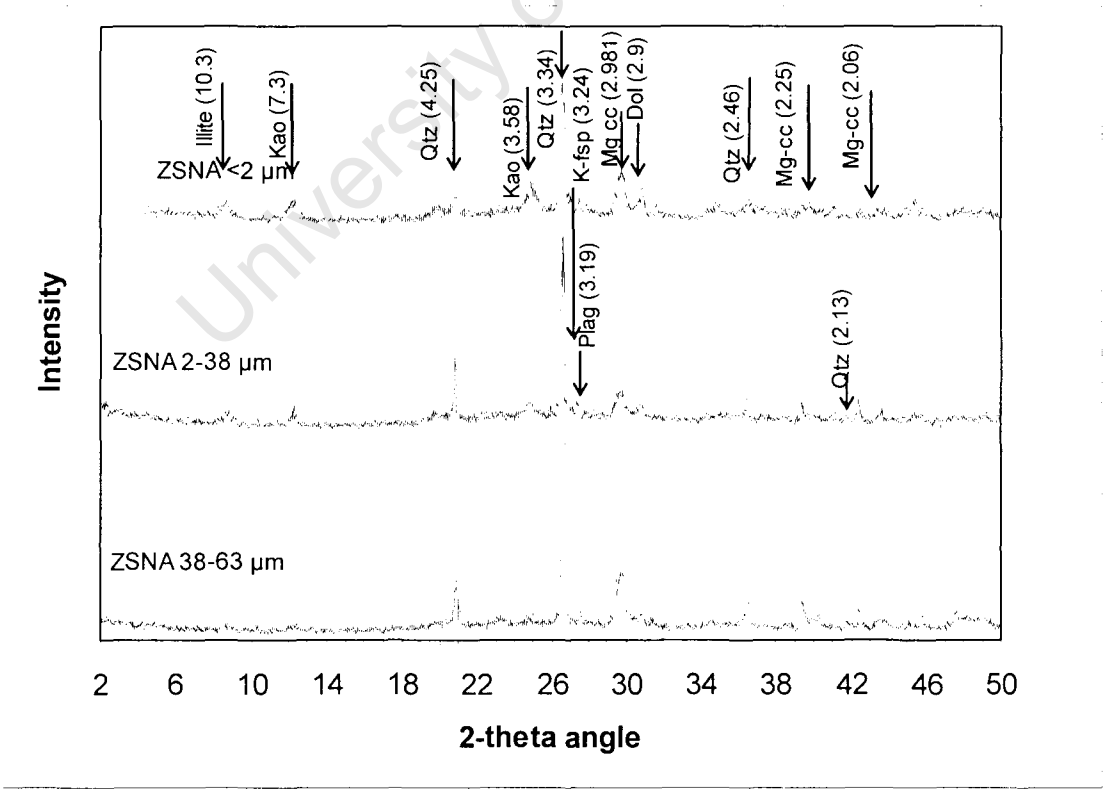

Figure 23. XRD scan showing mineralogy of sample ZSNA

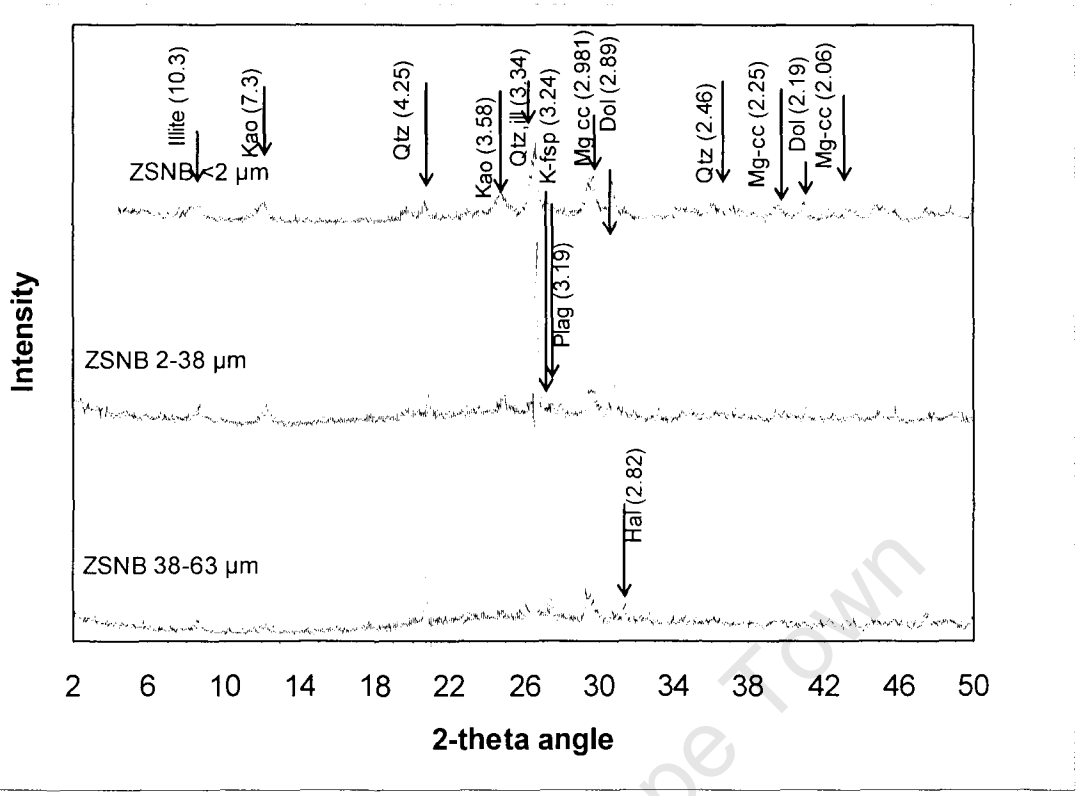

Figure 24. XRD scan showing mineralogy of sample ZSNB

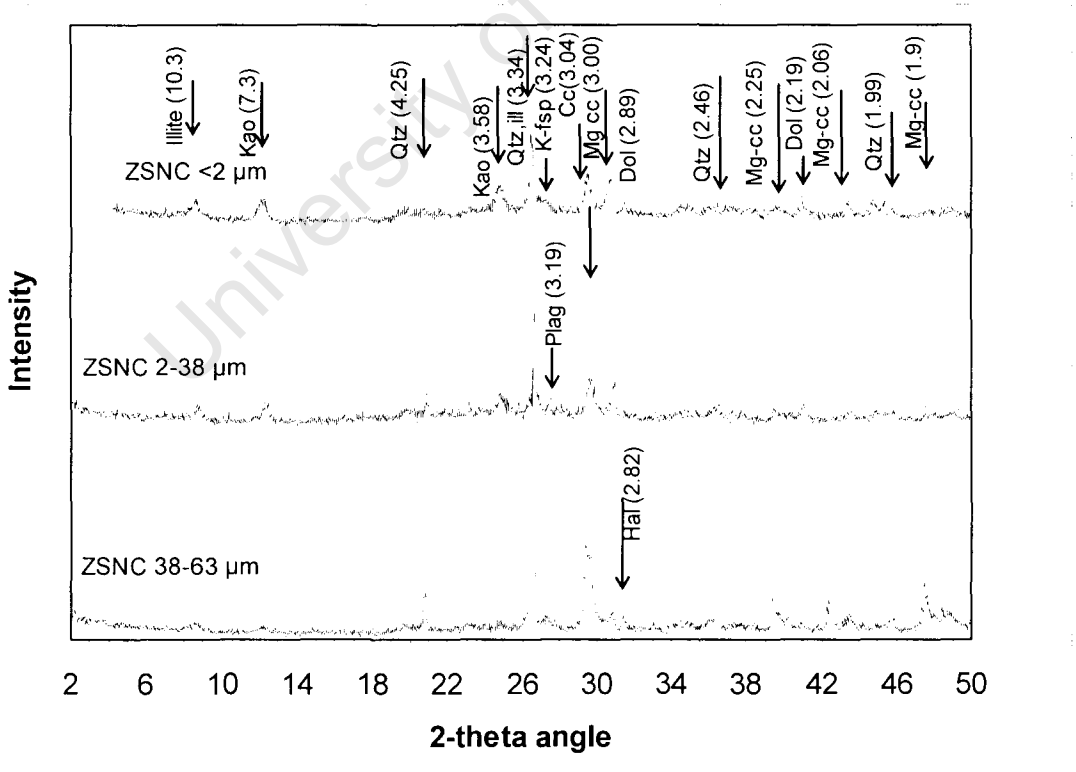

Figure 25. XRD scan showing mineralogy of sample ZSNC

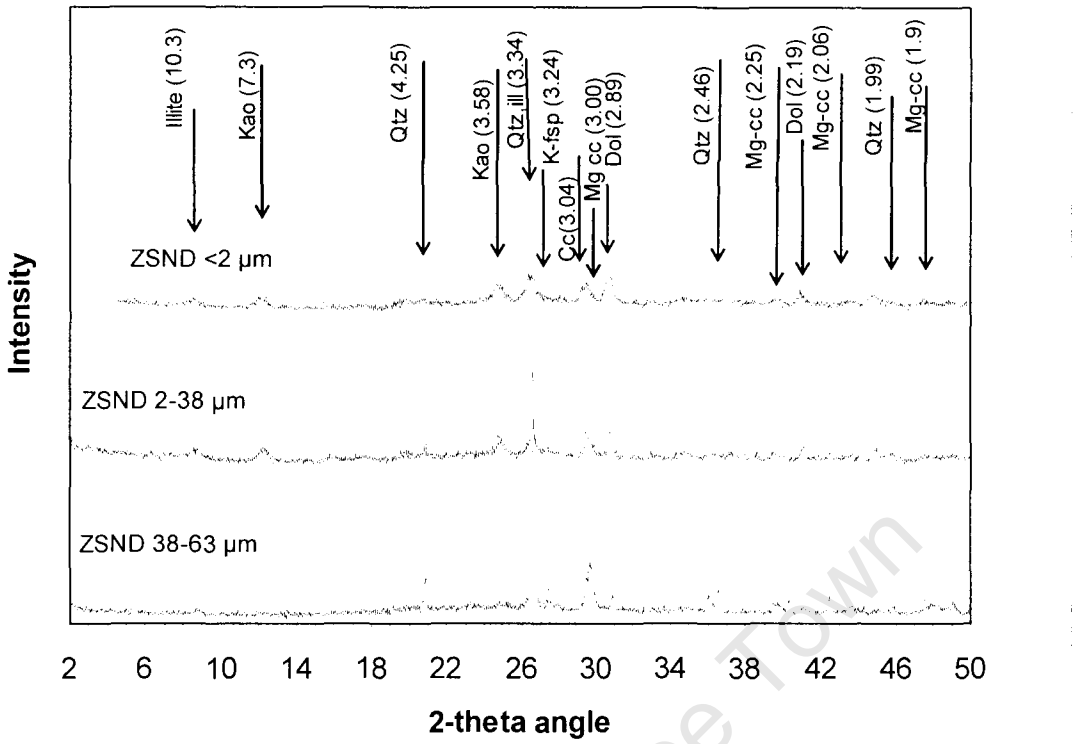

Figure 26. XRD scan showing mineralogy of sample ZSND

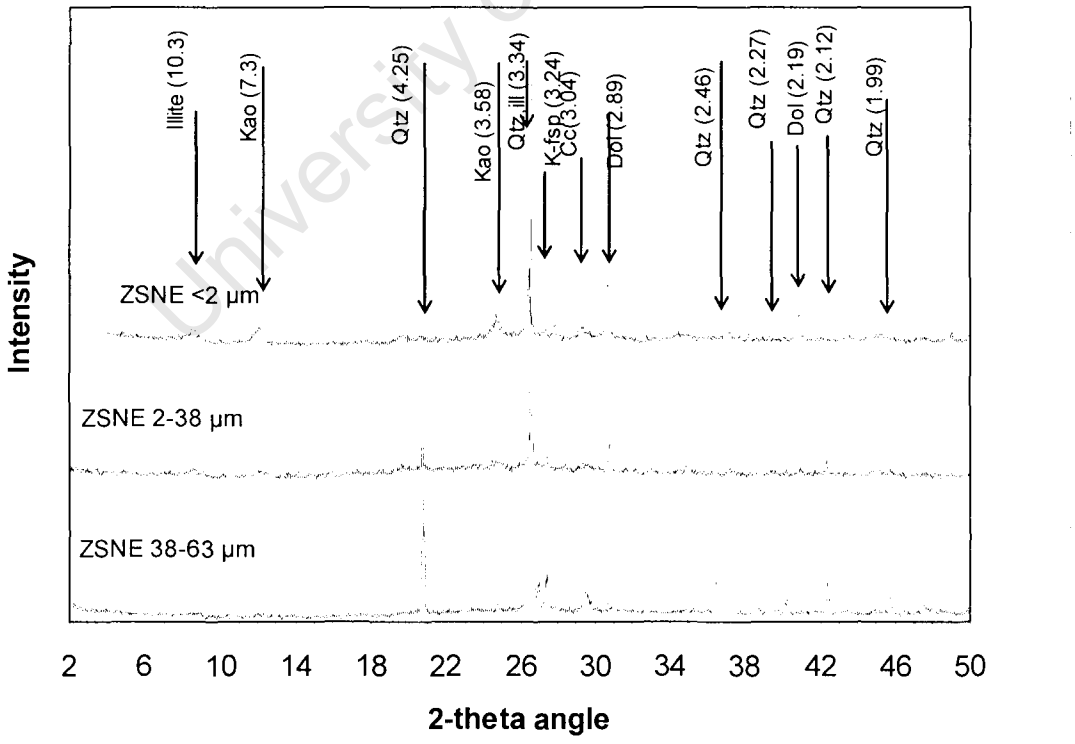

Figure 27. XRD scan showing mineralogy of sample ZSNE

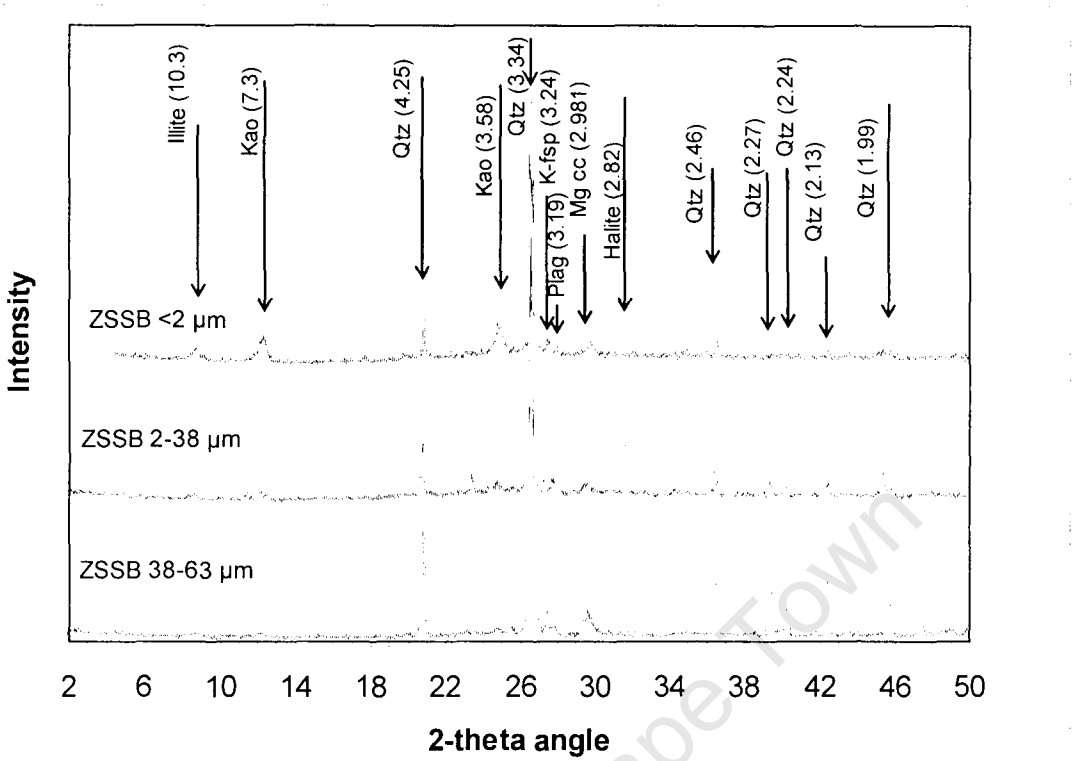

Figure 28. XRD scan showing mineralogy of sample ZSSB

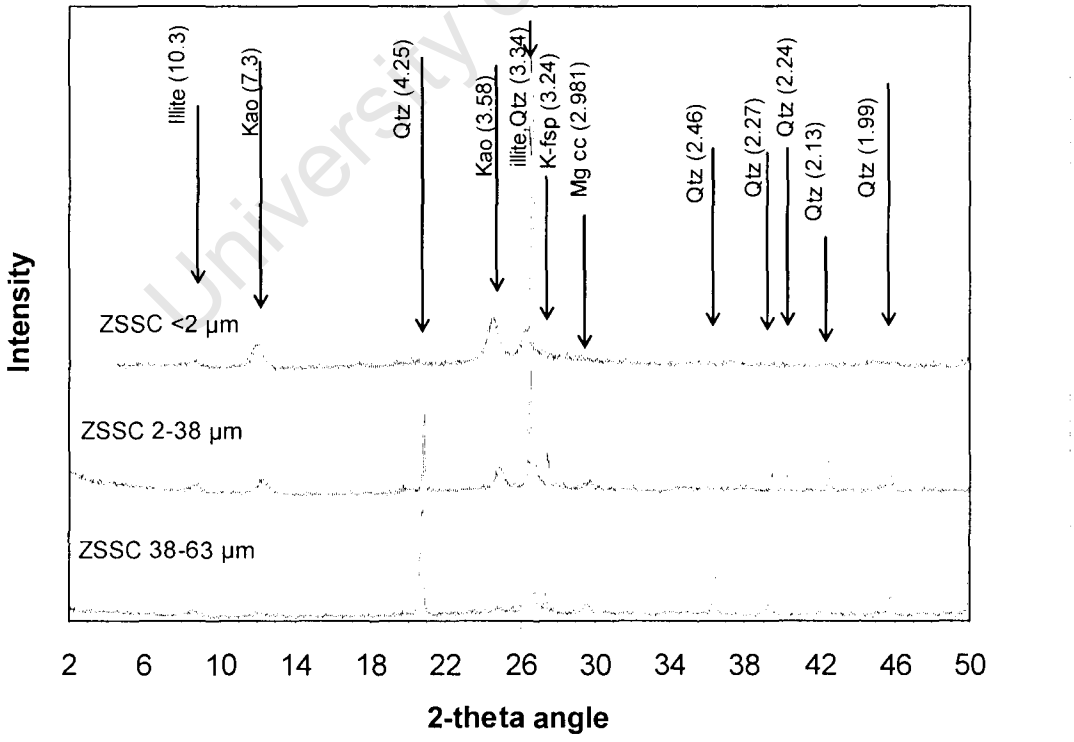

Figure 29. XRD scan showing mineralogy of sample ZSSC

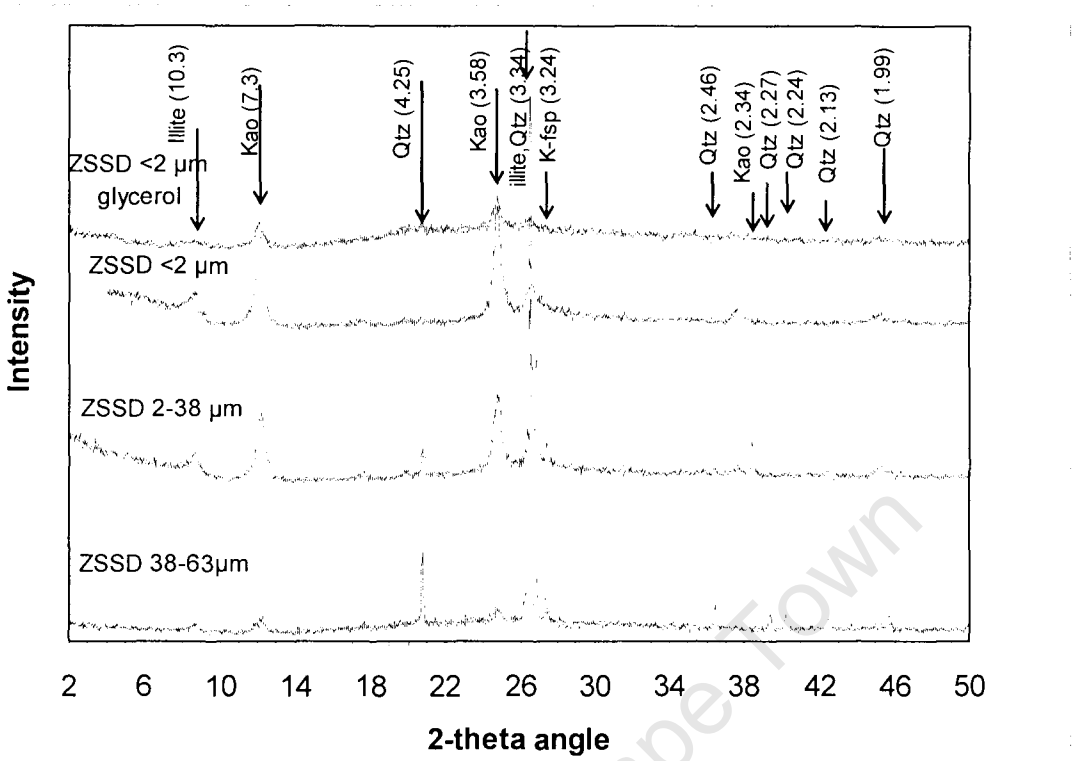

Figure 30. XRD scan showing mineralogy of sample ZSSD

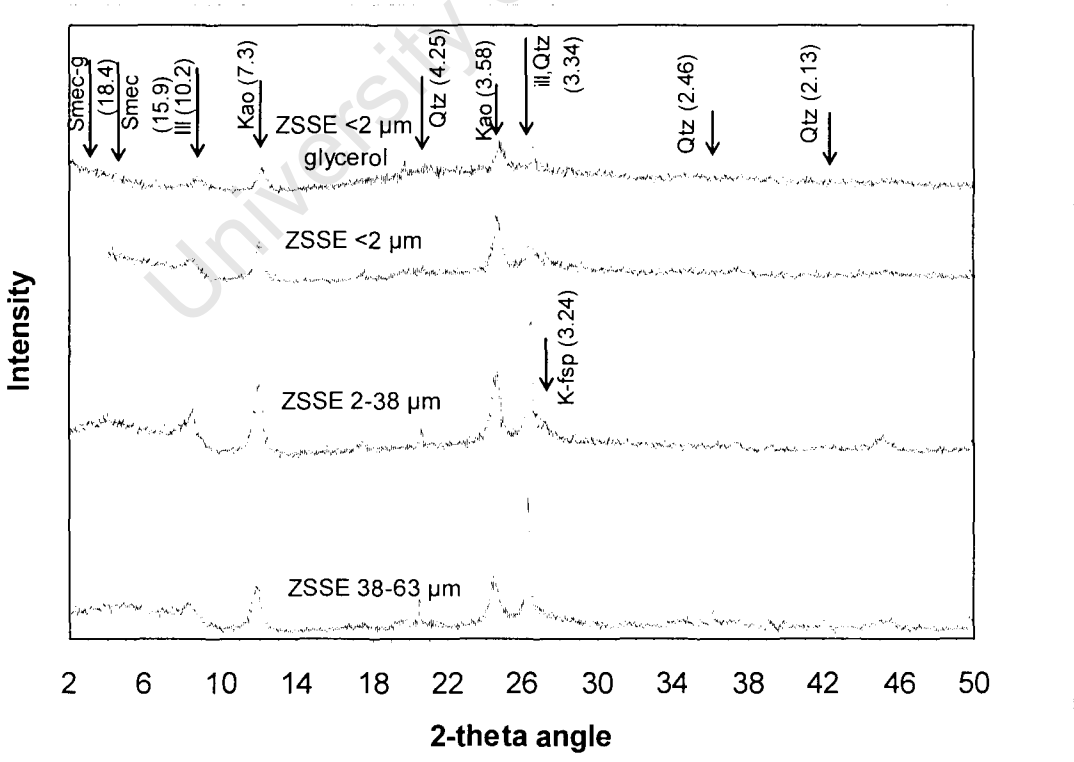

Figure 31. XRD scan showing mineralogy of sample ZSSE

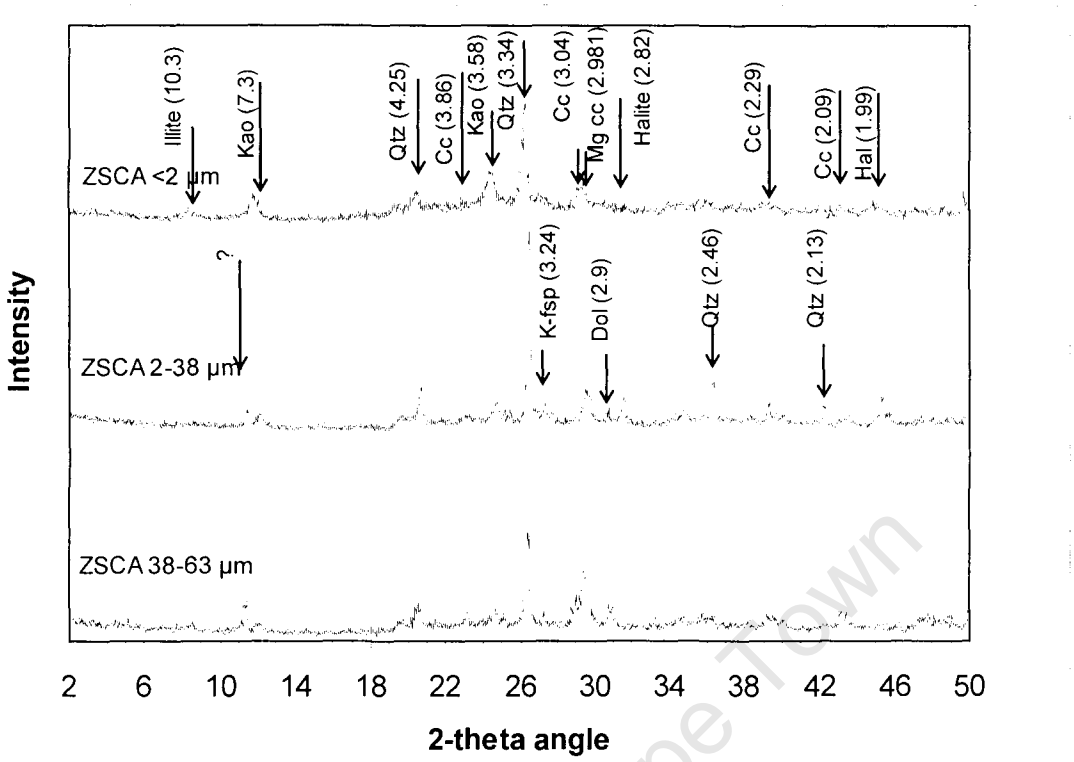

Figure 32. XRD scan showing mineralogy of sample ZSCA

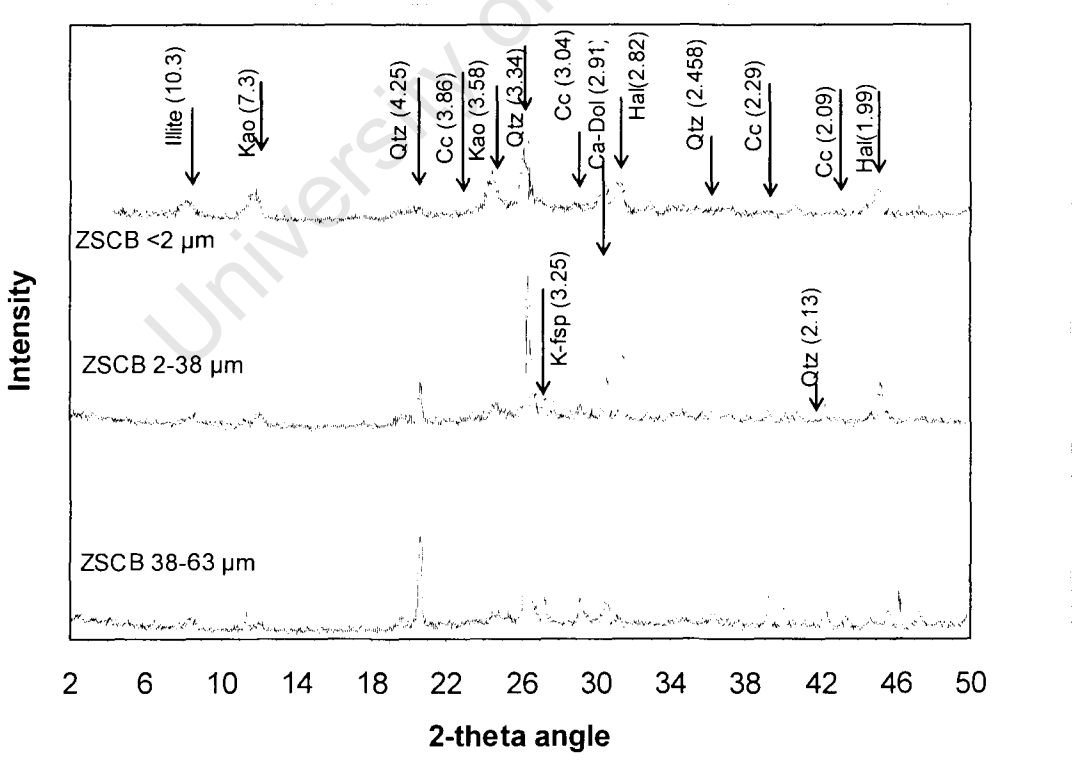

Figure 33. XRD scan showing mineralogy of sample ZSCB

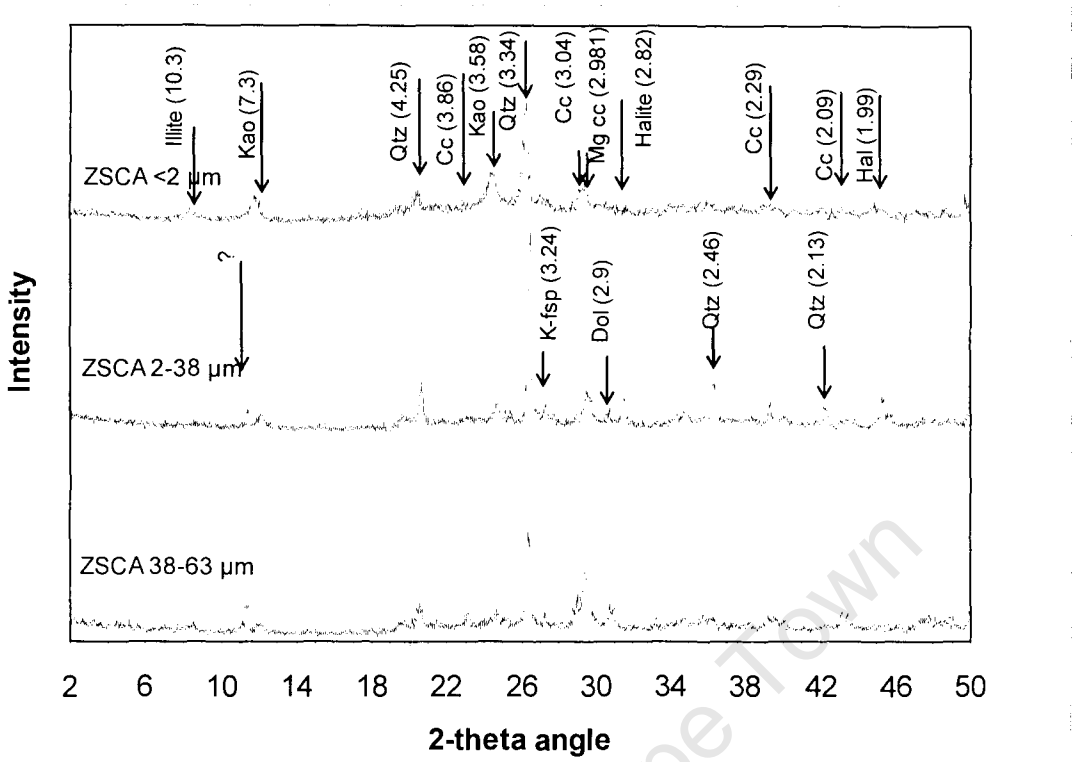

Figure 34. XRD scan showing mineralogy of sample ZSCC

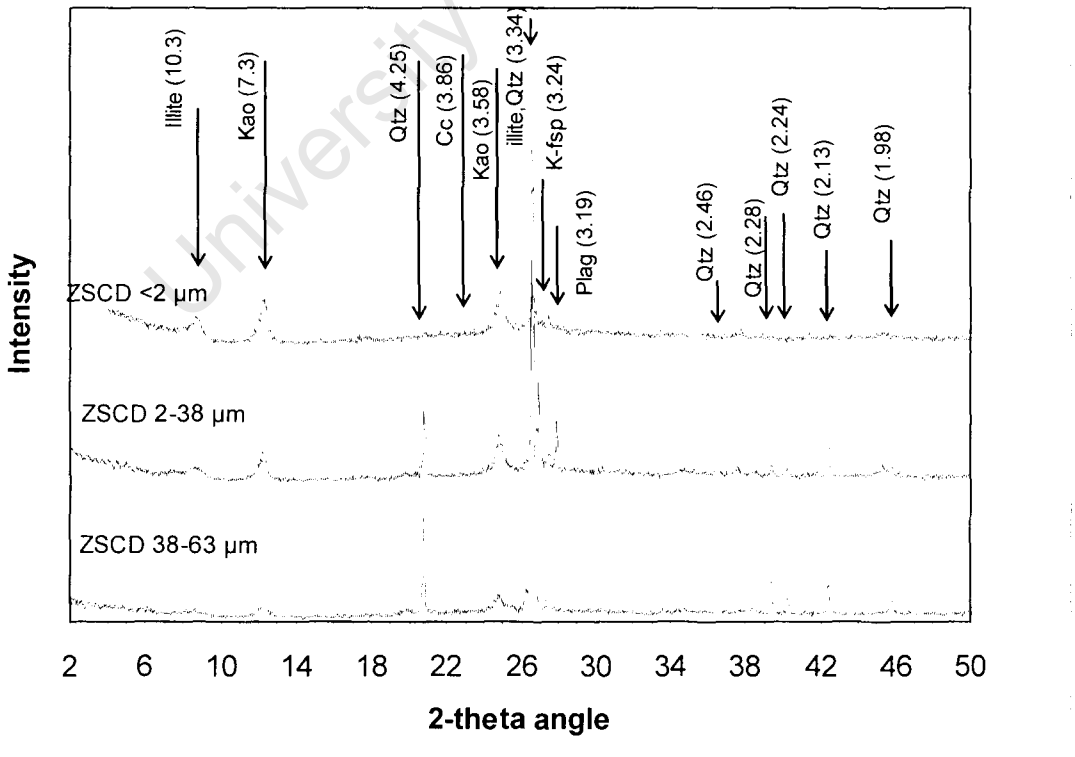

Figure 35. XRD scan showing mineralogy of sample ZSCD

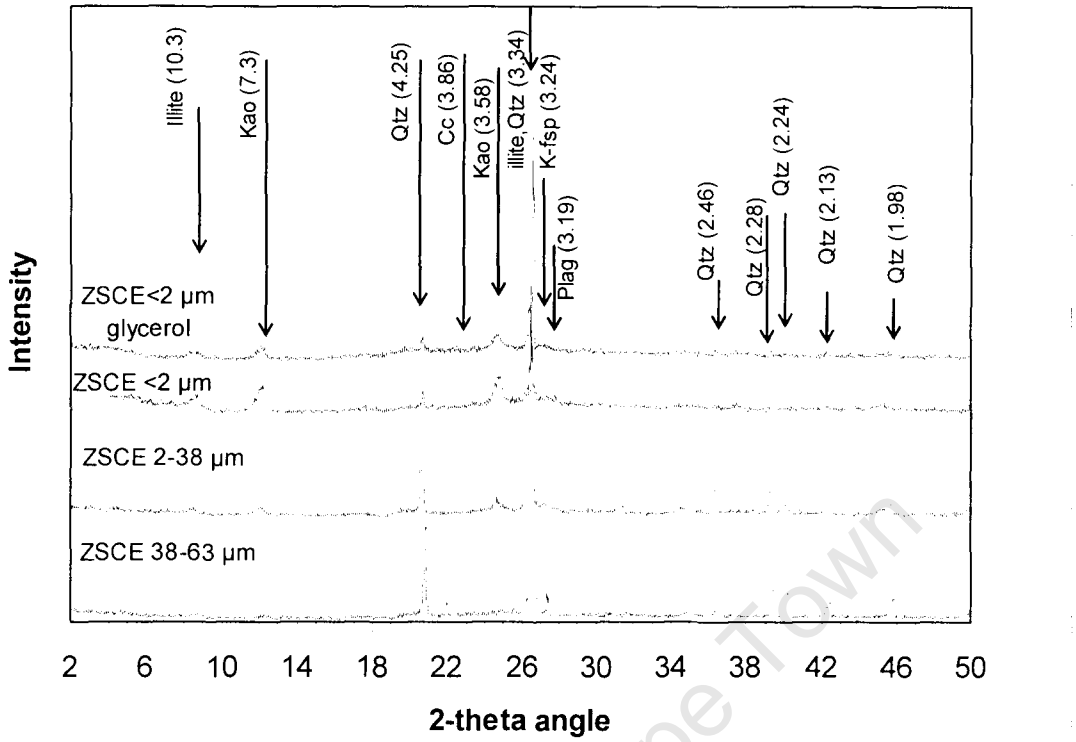

Figure 36. XRD scan showing mineralogy of sample ZSCE

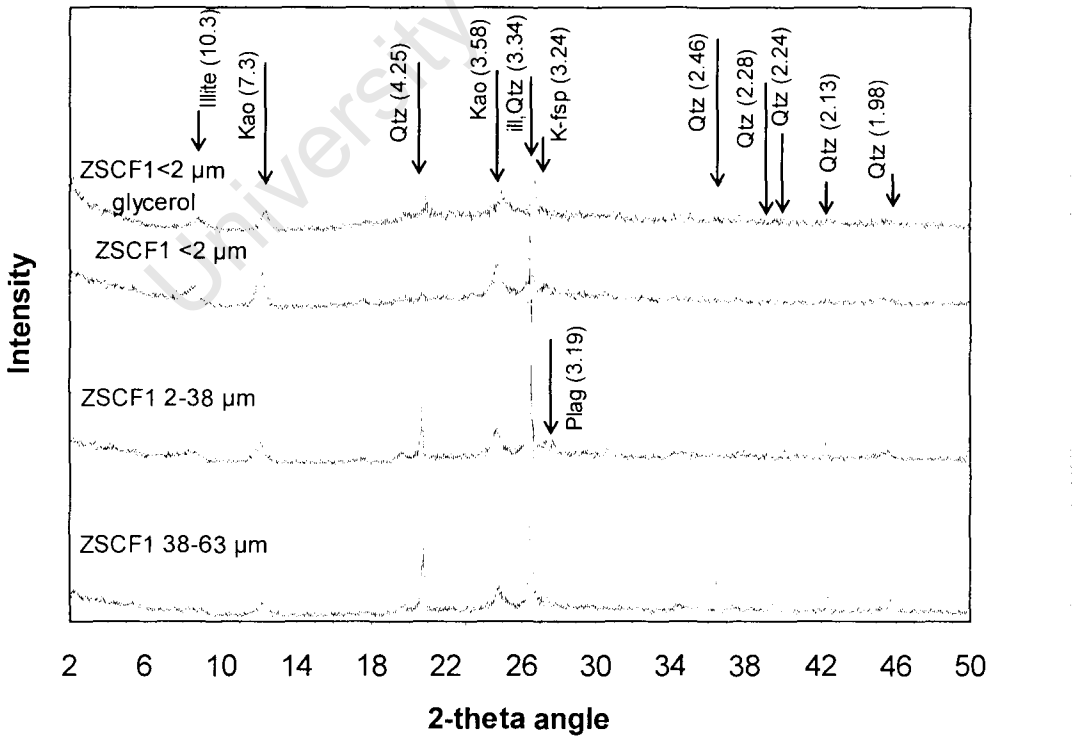

Figure 37. XRD scan showing mineralogy of sample ZSCF1

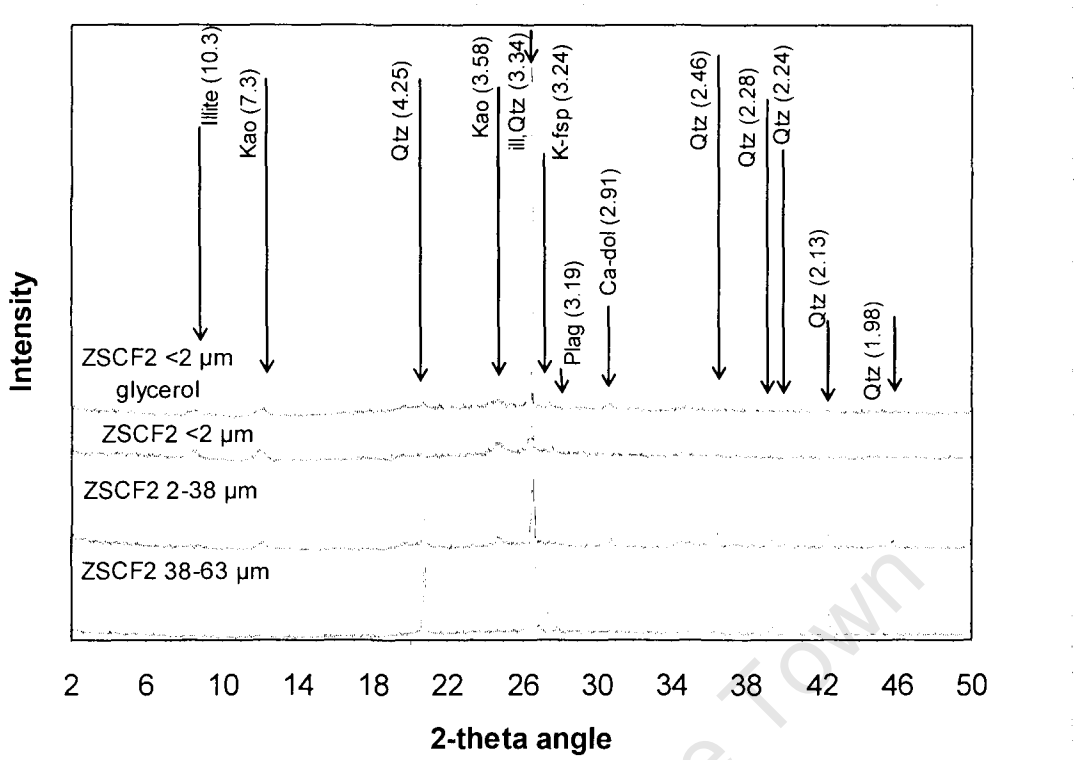

Figure 38. XRD scan showing mineralogy of sample ZSCF2

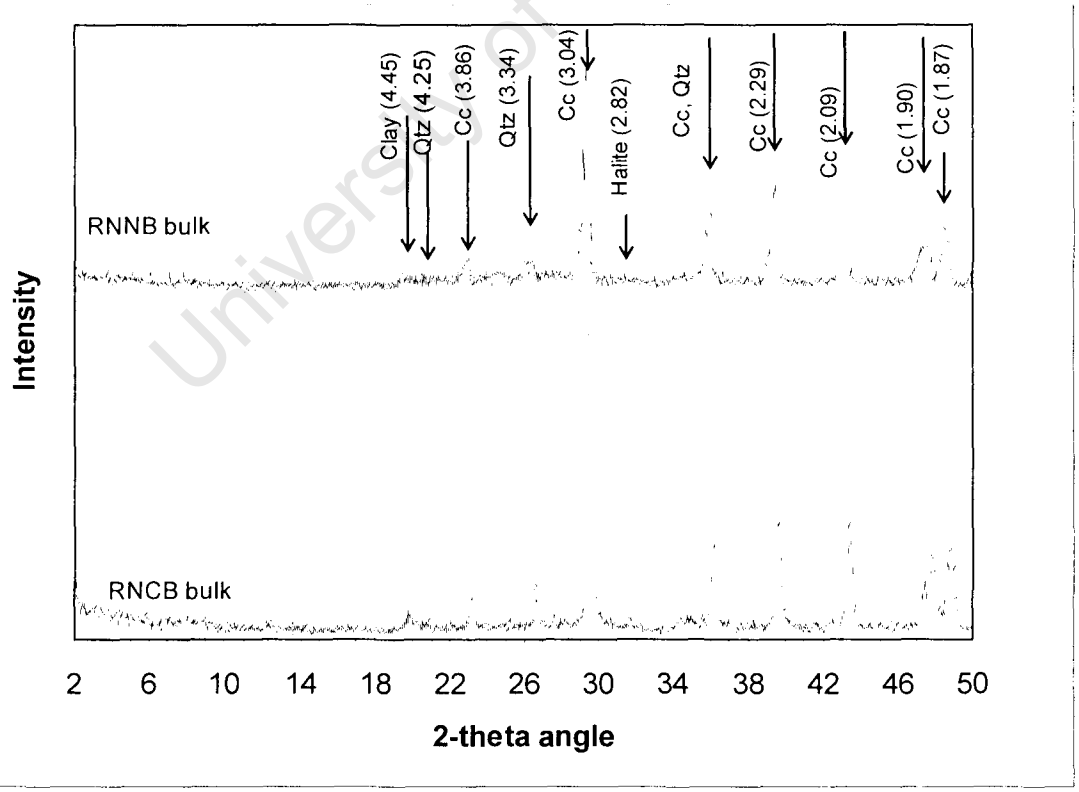

Figure 39. XRD scan showing mineralogy of sample RNNB and RNCB

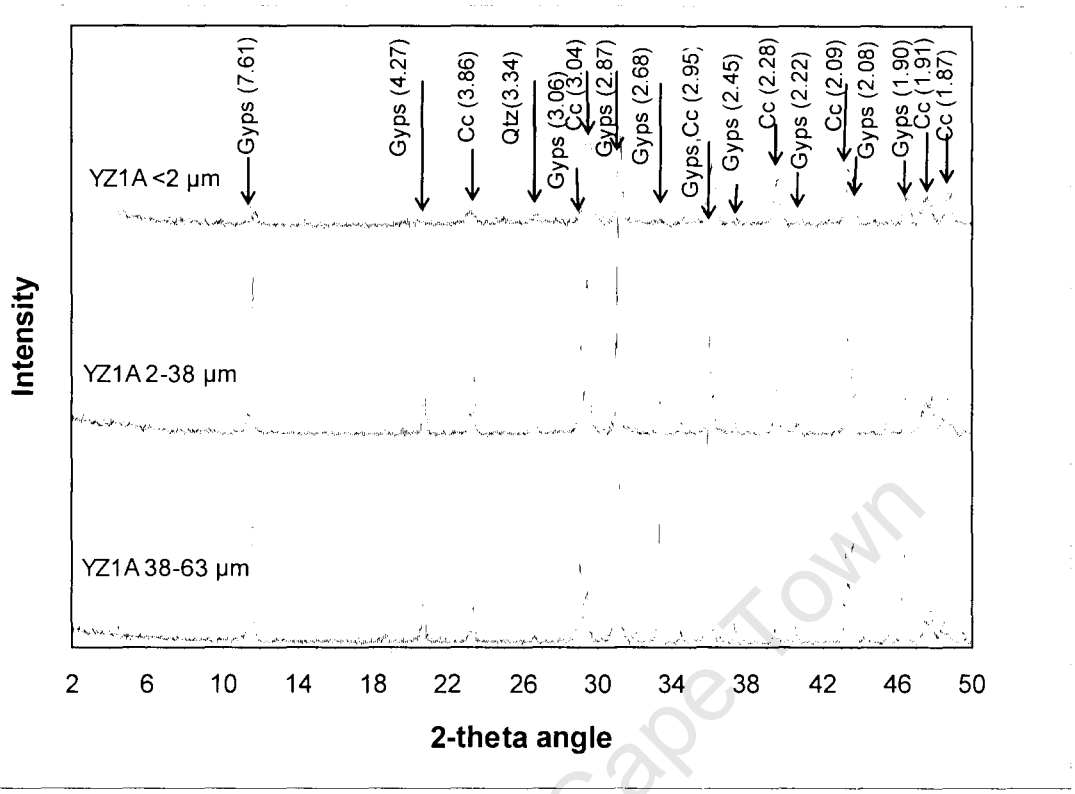

Figure 40. XRD scan showing mineralogy of sample YZ1A

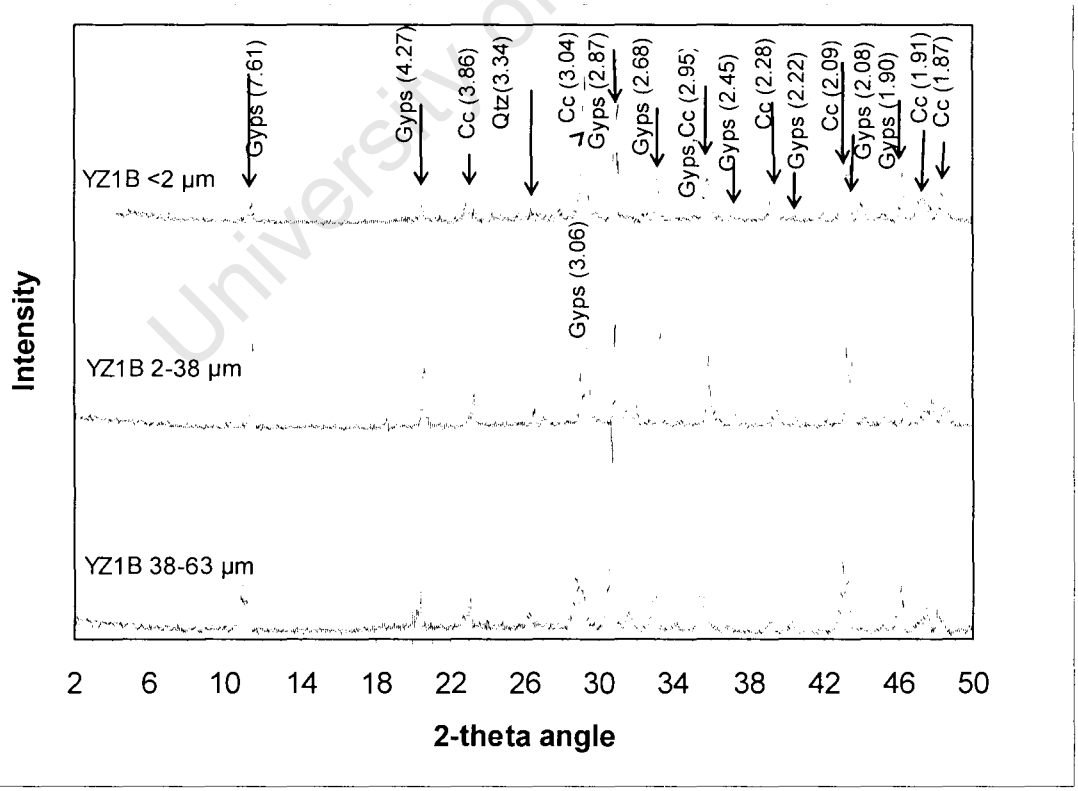

Figure 41. XRD scan showing mineralogy of sample YZ1B

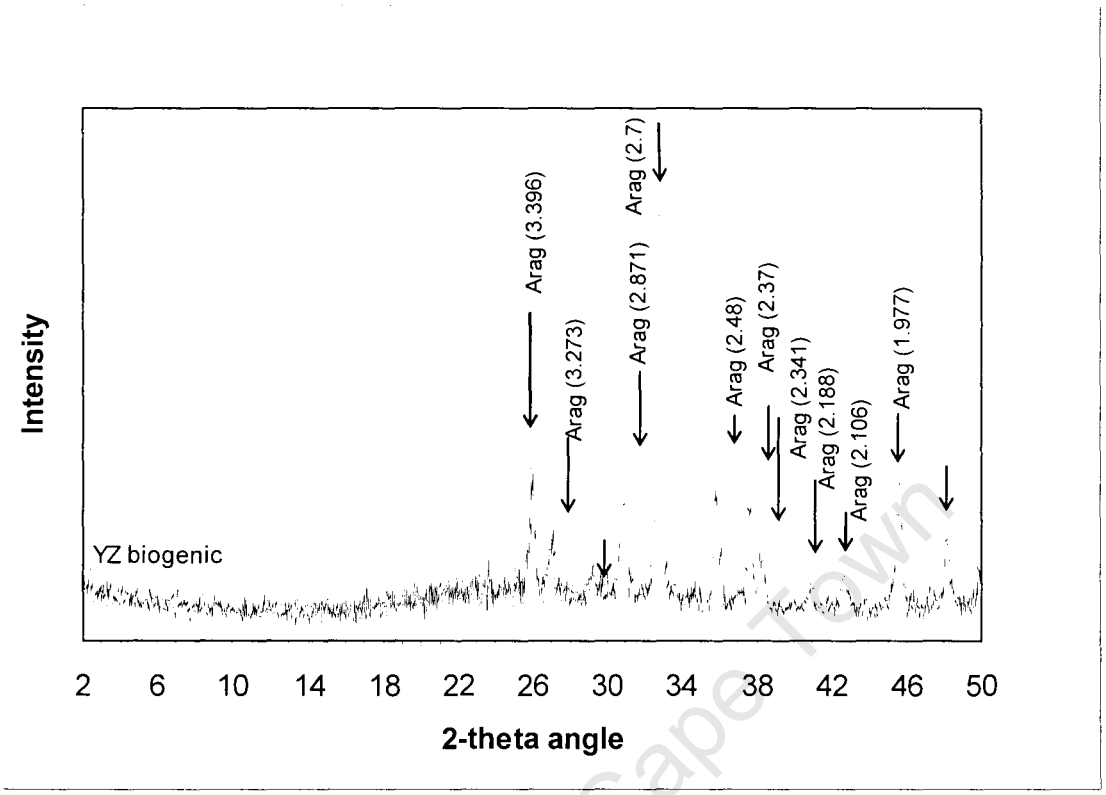

Figure 42. XRD scan showing mineralogy of sample YZ1-T (gastropod *T. ventricosa*)

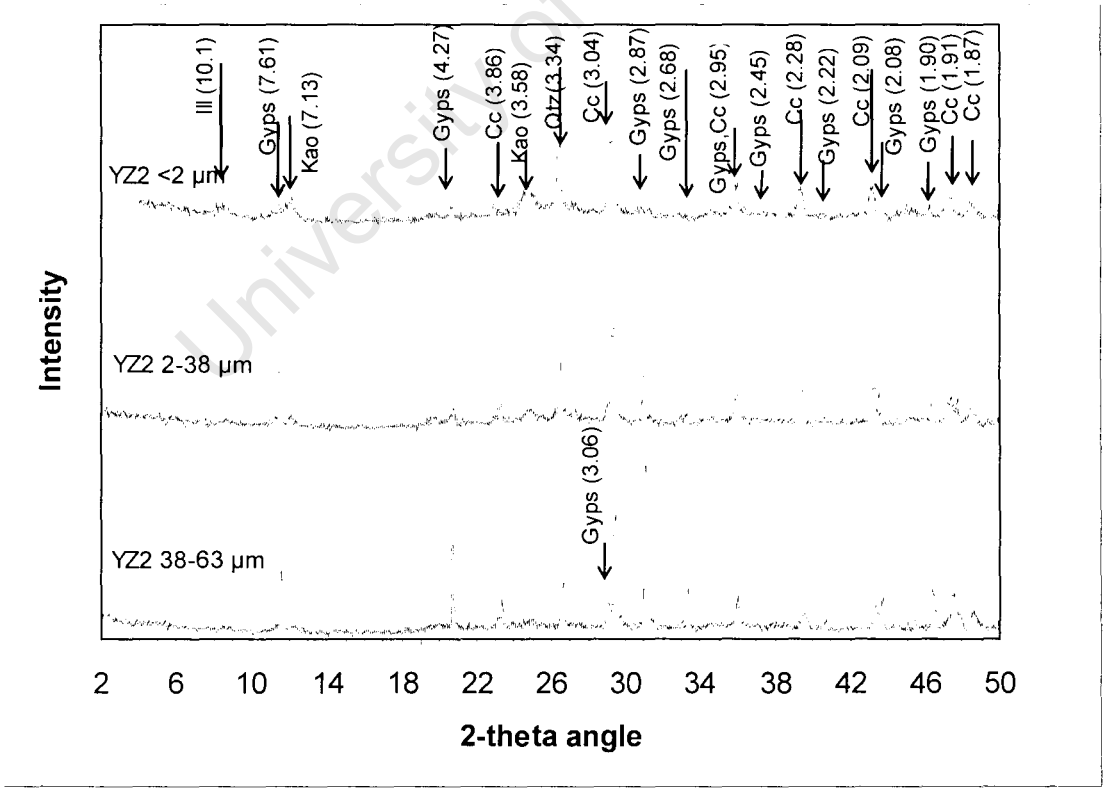

Figure 43. XRD scan showing mineralogy of sample YZ2

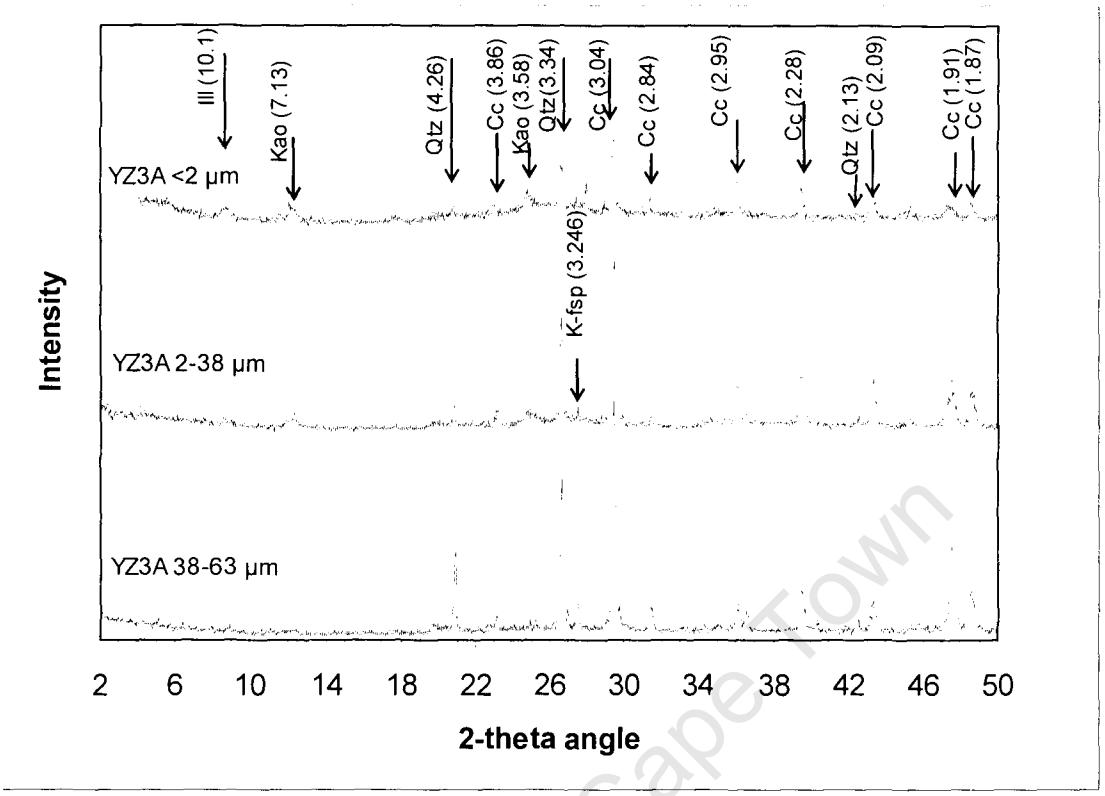

Figure 44. XRD scan showing mineralogy of sample YZ3A

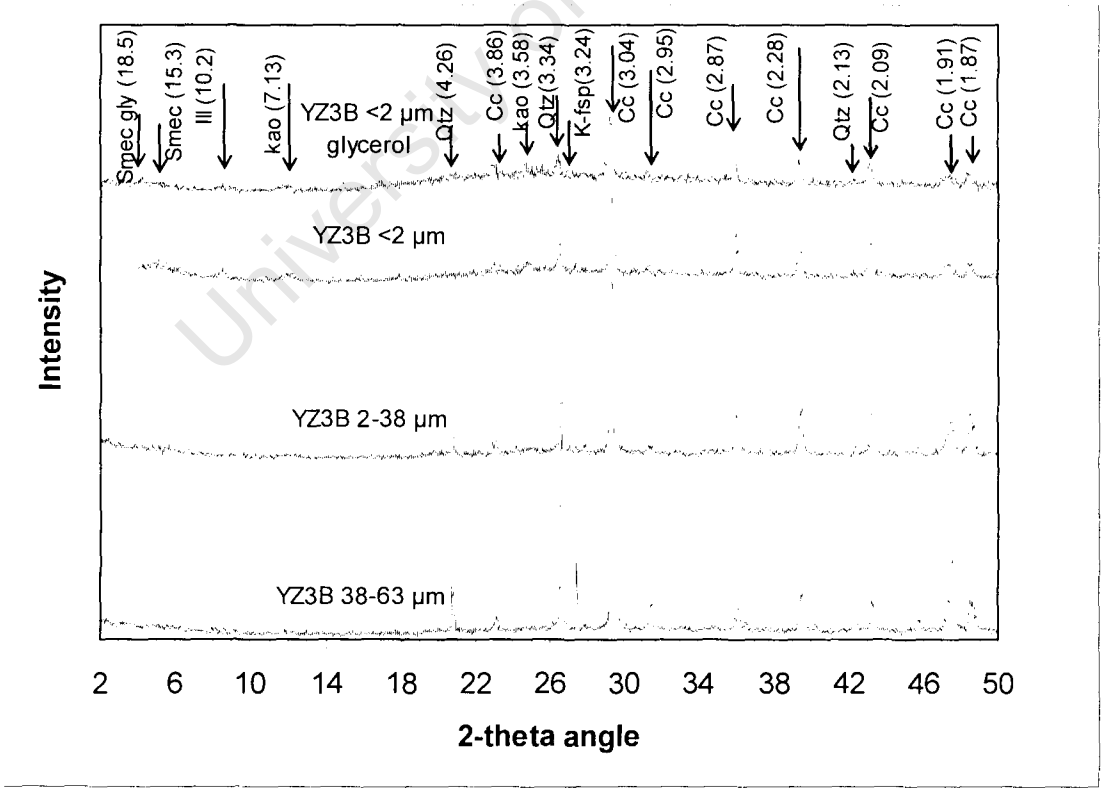

Figure 45. XRD scan showing mineralogy of sample YZ3B

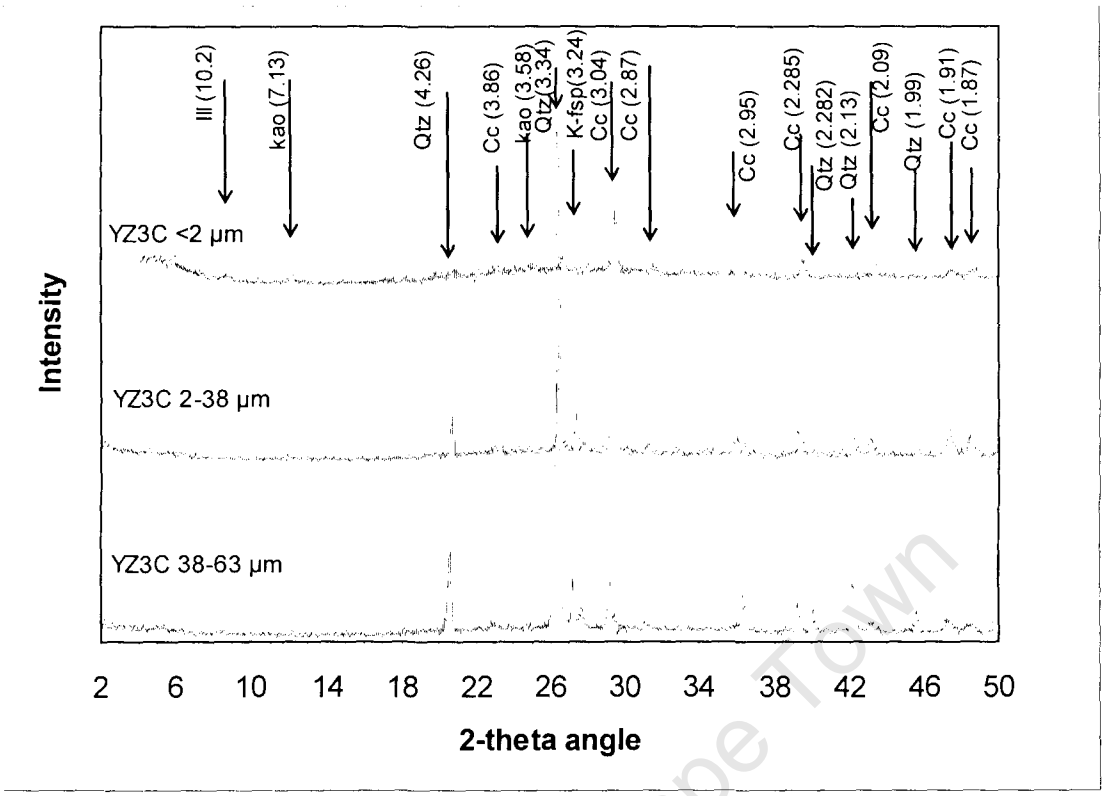

Figure 46. XRD scan showing mineralogy of sample YZ3C

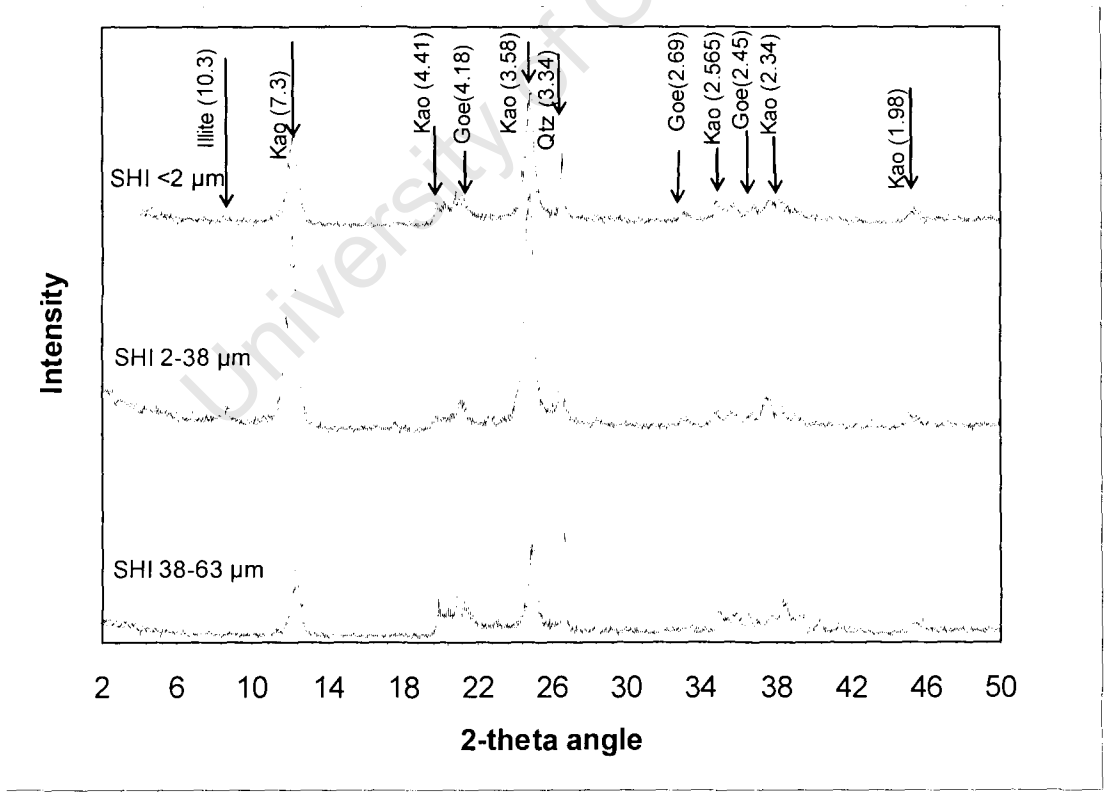

Figure 47. XRD scan showing mineralogy of sample SH1